



NUCLEAR WASTE MANAGEMENT ORGANIZATION SOCIÉTÉ DE GESTION DES DÉCHETS NUCLÉAIRES

# Phase 1 Geoscientific Desktop Preliminary Assessment, Lineament Interpretation

TOWNSHIP OF SCHREIBER, ONTARIO



**APM-REP-06144-0038**

**NOVEMBER 2013**

*This report has been prepared under contract to the NWMO. The report has been reviewed by the NWMO, but the views and conclusions are those of the authors and do not necessarily represent those of the NWMO.*

*All copyright and intellectual property rights belong to the NWMO.*

*For more information, please contact:*

**Nuclear Waste Management Organization**

22 St. Clair Avenue East, Sixth Floor

Toronto, Ontario M4T 2S3 Canada

Tel 416.934.9814

Toll Free 1.866.249.6966

Email [contactus@nwmo.ca](mailto:contactus@nwmo.ca)

[www.nwmo.ca](http://www.nwmo.ca)

**Phase 1 Geoscientific Desktop Preliminary Assessment**

# **Lineament Interpretation**

## **Township of Schreiber, Ontario**

**Report Prepared for:**

**AECOM**

AECOM Canada Ltd.

&

**nwmo**  
NUCLEAF WASTE MANAGEMENT ORGANIZATION SOCIÉTÉ DE GESTION DES DÉCHETS NUCLÉAIRES

Nuclear Waste Management Organization  
NWMO Report Number: APM-REP-06144-0038

**Report Prepared by:**

 **srk** consulting

SRK Consulting (Canada) Inc.  
SRK Project Number: 3CN020.001

November, 2013

---

# Lineament Interpretation

## Township of Schreiber, Ontario

### **AECOM Canada Ltd.**

215 – 55 Wyndham Street North  
Guelph, ON, Canada N1H 7T8

[www.aecom.com](http://www.aecom.com)

### **Nuclear Waste Management Organization**

22 St. Clair Avenue East, 6<sup>th</sup> Floor  
Toronto, Ontario

M4T 2S3

[www.nwmo.ca](http://www.nwmo.ca)

### **SRK Consulting (Canada) Inc.**

Suite 2100, 25 Adelaide Street East  
Toronto, Ontario, Canada

M5C 3A1

E-mail: [toronto@srk.com](mailto:toronto@srk.com)

Website: [www.srk.com](http://www.srk.com)

Tel: +1 416 6011445

Fax: +1 416 601 9046

**SRK Project Number: 3CN020.001**

**NWMO Report Number: APM-REP-06144-0038**

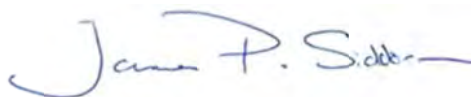
**November, 2013**

### **Authored by:**



Ivo Vos, Ph.D., P.Geol.  
Senior Consultant (Structural Geology)

### **Reviewed by:**



James P. Siddorn, Ph.D., P.Geol.  
Principal Consultant (Structural Geology)

---



## Executive Summary

In December, 2011, the Township of Schreiber, Ontario, expressed interest in continuing to learn more about the Nuclear Waste Management Organization nine-step site selection process, and requested that a preliminary assessment be conducted to assess potential suitability of the Schreiber area for safely hosting a deep geological repository (Step 3). This request followed a successful completion of an initial screening conducted during Step 2 of the site selection process.

The preliminary assessment is a multidisciplinary desktop study integrating both technical and community well-being studies, including geoscientific suitability, engineering, transportation, environment and safety, as well as social, economic and cultural considerations. The findings of the overall preliminary assessment are reported in an integrated report (NWMO, 2013). The objective of the desktop geoscientific preliminary assessment is to determine whether the Township of Schreiber and its periphery, referred to as the “Schreiber area”, contains general areas that have the potential to meet NWMO’s geoscientific site evaluation factors.

This report presents the findings of a lineament investigation assessment completed as part of the desktop geoscientific preliminary assessment of the Schreiber area (AECOM, 2013a). The lineament assessment focused on identifying surficial and geophysical lineaments and their attributes using publicly-available digital data sets, including geophysical (aeromagnetic and electromagnetic) and surficial (satellite imagery, digital elevation) data sets for the Schreiber area in northwestern Ontario. The assessment of interpreted lineaments in the context of identifying general areas that have the potential to meet NWMO’s geoscientific site evaluation factors is provided in the desktop preliminary geoscientific assessment report (AECOM 2013a). The lineament investigation interprets the location and orientation of potential bedrock structural features (e.g., individual fractures or fracture zones) within the context of the local and regional geological setting. The approach undertaken in this desktop lineament investigation is based on the following:

- Lineaments were interpreted from multiple, readily-available data sets (aeromagnetic, electromagnetic, CDED, SPOT and Landsat);
- Lineament interpretations were made by documented specialist observers and using a standardized workflow;
- Lineament interpretations were analyzed based on an evaluation of the quality and limitations of the available data sets;
- Interpreted lineaments were separated into three categories (ductile, brittle, dyke) based on their character;
- Lineament interpretations were analyzed using reproducibility tests, particularly the coincidence of lineaments extracted by different observers, coincidence of lineaments extracted from different data sets, relative ages and/or documentation in literature; and
- Final classification of the lineament interpretation was done based on length and reproducibility.

The distribution of lineaments in the Schreiber area reflects the bedrock structure, resolution of the data sets used, and surficial cover. Surface lineament density, as demonstrated in this assessment, is high and relatively uniform since only minor areas of significant overburden cover occur that may mask the surficial expression of bedrock structures. The greatest density of lineaments occurs within portions of the Schreiber area that are underlain by metavolcanic rocks of the Schreiber greenstone belt. In addition, an approximately 10 kilometre wide corridor of high lineament density occurs through the center of the Schreiber area. The lineaments in this area trend in a northwest-southeast direction. Although the lineament density in the Schreiber area is generally high, few areas with a relatively low density of lineaments were identified. These are restricted to granitoid batholiths, mostly within the Crossman Lake batholith.

On the basis of the structural history of the Schreiber area, a framework was also developed to constrain the relative age relationships of the interpreted lineaments.

## Important Notice

AECOM Canada Ltd. (AECOM), on behalf of the Nuclear Waste Management Organization (NWMO), commissioned SRK Consulting (Canada) Inc. (SRK) to compile a structural lineament interpretation of remote sensing data for the Schreiber area in Ontario. The opinions expressed in this report have been based on the information supplied to SRK by AECOM and NWMO. These opinions are provided in response to a specific request from NWMO, and are subject to the contractual terms between SRK and AECOM. SRK has exercised all due care in reviewing the supplied information. Whilst SRK has compared key supplied data with expected values, the accuracy of the results and conclusions from the review are entirely reliant on the accuracy and completeness of the supplied data. SRK does not accept responsibility for any errors or omissions in the supplied information and does not accept any consequential liability arising from commercial decisions or actions resulting from them. Opinions presented in this report apply to the site conditions and features as they existed at the time of SRK's investigations, and those reasonably foreseeable. These opinions do not necessarily apply to conditions and features that may arise after the date of this report.

All title and beneficial ownership interests to all intellectual property, including copyright, of any form, including, without limitation, discoveries (patented or otherwise), software, data (hard copies and machine readable) or processes, conceived, designed, written, produced, developed or reduced to practice pertaining to this study shall vest in and remain with NWMO. For greater certainty, (a) ownership of all rights, title and interest, including intellectual property, in the work or deliverables are owned by NWMO and (b) ownership of all intellectual property created, developed or reduced to practice in the course of conducting this study and creating this report are exclusively owned by NWMO. SRK hereby grants NWMO a fully paid up irrevocable licence for all such intellectual property for its own non-commercial use.

# Table of Contents

<b>Executive Summary</b> .....	<b>i</b>
<b>Important Notice</b> .....	<b>ii</b>
<b>Table of Contents</b> .....	<b>iii</b>
<b>List of Tables</b> .....	<b>iv</b>
<b>List of Figures (in order following text)</b> .....	<b>iv</b>
<b>1 Introduction</b> .....	<b>1</b>
1.1 Scope of Work and Work Program .....	1
1.2 Qualifications of SRK and SRK Team.....	2
1.3 Acknowledgements .....	3
1.4 Report Organization .....	3
<b>2 Summary of Physical Geography and Geology</b> .....	<b>4</b>
2.1 Physical Geography .....	4
2.2 Bedrock Geology.....	6
2.2.1 Granitoid Intrusive Rocks.....	6
2.2.2 Schreiber-Hemlo Greenstone Belt.....	7
2.2.3 Mafic Dykes .....	8
2.2.4 Faults .....	8
2.2.5 Metamorphism .....	9
2.3 Geological and Structural History.....	10
2.4 Quaternary Geology.....	13
2.5 Land Use.....	15
<b>3 Methodology</b> .....	<b>15</b>
3.1 Source Data Descriptions .....	15
3.1.1 Geophysical Data .....	16
3.1.2 Surficial Data.....	17
3.2 Lineament Interpretation Workflow .....	19
3.2.1 Step 1: Lineament Interpretation and Certainty Level .....	21
3.2.2 Step 2: Reproducibility Assessment 1 (RA_1).....	22
3.2.3 Step 3: Coincidence Assessment 2 (RA_2) .....	24
<b>4 Findings</b> .....	<b>26</b>
4.1 Description of Lineaments by Data Set.....	26
4.1.1 Geophysical Data .....	26
4.1.2 Surficial Data (CDED topography and satellite imagery) .....	28
4.2 Description and Classification of Integrated Lineament Coincidence (RA_2).....	28
4.3 Description of Lineaments by Batholiths and Plutons in the Schreiber Area .....	29
<b>5 Discussion</b> .....	<b>30</b>
5.1 Lineament Density .....	30
5.2 Lineament Reproducibility and Coincidence .....	31
5.3 Lineament Length .....	32
5.4 Fault and Lineament Relationships.....	33
5.5 Relative age relationships .....	34
<b>6 Summary</b> .....	<b>34</b>
<b>7 References</b> .....	<b>36</b>

## List of Tables

Table 1: Summary of the Geological and Structural History of the Schreiber Area (adapted from AECOM, 2013a).....	12
Table 2: Summary of Source Data Information for the Lineament Interpretation, Schreiber area.....	16
Table 3: Summary of Geophysical Survey Acquisition Parameters for the Lineament interpretation .....	17
Table 4: Summary of 1:50,000 scale CDED tiles used for Lineament interpretation.....	18
Table 5: Summary of SPOT imagery scenes used for the Lineament interpretation.....	18
Table 6: Summary of Landsat 7 imagery scenes used for the Lineament interpretation.....	19
Table 7: Summary of Attribute Table Fields Populated for the Lineament Interpretation .....	20

## List of Figures (in order following text)

Figure 1: Township of Schreiber and Surrounding Area	
Figure 2: Regional Tectonic Setting of Schreiber and Surrounding Area	
Figure 3: Local Bedrock Geology of the Schreiber Area	
Figure 4: Terrain Features of the Schreiber Area	
Figure 5: Pole Reduced Magnetic Data (first vertical derivative) for the Schreiber Area	
Figure 6: Apparent Resistivity from Low Frequency (877 Hz) Electromagnetic Data for the Schreiber Area	
Figure 7: CDED Digital Elevation Model for the Schreiber Area	
Figure 8: Satellite Data (LandSAT) for the Schreiber Area	
Figure 9: Ductile Features for the Schreiber Area	
Figure 10: Lineaments by Reproducibility (RA_1) Interpreted from Pole Reduced Magnetic Data (1VD) for the Schreiber Area	
Figure 11: Lineaments by Reproducibility (RA_1) interpreted from Low-Frequency (877 Hz) EM data for the Schreiber Area	
Figure 12: Lineaments by Reproducibility (RA_1) Interpreted from CDED Digital Elevation Data for the Schreiber Area	
Figure 13: Lineaments by Reproducibility (RA_1) Interpreted from Satellite Data (LandSAT) for the Schreiber Area	
Figure 14: Interpreted Lineaments by Reproducibility (RA_2) Overlying Bedrock Geology for the Schreiber Area	
Figure 15: Interpreted Lineaments by Length Overlying Bedrock Geology for the Schreiber Area	
Figure 16: Interpreted Lineaments by Length Overlying Bedrock Geology for the Schreiber Area	

# 1 Introduction

In December, 2011, the Township of Schreiber, Ontario, expressed interest in continuing to learn more about the Nuclear Waste Management Organization nine-step site selection process, and requested that a preliminary assessment be conducted to assess potential suitability of the Schreiber area for safely hosting a deep geological repository (Step 3). This request followed a successful completion of an initial screening conducted during Step 2 of the site selection process.

The preliminary assessment is a multidisciplinary desktop study integrating both technical and community well-being studies, including geoscientific suitability, engineering, transportation, environment and safety, as well as social, economic and cultural considerations. The findings of the overall preliminary assessment are reported in an integrated report (NWMO, 2013). The objective of the desktop geoscientific preliminary assessment is to determine whether the Township of Schreiber and its periphery, referred to as the “Schreiber area”, contains general areas that have the potential to meet NWMO’s geoscientific site evaluation factors.

This report presents the findings of a lineament investigation assessment completed by SRK Consulting (Canada) Inc. (SRK) as part of the desktop geoscientific preliminary assessment of the Schreiber area (AECOM, 2013a). The lineament assessment focussed on identifying surficial and geophysical lineaments and their attributes using publicly-available digital data sets, including surficial (satellite imagery, digital elevation) and geophysical (aeromagnetic, electromagnetic) data sets for the Schreiber area in northwestern Ontario. The assessment of interpreted lineaments in the context of identifying general areas that have the potential to meet NWMO’s geoscientific site evaluation factors is provided in the desktop preliminary geoscientific assessment report (AECOM, 2013a).

## 1.1 Scope of Work and Work Program

The scope of work includes the completion of a desktop structural lineament interpretation of remote sensing (AECOM, 2013b) and geophysical (Mira, 2013) data for the Schreiber area in northwestern Ontario (Figure 1).

The Schreiber area used for the interpretation is approximately 1,100 square kilometres (km<sup>2</sup>) and was provided by NWMO as a shape file for a square area (Figure 1).

The lineament study involved the interpretation of remotely-sensed data sets, including surficial (satellite imagery, digital elevation) and geophysical (aeromagnetic and electromagnetic) data sets for the Schreiber area. The investigation interpreted the implication of lineament location and orientation as potential bedrock structural features (e.g., individual fractures or fracture zones) and evaluated their relative timing relationships within the context of the local and regional geological setting. For the purpose of this report, a lineament was defined as, ‘an extensive linear or arcuate geologic or topographic feature’. The approach undertaken in this desktop lineament investigation is based on the following:

- Lineaments were mapped from multiple, readily-available data sets that include geophysical (aeromagnetic and electromagnetic) data, satellite imagery (Landsat, SPOT) and digital elevation models (Canadian Digital Elevation Data (CDED));
- Lineament interpretations from each source data type were made by two specialist observers for each data set using a standardized workflow;

- Lineaments were interpreted as brittle, dyke or ductile features by each observer;
- Lineaments were analyzed based on an evaluation of the quality and limitations of the available data sets;
- Lineaments were evaluated using: age relationships; reproducibility tests, particularly the coincidence of lineaments extracted by different observers; coincidence of lineaments extracted from different data sets; and comparison to literature; and
- Classification was applied to indicate the significance of lineaments based on length and reproducibility.

These elements address the issues of subjectivity and reproducibility normally associated with lineament investigations and their incorporation into the methodology increases the confidence in the resulting lineament interpretation.

At this desktop stage, the interpreted features were classified into three general categories based on a working knowledge of the structural history and bedrock geology of the Schreiber area. These categories include ductile, brittle and dyke lineaments, described as follows:

- **Ductile lineaments:** Features which were interpreted as being associated with the internal fabric of the rock units (including sedimentary or volcanic layering, tectonic foliation or gneissosity, and magmatic foliation) were classified as ductile lineaments. This category also includes recognizable penetrative shear zone fabric.
- **Brittle lineaments:** Features interpreted as fractures (joints or joint sets, faults or fault zones, and veins or vein sets), including those that offset the continuity of the ductile fabric described above, were classified as brittle lineaments. This category also includes brittle-ductile shear zones, and brittle partings interpreted to represent discontinuous re-activation parallel to the ductile fabric. At the desktop stage of the investigation, this category also includes features of unknown affinity. This category does not include interpreted dykes, which are classified separately (described below).
- **Dyke lineaments:** For this preliminary desktop interpretation, any features which were interpreted, on the basis of their distinct character, e.g., scale and composition of fracture in-fill, orientation, geophysical signature and topographic expression, were classified as dykes. Dyke interpretation is largely made using the aeromagnetic data set, and is often combined with pre-existing knowledge of the bedrock geology of the Schreiber area.

## 1.2 Qualifications of SRK and SRK Team

The SRK Group comprises of more than 1,200 professionals, offering expertise in a wide range of resource engineering disciplines. The independence of the SRK Group is ensured by the fact that it holds no equity in any project it investigates and that its ownership rests solely with its staff. These facts permit SRK to provide its clients with conflict-free and objective recommendations on crucial issues. SRK has a proven track record in undertaking independent assessments of mineral resources and mineral reserves, project evaluations and audits, technical reports and independent feasibility evaluations to bankable standards on behalf of exploration and mining companies, and financial institutions worldwide. Through its work with a large number of major international mining companies, SRK Group has established a reputation for providing valuable consultancy services to the global mining industry.

The following is a brief description of the qualifications and roles of project team members.

**Dr. Ivo Vos, P.Geo.** is a Senior Consultant (Structural Geology) with SRK who has a broad background in geoscience with a focus on deciphering structural controls on the distribution of mineralization for a variety of mineral deposit styles. He has undertaken numerous structural and geological interpretations of remote sensing data for areas in Canada, South America, West Africa and the Middle East. Dr. Vos holds a Bachelor's and Master's Degree in Geology from the University of Utrecht (The Netherlands) and a Doctoral Degree in Earth Sciences from Monash University (Australia). In this study, Dr. Vos was the lead interpreter.

**Simon Craggs, M.Sc.** is a Senior Consultant (Structural Geology) with SRK who has a broad background in geoscience and specializes in regional mapping, and detailed analysis of fracture/fluid flow mechanics and the structural controls on epithermal ore deposit formation. Mr. Craggs holds a Bachelor's Degree in Geological Science from the University of Leeds, UK, and a Master's Degree in Structural Geology from the University of New Brunswick. In this study, Mr. Craggs was the second interpreter.

**Dr. James Siddorn, P.Geo.** is a Practice Leader and Principal Consultant (Structural Geology) with SRK who has a broad background in geoscience. Dr. Siddorn specializes in building 4D deposit to district scale models to evaluate the structural controls on ore distribution, rock stability, and hydrogeology, and is highly proficient in computer based 2D/3D GIS and geological modeling. He has over 16 years of experience in the consulting field, including the management of a number of high profile and multidisciplinary projects. He has managed and completed numerous studies involving the structural and geological interpretation of remote sensing data in Northern Ontario for mineral exploration and geotechnical/hydrogeological studies. Dr. Siddorn holds a Bachelor's Degree in Geology from the University of Durham, UK, a Master's Degree in Geology and a Doctoral Degree in Structural Geology from the University of Toronto. In this study, Dr. Siddorn supervised all work completed and reviewed drafts of this report prior to their delivery to AECOM and NWMO as per SRK internal quality management procedures.

**Jason Adam** is an Associate Consultant (GIS) who has a broad experience in GIS. Mr. Adam provided GIS support for the study, mainly for the preparation of figures, under the direction of Dr. Vos.

## 1.3 Acknowledgements

SRK would like to thank Mr. Cam Baker and Mr. Bob Leech from AECOM and Mr. Thomas Campagne and Mr. Nigel Phillips from Mira Geosciences for a fruitful collaboration on this project.

## 1.4 Report Organization

The report is organized into sections that describe the geological setting of the Schreiber area, the methodology used in identifying lineaments, the findings of the lineament interpretation, and a discussion of the results in the context of the local and regional geological framework.

Section 1 of this report includes an introduction and background for the completed structural lineament investigation.

Section 2 provides an overview of the geological setting of the Schreiber area and documents its structural history on the basis of available literature. A brief outline of the physical geography, Quaternary geology and land use in the Schreiber area are also included in this section.

Section 3 documents the methodology applied for the lineament investigation for the Schreiber area. The source data used for the lineament interpretation are outlined and the interpretation workflow for the subsequent steps of the investigation is described.

Section 4 documents the findings of the lineament investigation in the Schreiber area. This includes a description of interpreted lineaments by data set and describes the classification of the integrated data set by major geological unit.

Section 5 discusses lineament length, density and reproducibility, as well as their relative age relationships and fit with mapped features

Section 6 is a brief summary of the main findings of this investigation.

## 2 Summary of Physical Geography and Geology

The Schreiber area is primarily located in the Archean Wawa Subprovince, Superior Province (Figure 2). The Wawa Subprovince comprises a volcano-sedimentary-plutonic terrane bounded to the east by the Kapuskasing structural zone (beyond the area of investigation) and to the north by the metasedimentary-dominated Quetico Subprovince. The western end of the Wawa Subprovince is bordered by the Proterozoic Trans-Hudson orogen. To the south, the Schreiber area is flanked by the Early Proterozoic Southern Province. A discontinuity in mapped Marathon mafic dykes on Figure 2 is related to map boundaries, where the Marathon mafic dykes are not included in the public data for the southern map sheet covering the Schreiber area.

The Wawa Subprovince is composed of two semi-linear zones of greenstone belts, the northern of which includes the Shebandowan, Schreiber-Hemlo, Manitouwadge-Hornepayne, White River, Dayohessarah, and Kabinakagami greenstone belts (a portion of which is shown on Figure 2). The Schreiber area is situated in the western portion of the Schreiber-Hemlo greenstone belt (sometimes referred to as the Terrace Bay-Schreiber greenstone belt). This greenstone belt is divided into western and eastern portions by the Proterozoic Coldwell alkalic complex. The Schreiber-Hemlo greenstone belt consists of a number of narrow, arcuate segments of supracrustal rocks that are bounded and enclosed by granitoid bodies, including the Crossman and Whitesand Lake batholiths. The Schreiber-Hemlo greenstone belt is divided into three lithotectonic assemblages by Williams et al. (1991); the Schreiber, Hemlo-Black River, and Heron Bay assemblages. The Schreiber and Hemlo-Black River assemblages are separated by the Proterozoic Coldwell alkalic complex (north of the town of Marathon). The Hemlo-Black River and Heron Bay assemblages are located to the north and south of the Lake Superior Hemlo fault zone (LSHFZ; Figure 2), respectively.

### 2.1 Physical Geography

Physical Geography of the Schreiber area is described in detail in AECOM (2013a,b). A summary of the main features is provided here for reference.



The elevation difference within the Schreiber area is significant with a maximum range of approximately 402 metres. The highest relief occurs just north of the Township of Schreiber, where land elevation is approximately 585 metres above sea level (masl). The lowest point equals the elevation of Lake Superior, approximately 183 masl.

The Schreiber area is characterized by predominantly moderate to high relief over short distances, and rugged topography consisting of knobby bedrock hills and steep escarpments. The orientation of escarpments is parallel to the trend of major faults and lineaments which transect the area. Local areas of low relief (<20 m) occur between the Townships of Terrace Bay and Schreiber, and along the Aguasabon River system.

Across the Schreiber area, the elevation of hills and ridges is commonly between 400 and 500 metres. There is, however, a general southward decrease in the elevation of hill tops from the 400 to 500 metres range in the north to 300 to 400 metres range in the south. Lower elevations are encountered along the Aguasabon River in the east and in the vicinity of Whitesand and Lyne lakes in the southwest. A region of lower elevation, approximately 300 masl, characterizes the southeastern corner of the Schreiber area, around Hays Lake and the mouth of the Aguasabon River.

The Schreiber area is within the Little Pic tertiary watershed, which drains via the Great Lakes water system and the St. Lawrence River, and can be sub-divided into four watersheds at the quaternary scale. The Pays Plat River watershed is located in the northwestern part of the Schreiber area and enters into Lake Superior through the Pays Plat First Nation Reserve 51, 6 kilometres west of Rosspoint. The Whitesand River watershed is located immediately to the east and enters Lake Superior near Selim, approximately 8 kilometres west of Schreiber. The central portion of the Schreiber area is drained by the Big Duck Creek watershed, which drains into the Aguasabon River watershed at Hays Lake. The Aguasabon River watershed drains the eastern portion of the Schreiber area and enters Lake Superior near Terrace Bay.

The orientation of the drainage network within the Schreiber area is largely controlled by bedrock structural features and the irregular surface of the topography. Due to this control, the majority of waterways, including lakes, have a north, northwestward or northeastward orientation. While the overall drainage in the area is southward, the catchment areas of individual lakes within the watersheds results in short segments of northward flow.

The larger rivers draining the watersheds noted above are fed by numerous smaller creeks and rivers that effectively drain all parts of the Schreiber area. An exception is a portion of the region underlain by notable thicknesses of glaciolacustrine and glaciofluvial deposits in the area surrounding Terrace Bay. Typically, segments of the area's waterways are short, on the order of less than 2 kilometres, as they flow into and out of lakes occurring along the drainage paths.

The numerous lakes within the Schreiber area occupy approximately 7.6 percent of the land surface (i.e., excluding Lake Superior) and occur with an even distribution, excluding the area near Terrace Bay.. These lakes, many of which are elongate in shape, are generally small with only five lakes having a surface area of greater than 2 km<sup>2</sup>. Larger lakes in the interior of the Schreiber area include Pays Plat, along the western boundary, and Winston, Charlotte and Big Duck lakes in the north-central region (Figure 1).

## 2.2 Bedrock Geology

The bedrock geology of the Schreiber area is shown in Figure 3. The main geological units in the Schreiber area include, several large granitoid intrusions (Terrace Bay, Crossman Lake and Whitesand Lake batholiths, and the Mount Gwynne pluton), the supracrustal rocks of the Schreiber assemblage of the Schreiber-Hemlo greenstone belt, and the several suites or swarms of mafic diabase dykes. Each of these sets of rock units is discussed in more detail below. In addition, the bedrock in the Schreiber area is overprinted by several orientations of brittle faults and the individual rock units have been subjected to varying amounts of metamorphism.

### 2.2.1 Granitoid Intrusive Rocks

Massive granite to granodiorite intrusions comprise a voluminous suite of rocks within and adjacent to the Schreiber-Hemlo greenstone belt (Figure 3). These are typically composite, ovoid intrusions that vary in size up to twenty-five kilometres in diameter. Their composite nature includes lithologies ranging from dominantly granite and granodiorite to quartz diorite, syenite and quartz monzonite (and their gneissic equivalents), as well as aplite and pegmatite dykes. These intrusions likely formed by partial melting of mafic to ultramafic sources (e.g., Polat, 1998).

Granitoid intrusions in the Hemlo assemblage of the Schreiber-Hemlo greenstone belt returned ages between ca. 2.688 and 2.678 billion years (Ga) (Corfu and Muir 1989). Due to the similar character and emplacement style of granitoid intrusions in the Schreiber area compared to the Hemlo area, and an absence of more precise age dating, the granitoid intrusions in the Schreiber area are also considered to be emplaced between ca. 2.690 and 2.680 Ga (Smyk and Schnieders, 1995; Corfu and Muir, 1989).

The granitoid intrusions in the Schreiber area include the Terrace Bay, Crossman Lake and Whitesand Lake batholiths, and the Mount Gwynne pluton (Figure 3). These intrusions cover approximately 495 km<sup>2</sup> within the Schreiber area. The emplacement of these batholiths overlapped with regional metamorphism dated at ca. 2.688 to 2.675 Ga (Muir, 2003) and resulted in the development of amphibolite grade contact aureoles within the surrounding greenschist grade greenstone belt rocks (Marmont, 1984).

The Terrace Bay batholith is located in the southeastern part of the Schreiber area (Figure 3) and trends northeast, at an angle to the generally east-trending greenstone belt rocks. The bulk of the Terrace Bay batholith is a massive, homogeneous, equigranular and medium-grained granodiorite with common variations in texture, grain size and colour, with minor masses of quartz monzodiorite and quartz-monzonite (Marmont, 1984; Carter, 1988). Apophyses and dykes derived from the Terrace Bay batholith intrude the greenstone belt rocks (discussed in Section 2.2.2) within the vicinity of the batholith contact. These minor phases include: 1) aplite and pegmatite dykes; 2) quartz-feldspar, feldspar and hornblende porphyries; 3) carbonate-rich lamprophyre dykes; and 4) narrow, magnetic diabase dykes. The Terrace Bay batholith covers 67 km<sup>2</sup> within the Schreiber area.

The Crossman Lake batholith occupies the majority of the northern part of the Schreiber area (Figure 3). The batholith is predominantly massive and consists of a mixture of medium-grained quartz-monzonite and monzodiorite, (alkali-feldspar) granite, tonalite and granodiorite. Minor dykes and irregular masses of microgranite, quartz (-feldspar) porphyry and aplite occur along the margins of the batholith. The Crossman Lake batholith covers 300 km<sup>2</sup> within the Schreiber area.

The Whitesand Lake batholith occurs in the southwestern portion of the Schreiber area (Figure 3). This batholith is elongate in an east-west direction parallel to the structural trend within the surrounding greenstone belt rocks. The batholith consists of mostly massive (alkali-feldspar) granite with lesser

porphyritic granite, monzodiorite, quartz monzonite and rare aplite. The Whitesand Lake batholith covers 123 km<sup>2</sup> within the Schreiber area.

The boundary between the Whitesand Lake and Crossman Lake batholiths is poorly defined. However, Carter (1988) places the boundary between the two batholiths along narrow septa of east-trending greenstone belt rocks along the western margin of the Schreiber area (Figure 3).

The Mount Gwynne pluton is located near the southern margin of the Schreiber area (Figure 3). It is located along the southern boundary of the supracrustal rocks of the Schreiber-Hemlo greenstone belt. The pluton comprises massive, medium-grained alkali-feldspar granite and biotite-hornblende granodiorite. The Mount Gwynne pluton covers 5 km<sup>2</sup> within the Schreiber area.

### 2.2.2 Schreiber-Hemlo Greenstone Belt

Supracrustal rocks in the Schreiber area occur in the western part of the Schreiber-Hemlo greenstone belt and are considered to be part of the Schreiber assemblage (Williams et al., 1991; Figure 3). Carter (1988) identified three major types of supracrustal rocks in the Schreiber assemblage: 1) tholeiitic, mafic metavolcanic rocks comprising mainly massive to pillow basalt, tuff and related breccias; 2) calc-alkalic, mafic to felsic metavolcanic rocks dominated by pyroclastic units; and 3) clastic metasedimentary rocks of turbiditic origin interbedded with minor banded iron formation. These three supracrustal rock types are described in further detail below.

Tholeiitic, mafic metavolcanic rocks are massive or schistose and variably metamorphosed ranging from dominantly greenschist facies to amphibolite facies and locally pyroxene hornfels facies. Greenschist facies mafic volcanic rocks are either massive or foliated and are aphanitic to medium-grained, whereas amphibolite facies mafic volcanic rocks are medium-grained and well foliated (Carter, 1988). The greenschist facies tholeiitic rocks comprise aphanitic, fine-grained massive and pillowed flows, as well as porphyritic, amygdaloidal and variolitic flows. Interbedded with these flows are minor autoclastic flow breccias and mafic to intermediate tuff horizons. The amphibolite facies tholeiitic rocks include fine- to medium-grained foliated amphibolite and garnet amphibolite. The minimum age of mafic volcanism is constrained by crosscutting pluton apophyses in the eastern half of the Schreiber-Hemlo greenstone belt at ca. 2.697 Ga (Muir, 2003).

Calc-alkalic mafic to felsic metavolcanic rocks are mainly greenschist facies massive, aphanitic to fine-grained andesite to porphyritic dacite flows. Minor amygdaloidal felsic interbeds occur with the massive flows. In addition, fine-grained to aphanitic tuff units with rare lapilli tuff and tuff breccia are interlayered with the mafic to felsic flows. Muir (2003) indicated that felsic calc-alkalic volcanism occurred from ca. 2.698 to 2.692 Ga, and intermediate volcanism occurred around 2.689 Ga in the eastern half of the Schreiber-Hemlo greenstone belt. This is compatible with U-Pb zircon age determinations for calc-alkaline volcanism that are generally within a narrow range between 2.698 and 2.688 Ga (Corfu and Muir, 1989).

Metasedimentary rocks are composed of greenschist facies wacke, silicified shale (including graphitic intervals), chert horizons and banded iron formation as well as minor amphibolite facies garnet- and sillimanite-bearing wacke. The wacke comprises foliated, fine- to medium-grained quartz-plagioclase-biotite rocks with minor epidote, apatite, muscovite and pyrite. Banded iron formations form thinly bedded units interlayered with the metavolcanic rocks comprising magnetite-chert or magnetite-only (oxide-facies) and pyrite-pyrrhotite-chert (sulphide-facies) horizons. Sedimentation of turbiditic wacke-mudstone in the Schreiber-Hemlo greenstone belt occurred after ca. 2.693 Ga for volcanoclastic deposits and possibly as late as ca. 2.685 Ga for wacke (Muir, 2003).

Rocks of the Quetico Subprovince consisting of metamorphosed turbiditic wacke with subordinate arenite-pegmatite migmatite and feldspar gneiss occupy the northern fringe of the Schreiber area (Carter, 1988). Deposition of these sedimentary rocks took place between 2.70 to 2.69 Ga, and amphibolite facies metamorphism occurred during the period 2.67 to 2.65 Ga (Williams et al., 1991).

Along the shore of Lake Superior in the Schreiber area, Mesoproterozoic sedimentary rocks of the ca. 2.200 Ga Animikie Group (Gunflint Formation, 24 in legend of Figure 3; Carter, 1988), the ca. 1.500 Ga Sibley and ca. 1.100 Ga Osler groups unconformably overlie Archean granitic and mafic metavolcanic rocks. These form discontinuous erosional remnants of an ancient fluvial-lacustrine system that comprises interbedded sandstone, conglomerate, ironstone, chert, shale, mudstone and limestone. These rocks are not metamorphosed and dip gently from 10 to 15 degrees to the southwest.

### 2.2.3 Mafic Dykes

Several suites of diabase dykes crosscut the Schreiber area (Figures 2 and 3), including:

- Northwest-trending Matachewan Suite dykes (ca. 2.473 Ga; Buchan and Ernst, 2004). This dyke swarm is one of the largest in the Canadian Shield. Individual dykes are generally up to 10 metres wide, and have vertical to subvertical dips. The Matachewan dykes comprise mainly quartz diabase dominated by plagioclase, augite and quartz (Osmani, 1991).
- North-trending Marathon Suite dykes (ca. 2.121 Ga; Buchan et al. (1996). These form a fan-shaped distribution pattern around the northern, eastern and western flanks of Lake Superior. The dykes vary in orientation from northwest to northeast, and occur as steep to subvertical sheets, typically a few metres to tens of metres thick, but occasionally up to 75 metres thick (Hamilton et al., 2002). The Marathon dykes comprise quartz tholeiite dominated by equigranular to subophitic clinopyroxene and plagioclase.; and
- East-west-trending, reversely polarized Keweenaw Suite dykes related to ca. 1.100 Ga mid-continental rifting that was centred on proto-Lake Superior (Thurston, 1991).

Potentially, a western extension of the ca. 2.167 Ga Biscotasing dyke swarm also occurs in the Schreiber area (Hamilton et al., 2002). These generally trend northeast; however, how these may be distinguished from northeast-trending Marathon dykes in the Schreiber area is undefined.

### 2.2.4 Faults

In the Schreiber area, several faults are indicated on public domain geological maps. These include the major (from west to east) Sox Creek, Ross Lake, and Cook Lake southeast-trending faults (Figure 3). Several northeast-trending faults are indicated on public domain maps including the Schreiber Point fault, the Worthington Bay fault (with the Syenite Lake fault along its extension), and the Ellis Lake fault. The timing and kinematics of these faults are not described in literature.

Carter (1988) conducted a field mapping program and developed a geological map for the Schreiber area, primarily on the basis of 1:15,840 scale aerial photographs and north-south trending traverse mapping at roughly quarter mile intervals. As a result of this mapping program, Carter (1988) attempted an interpretation of the fault movement along some of the faults shown on public domain geological maps. No supporting structural information was included in Carter (1988), so it is assumed that the fault movement interpretation was derived from aerial photographs. Carter's (1988) interpretation is only included here for historical reference. Carter (1988) interpreted the Sox Lake fault and the Schreiber Point fault as dextral strike-slip faults; the Cook Lake fault and Syenite Lake fault as dip-slip faults; and the Worthington Bay fault as a sinistral strike-slip fault. The current lineament study presents a different interpretation which is described below in Section 4.2.

## 2.2.5 Metamorphism

Studies on metamorphism in Precambrian rocks across the Canadian Shield have been summarized in a few publications since the 1970s (e.g., Fraser and Heywood 1978; Kraus and Menard, 1997; Menard and Gordon, 1997; Berman et al., 2000; Easton, 2000a and Easton, 2000b; and Berman et al., 2005) and the thermochronologic record for large parts of the Canadian Shield is documented in a number of studies (Berman et al., 2005; Bleeker and Hall, 2007; Corrigan et al., 2007; and Pease et al., 2008).

The Superior Province of the Canadian Shield largely preserves low pressure – high temperature Neoproterozoic (ca. 2.710-2.640 Ga) metamorphic rocks. The relative timing and grade of regional metamorphism in the Superior Province corresponds to the lithological composition of the subprovinces (Easton, 2000a; Percival et al., 2006). Subprovinces comprising volcano-sedimentary assemblages and synvolcanic to syntectonic plutons (i.e. granite-greenstone terranes) are affected by relatively early lower greenschist to amphibolite facies metamorphism. Subprovinces comprising both metasedimentary- and migmatite-dominated lithologies, such as the English River and Quetico, and dominantly plutonic and orthogneissic domains, such as the Winnipeg River, are affected by relatively late middle amphibolite to granulite facies metamorphism (Breaks and Bond, 1993; Corfu et al., 1995). Subgreenschist facies metamorphism in the Superior Province is restricted to limited areas, notably within the central Abitibi greenstone belt (e.g., Jolly, 1978; Powell et al., 1993).

A widespread Paleoproterozoic tectonothermal event, the Trans-Hudson Orogeny, involved volcanism, sedimentation, plutonism and deformation that affected the Churchill Province through northernmost Ontario, western Manitoba, northern Saskatchewan and Nunavut (e.g., Skulski et al., 2002; Berman et al., 2005). This event was associated with ca. 1.84 to 1.8 Ga collisional convergence of the Archean Hearne domain and Superior Province (Kraus and Menard, 1997; Menard and Gordon, 1997; Corrigan et al., 2007). Associated tectonometamorphism at moderate to high temperatures and low to moderate pressures resulted in amphibolite facies metamorphism that overprinted Archean metamorphic signatures in Archean rocks of the Churchill Province, and a complex brittle overprint in Archean rocks of the Superior Province (e.g., Kamineni et al., 1990).

Along the eastern flank of the Canadian Shield, the Grenville Province records a complex history of episodic deformation and subgreenschist to amphibolite and granulite facies metamorphism, from ca. 1.300 to 0.950 Ga (Easton, 2000b; Tollo et al., 2004 and references therein).

Lower greenschist metamorphism was documented along faults in the vicinity of Lake Nipigon and Lake Superior and is inferred to be the result of ca. 1.0 Ga far-field reactivation during the Grenville Orogeny (Manson and Halls, 1994).

In northwestern Ontario, the concurrent post-Archean effects, including the Trans-Hudson Orogen, are limited to poorly documented reactivation along faulted Archean terrane boundaries (e.g., Kamineni et al., 1990 and references therein). Most late orogenic shear zones in the Superior Province and Trans-Hudson Orogen experienced lower to middle greenschist retrograde metamorphism (e.g. Kamineni et al., 1990 and references therein).

Overall, most of the Canadian Shield preserves a complex episodic history of Neoproterozoic tectonometamorphism overprinted by Paleoproterozoic tectonothermal events culminating at the end of the Grenville orogeny ca. 0.950 Ga. The distribution of contrasting metamorphic domains in the Canadian Shield is a consequence of relative uplift, block rotation and erosion resulting from Neoproterozoic orogenesis, subsequent local Proterozoic orogenic events and broader epeirogeny during later Proterozoic and Phanerozoic eons.

In the Schreiber area, the metamorphic grade of exposed Archean rocks is upper greenschist facies (Williams et al., 1991). Locally, higher metamorphic grades up to upper amphibolite facies are recorded in rocks along the margins of plutons. No records exist that suggest that rocks in the Schreiber area may have been affected by thermotectonic overprints related to post-Archean events.

## 2.3 Geological and Structural History

Direct information on the geological and structural history of the Schreiber area is limited. The geological and structural history summarized below integrates the results from studies undertaken elsewhere throughout and proximal to the regional area shown in Figure 2, including structural investigations on the Hemlo gold deposit and surrounding region (i.e., the eastern portion of the Schreiber-Hemlo greenstone belt). It is understood that there are potential problems in applying a regional  $D_x$  numbering system into a local geological history. Nonetheless, the summary below represents an initial preliminary interpretation for the Schreiber area, which may be modified after site-specific information has been collected, if the community is selected by the NWMO and remains interested in continuing with the site selection process.

Regional studies revealed that the region has undergone complicated polyphase deformation but do not clarify the relationship between various structures and their significance for the regional tectonic evolution (Polat et al., 1998). Since the various structural studies were carried out on various scales and from different perspectives, disparate structural models and associated terminologies have developed for the Schreiber-Hemlo greenstone belt. In addition, because more than one generation of structures may develop in a single episode of progressive deformation, correlating the different structural studies is a challenge.

The most comprehensive structural study of the Schreiber-Hemlo greenstone belt was conducted by Muir (2003). Since no previous detailed structural studies have been undertaken in the Schreiber area, Muir's (2003) findings on the structural history are included in the summary below, and may be used as a "best-fit" for the structural history of the Schreiber area. The summary below integrates findings from Muir (2003) with information based on Carter (1988), Polat et al. (1998), Jackson (1998), Polat and Kerrich (1999) and Davis and Lin (2003).

Polat et al. (1998) interpreted that the Schreiber-Hemlo and surrounding greenstone belts represent collages of oceanic plateaus, oceanic arcs, and subduction-accretion complexes amalgamated through subsequent episodes of compressional and transpressional collision. On the basis of overprinting relationships between different structures, Polat et al. (1998) suggested that the Schreiber-Hemlo greenstone belt underwent at least two main episodes of deformation. These can both be correlated with observations from Muir (2003), who reported at least six generations of structural elements. Muir (2003) is therefore considered the better study to be used as a "best-fit" for the Schreiber area. Two of the six generations of structures account for most of the ductile strain, and although others can be distinguished on the basis of crosscutting relationships, they are likely the products of progressive strain events. The main characteristics of these deformation phases are described below.

The earliest deformation phase ( $D_1$ ) is associated with the development of  $S_1$  slaty cleavage and asymmetric boudins in metasedimentary rocks, and asymmetric boudins, mesoscopic closed to isoclinal (overturned)  $F_1$  folds and associated  $D_1$  thrust faults in the metavolcanic rocks. Muir (2003) included the development of  $S_1$  compositional layering as part of this deformation event. The orientation of  $F_1$  folds was modified during subsequent deformation; however, the regionally consistent asymmetry of the  $F_1$

overturned folds, combined with S-C fabrics along ductile D<sub>1</sub> thrust faults, suggests a south-southeast tectonic vergence. Muir (2003) suggested that D<sub>1</sub> likely occurred from ca. 2.719 to ca. 2.691 Ga.

D<sub>2</sub> deformation structures (D<sub>1</sub> in Jackson et al., 1998) are ubiquitous in the Schreiber-Hemlo greenstone belt and include dominantly east-northeast trending overturned tight to isoclinal F<sub>2</sub> folds, D<sub>2</sub> thrust faults, and northeast- to east-trending D<sub>2</sub> strike-slip faults (collectively forming D<sub>2</sub> fold and thrust duplexes) that overprint or fold D<sub>1</sub> structural elements. During D<sub>2</sub> deformation, the dominantly steeply northward dipping S<sub>2</sub> foliation was developed. The S<sub>2</sub> foliation is characterized by a preferred alignment of phyllosilicate and mafic minerals and flattening and (or) elongation of clasts (Davis and Lin, 2003; Muir, 2003). Several kilometre-scale F<sub>2</sub> folds, with dominant S-shaped asymmetry developed during D<sub>2</sub> deformation (Muir, 2003). Whereas Polat et al. (1998) interpreted that D<sub>2</sub> developed during dextral transpression, Lin (2001) interpreted D<sub>2</sub> deformation as an episode of sinistral transpression based on local observations from the Hemlo shear zone. Muir (2003) suggested that D<sub>2</sub> likely initiated at ca. 2.691 Ga and continued until ca. 2.683 Ga.

Lin (2001) further distinguished open to tight folds with a well-developed axial planar cleavage associated with north over south compression with a dextral strike-slip component. It is not clear whether these structures represent a separate deformation event. If D<sub>2</sub> deformation represents a stage of dextral transpression, as interpreted by Polat et al. (1998), these structures can be interpreted to result from the prolongation of D<sub>2</sub> deformation. However, if D<sub>2</sub> represents a stage of sinistral transpression, it follows that these structures must be related to a separate D<sub>3</sub> deformation phase.

Based on observations in the vicinity of the Hemlo gold deposit, Muir (2003) distinguished a variably developed S<sub>3</sub> mineral and (or) crenulation foliation associated with F<sub>3</sub> folds, which overprint D<sub>2</sub> structural elements. Muir (2003) noted that these features are particularly well-developed within schistose units. Local D<sub>3</sub> S-C shear fabrics and extensional shear bands record a dextral sense of shear, which conforms to their development during dextral transpression as interpreted by Lin (2001). Muir (2003) interpreted that a period of near peak metamorphic temperatures overlapped with the D<sub>2</sub>-D<sub>3</sub> transition from ca. 2.688 to ca. 2.675 Ga.

Again, founded on observations in the vicinity of the Hemlo gold deposit, Lin (2001) and Muir (2003) recognized D<sub>4</sub> structural elements, including F<sub>4</sub> kink folds and various sets of D<sub>4</sub> fractures and small-scale faults. Muir (2003) interpreted that the orientation of conjugate sets of D<sub>4</sub> contractional kink bands is consistent with their development during northwest- to west-northwest-directed shortening. Northwest-directed D<sub>3</sub>-D<sub>4</sub> shortening is estimated to have occurred from ca. 2.682 to ca. 2.679 Ga (Muir, 2003).

Based on this summary, it may be surmised that a protracted period of brittle-ductile deformation spanning D<sub>1</sub> to D<sub>4</sub> comprising elements of compression and sinistral and dextral transpression occurred between ca. 2.719 and ca. 2.679 Ga. It should be noted that this age range partly overlaps with the inferred ages for granitoid intrusions (ca. 2.690 to ca. 2.680 Ga) which suggests that these intrusions may have been affected by D<sub>2</sub>-D<sub>4</sub> deformation.

Lin (2001) highlighted the presence of post-D<sub>4</sub> brittle faults at various scales and with various orientations in the Schreiber-Hemlo greenstone belt. One set of post-D<sub>4</sub> brittle faults is parallel to the S<sub>2</sub> foliation, contains cataclasite, fault breccia and local pseudotachylite and commonly offsets Proterozoic diabase dykes. Another post-D<sub>4</sub> brittle fault set strikes southeast and displays a consistent dextral sense of shear. Other than that these faults post-date the intrusion of Proterozoic diabase dykes, no estimates for the timing of this post-D<sub>4</sub> brittle deformation are present in literature. Peterman and Day (1989) recorded reactivation of the Late Archean Quetico and Rainy Lake-Seine River faults at ca. 1.943 Ga in the Rainy Lake region of Minnesota and Ontario. It is possible that at least one stage of D<sub>4</sub> faulting

occurred during this regional tectonic event, which coincides with the ca. 2.100 to 1.860 Ga Penokean Orogen.

No neotectonic structural features are known to occur within the Schreiber area. Neotectonics refers to deformation, stress and displacements in the earth's crust of recent age or which are still occurring. The Schreiber area lies within the Superior Province of the Canadian Shield where large parts have remained tectonically stable for the last 1.9 billion years (Percival and Easton, 2007; Peterman and Day, 1989). Although Hayek et al. (2009) indicated that the general western Superior Province has experienced a number of small magnitude seismic events, all recorded earthquakes in the Schreiber area are of a magnitude less than 3.

The geological and structural history of the Schreiber area is summarized in Table 1.

**Table 1: Summary of the Geological and Structural History of the Schreiber Area (adapted from AECOM, 2013a).**

<b>Time period (years before present)</b>	<b>Geological Event</b>
ca. 3.0 to 2.770 Ga	Progressive growth of the Wawa-Abitibi terrane by accretion of oceanic plateau sequences; volcanic island arc sequences; and arc-derived, synkinematic siliciclastic trench turbidites collages along a south-southeast-facing convergent plate margin through compressional and transpressional collisions (Polat et al., 1998).
ca. 2.770 to 2.678 Ga	An extended period of volcanism and sedimentation associated with the formation of the Schreiber-Hemlo greenstone belt. <ul style="list-style-type: none"> <li>- ca. 2.770 Ga: Formation of the Hemlo-Black River Assemblage (Williams et al., 1991);</li> <li>- ca. 2.700 Ga: Formation of the Heron Bay Assemblage (Williams et al., 1991);</li> <li>- ca. 2.697 to ca. 2.688: Mafic, calc-alkalic and felsic volcanism (Corfu and Muir, 1989; Muir, 2003);</li> <li>- ca. 2.693 to ca. 2.685: Deposition of clastic and chemical sedimentary rocks (Muir, 2003);</li> <li>- ca.2690-2680: Inferred emplacement of granitoid intrusions in the Schreiber area (Smyk and Schnieders, 1995; Corfu and Muir, 1989).</li> </ul> <p>During the formation of the greenstone belt, four periods of ductile-brittle deformation (D<sub>1</sub>-D<sub>4</sub>) are recognized as occurring between ca. 2.719 and 2.679 Ga (Muir, 2003)</p>
ca. 2.690 to 2.684 Ga	Coalescence of the Wawa and Quetico subprovinces (Corfu and Stott, 1996)
ca. 2.688 to 2.675 Ga	Regional metamorphism (Muir, 2003)
ca. 2.688 to 2.675 Ga	Emplacement of granitoid intrusions including the Terrace Bay, Crossman Lake and Whitesand Lake batholiths, and the Mount Gwynne pluton (Santaguida, 2002).
ca. 2.473 Ga	Emplacement of northwest-trending Matachewan Suite of dykes (Buchan and Ernst, 2004)
ca. 2.400 to 2.200 Ga	Development of the Southern Province; possible deposition and subsequent erosion of sedimentary rocks in the Schreiber area (Young et al., 2001)
ca. 2.167 Ga	Possible emplacement of the northeast trending Biscotasing dyke swarm (Hamilton et al., 2002). These dykes cannot be separated with confidence from the Marathon dykes



**Table 1: Summary of the Geological and Structural History of the Schreiber Area (adapted from AECOM, 2013a).**

<b>Time period (years before present)</b>	<b>Geological Event</b>
ca. 2.121 Ga	Emplacement of north-trending Marathon Suite of dykes (Hamilton et al., 2002; Buchan et al., 1996)
ca. 2.100 to 1.860 Ga	Penokean Orogen; deposition of the Animikie Group sediment rocks to the west. Possible deposition and subsequent erosion in the Schreiber area (Sutcliffe, 1991; Fralick et al., 2002)
ca. 1.540 Ga	Possible deposition and subsequent erosion of Mesoproterozoic Sibley Group clastic sedimentary rocks (Sutcliffe, 1991)
ca. 1.150 to 1.090 Ga	Formation of the Midcontinent Rift that resulted in the deposition of volcanic rocks and minor sedimentary units. Emplacement of west-trending Keweenaw Suite of dykes related to mid-continental rifting that was centred on proto-Lake Superior (Sutcliffe, 1991; Thurston, 1991)
ca. 1.100 to 1.086 Ga	Deposition of the Osler Group (Sutcliffe, 1991)
ca. 540 to 355 Ma	Possible coverage of the area by marine seas and deposition of carbonate and clastic rocks subsequently removed by erosion (Johnson et al., 1992)
ca. 145 to 65 Ma	Possible deposition of marine and terrestrial sediments of Cretaceous age subsequently removed by erosion
ca. 2.6 to 0.01 Ma	Periods of glaciation and deposition of glacial sediments (Barnett, 1992)

## 2.4 Quaternary Geology

Quaternary geology in the Schreiber area is described in detail in AECOM (2013b). A summary of the main features is provided here for reference.

The Schreiber area is within the Abitibi Uplands physiographic region of Thurston (1991) who subdivided the extensive James Region physiographic region of Bostock (1970). The region is characterized by abundant bedrock outcrop with shallow drift cover and a rugged surface.

The Quaternary sediments, commonly referred to as drift, soil or overburden, are glacial and post-glacial materials which overlie the bedrock in the Schreiber area. The distribution, thickness and physical characteristics of these deposits have an important influence on several aspects of the current investigation. Areas of thicker drift can hinder the interpretation of lineaments by masking their presence or muting the response obtained from geophysical surveys. Coarser-grained surficial sediments typically have a moderate to high transmissivity and can serve as local aquifers as well as being a potential source of mineral aggregates for use in building and road construction.

All glacial landforms and related materials within the Schreiber area are associated with the Wisconsinan glaciation which began approximately 115 Ka before present (BP) (Barnett, 1992). The Quaternary (i.e., surficial) geology of the Schreiber area has been mapped at a regional scale (>1:100,000) by several authors, including Zoltai (1965), Sado and Carswell (1987), and Barnett et al. (1991) and at a higher resolution by Gartner (1979a, 1979b) and Morris (2000, 2001). Quaternary deposits and landforms in the area are thought to have formed during the latter stages of ice cover (i.e., during the Late Wisconsinan, which began 30 Ka BP).

Morris (2000) reports bedrock erosional features (e.g., striae, roche moutonnée) and landforms that indicate a regional ice flow direction of 194° with a range of measured directions, due to local topographic conditions, of between 165° to 238°. For the majority of the Schreiber area drift thickness over bedrock is limited and the ground surface reflects the bedrock topography. Over the majority of the area bedrock outcrops are common and the terrain is classified, for surficial purposes, as a bedrock-drift complex; i.e., thin drift cover that only locally achieves thicknesses that mask or subdue the bedrock topography.

The remote sensing and terrain evaluation completed as part of the Phase 1 study provides the most detailed assessment of the type, distribution and thickness of surficial deposits in the Schreiber area (AECOM, 2013b; Figure 4). The most common glacial deposit in the Schreiber area is a thin, discontinuous till, generally less than two to three metres thick. Greater accumulations of till are found within bedrock depressions, large scale lineaments and on the down-ice (lee) side of bedrock highs. The till has a silty-sand matrix and contains abundant clasts in the pebble to cobble size range.

Two types of glaciofluvial deposits are present in the Schreiber area: ice-contact stratified drift deposits (ICSD) and outwash deposits. The ICSDs are associated with recessional moraines, dead-ice topography, eskers and valley fills (Morris, 2000). The largest ice-contact deposit forms the core of a 9 kilometre long feature situated between Terrace Bay and Schreiber, south of Hays Lake. The ICSDs consist primarily of stratified, well to poorly sorted, sand and gravel that locally can achieve thicknesses of several tens of metres.

Glaciofluvial outwash deposits occur as relatively level areas within some narrow, bedrock controlled valleys (Figures 3). While valley controlled outwash deposits are found within the Schreiber area, significant deposits are also located along the Aguasabon, Whitesand and Pays Plat rivers, and Big Creek (which drains Clean and Deep lakes) and its tributaries. The thicknesses of these deposits are likely to be variable, and may be locally substantial. Outwash deposits are generally well-sorted and comprised of stratified sand, gravel and, locally, boulders.

Following retreat of the glacial ice approximately 9.5 Ka BP, the Lake Superior basin was occupied by a series of glacial lakes. It is likely that only the later of these lakes, Glacial Lake Minong and younger, affected the Schreiber area (Farrand and Drexler 1985; Barnett 1992). Lake inundation was limited to the area along the Lake Superior shoreline, to an elevation of ~305 m, and for a short distance inland within bedrock controlled valleys. Elevations of the various glacial lakes were controlled by the position of the ice mass and isostatic recovery of the land surface following deglaciation.

Fine-grained glaciolacustrine silts and clay deposits associated with the glacial lake have been encountered at depth in boreholes in the Terrace Bay area and other embayments further west along the Lake Superior shoreline (Gartner, 1979a). Overlaying these deposits are coarse-grained glaciolacustrine sediments that were deposited in a deltaic environment where bedrock valleys served as drainage channels discharging to the glacial lake. The largest glaciolacustrine delta is located in the Terrace Bay area where a sediment thickness of 48.3 m has been recorded. Another notable but smaller deltaic feature is found at Selim, at the mouth of the Whitesand River (Figure 4).

Bogs and organic-rich alluvial deposits are present along water courses in the area and in rock floored basins. These deposits tend to have a limited thickness, as determined by regional studies, and areal extent.

In summary, the extent and thickness of surficial deposits in the Schreiber area is limited, and SRK believes that it does not significantly influence the lineament interpretation. A correlation is present between the Aguasabon River and its floodplains only in the electromagnetic data. In part, the flow of

the river follows observed regional lineaments, and, therefore, this is not considered as a major impediment to lineament interpretation.

## 2.5 Land Use

Land use in the Schreiber area is described in detail in AECOM (2013b). The vast majority of the Schreiber area is undeveloped Crown Land with residences almost exclusively within the build-up areas of Terrace Bay and Schreiber or in close proximity to the Highway 17, the Trans Canada Highway. Infrastructure to support the population, in the form of roads, power and rail lines, etc., is largely concentrated within 5 kilometres of the Lake Superior shore. Mineral exploration is active in the area and numerous active mining claims are held by prospectors and mining companies (Campbell et al., 2012; MNDM, 2012a). The bulk of the claims are located over the two arms of the Schreiber-Hemlo greenstone belt and the immediate surrounding land. A number of aggregate operations are extracting sand and gravel in the area (MNR, 2012b). The majority of the pits are located close to the Trans Canada Highway in the vicinity of Terrace Bay and Schreiber. A small number of pits are located near Selim.

These features do not negatively impact the interpretation of bedrock lineaments.

## 3 Methodology

### 3.1 Source Data Descriptions

The lineament interpretation of the Schreiber area was based on publicly available remote sensing data sets, including airborne geophysical (aeromagnetic and electromagnetic), topographic (CDED elevation models), and satellite imagery data (SPOT and Landsat). A previous lineament interpretation was carried out by the Ontario Geological Survey on the basis of DEM data (Shirota and Barnett, 2004). This interpretation is not considered during the current study as the detail of the current study goes over and beyond the previous interpretation undertaken.

Available data were assessed for quality, processed and reviewed before use in the lineament interpretation. The geophysical data were used to evaluate deeper bedrock structures and proved invaluable to identify potential bedrock structures beneath areas of surficial cover and to aid in establishing the age relationships among the different lineament sets. Topography (CDED) and satellite imagery (SPOT and Landsat) data sets were used to identify surficial lineaments expressed in the topography, drainage, and vegetation. On the basis of comparative visibility of lineaments between data sets, it was determined that Landsat was the preferred satellite data set. Comparing surficial lineaments to aeromagnetic lineaments allows for the comparison of subsurface and surficial expressions of the bedrock structure. Throughout this study, the best resolution data available was used for the lineament interpretation.

Table 2 provides a summary of the source data sets, including their resolution, coverage and acquisition dates that were used for the lineament interpretation. All geophysical surveys listed were acquired from north-south oriented survey flight lines.

The lineament interpretation was built in two-dimensions in ArcGIS™ in UTM NAD83, Zone 16 North. Each data set used in the interpretation required manipulation in ErMapper™, including creating

ErMapper .ECW compressed raster images (mostly colour mosaics) as end products for each data set prior to import into ArcGIS.

**Table 2: Summary of Source Data Information for the Lineament Interpretation, Schreiber area**

Data Set	Product	Source	Resolution	Coverage	Acquired
<b>Geophysics</b>	Single master gravity and aeromagnetic data for Ontario (SMGA; GDS 1036)	Ontario Geological Survey	805 m line spacing; Sensor height 305 m	Entire Schreiber area	1962 (reprocessed in 1999)
	Schreiber magnetic and electromagnetic supergrid (GDS1104)	Ontario Geological Survey	200 m line spacing; Sensor height 30 m (EM) 30 - 45 m (mag)	Covers 837 km <sup>2</sup> of Schreiber area (excluding a narrow ~4 km wide strip along the western margin)	1999
	Schreiber aeromagnetic survey data (GSC2514)	Ontario Geological Survey	1000 m line spacing; Sensor height 120 m	Entire Schreiber area	1991
<b>DEM</b>	Canadian Digital Elevation Data (CDED); 1:50,000 scale	Geobase	8-23 m (0.75 arc seconds) depending on latitude	Entire Schreiber area	1995 (published in 2003)
<b>Satellite Imagery</b>	SPOT 5; Orthoimage, multispectral/panchromatic	Geobase	20 m (multispectral)	Entire Schreiber area	2009
	Landsat 7 orthorectified imagery	Geobase	30 m (multispectral)	Entire Schreiber area	2000
	Landsat 7 orthoimages of Canada	Geogratias	15 m (multispectral)	Entire Schreiber area	2006 (west) 2007 (east)

### 3.1.1 Geophysical Data

MIRA Geoscience identified and evaluated all available geophysical data sets for the Schreiber area (Mira, 2013). This evaluation highlighted the presence of a high-resolution geophysical data set, the Schreiber Magnetic Supergrid aeromagnetic data set that covers 837 km<sup>2</sup> of the area, excluding a narrow strip of approximately three kilometres wide on the western edge of the Schreiber area. In the area covered by this high-resolution data set, it is considered that other available data sets with lower resolution were not favorable for the use in the lineament investigation. The Schreiber Magnetic Supergrid (Ontario Geological Survey, 2003; GDS1104) includes measured vertical gradient (thscmvg83.grd), second vertical derivative (thsc2vdsup83.grd), levelled total magnetic field (thscmaggsc83.grd) and apparent resistivity from low, mid and high frequency electromagnetic data (thscreslow / thscresmid / thscreshigh83.grd) grids with a 40-metre grid cell size.

The magnetic data located within the Schreiber area were processed using several common geophysical techniques in order to enhance the magnetic response to assist with the interpretation of geophysical lineaments. The enhanced magnetic grids used in the lineament interpretation include the first and second vertical derivatives, and the tilt angle derivative. These enhanced grids were processed and imaged using WinDisp in the GOCAD Mira Mining Suite software package. Acquisition parameters, processing methods and enhanced grids associated with the geophysical datasets used in the lineament interpretation are discussed in detail in Mira (2013). The combination of all of the enhanced magnetic grids provide much improved resolution of subtle magnetic fabrics and boundaries in areas that appear featureless in the total magnetic field.

For the narrow strip of approximately three kilometres width on the western side of the Schreiber area, other geophysical data were available and evaluated (Mira, 2013). These data sets include the Single Master Gravity and Aeromagnetic Data for Ontario (SMGA; Ontario Geological Survey, 1999; GDS 1036) and the Schreiber Aeromagnetic Survey Data (GSC2514). Source data information for these two data sets is included in Table 2. Both data sets cover the entire Schreiber area. For the lineament investigation, SRK was provided with gridded data for total magnetic field and first vertical derivative filters, both reduced to the pole by MIRA Geoscience (Mira, 2013). Compressed raster images were created from the vertical magnetic gradient grid, including a colour-draped and shaded image. Figure 5 shows the first vertical derivative of combined aeromagnetic data for the Schreiber area.

A frequency domain electromagnetic survey was also collected from the Schreiber Supergrid area survey carried out by the Ontario Geological Survey (2003, GDS1104). MIRA Geoscience provided grids for three different frequencies (877 Hz, 4891 Hz and 33840 Hz) for the electromagnetic data. From these gridded data, SRK created compressed raster images for each frequency applying a colour-drape to enhance the image contrast. Figure 6 shows the low frequency electromagnetic data for the Schreiber area.

The resolution of each available data set has a strong impact on the resolution and number of interpreted lineaments. The SMGA data cover the entire Schreiber area, but have the lowest resolution of all data sets used in the interpretation (805 metre line spacing; 200-metre grid cells). The Schreiber Magnetic Supergrid data set has the highest resolution (200 metre line spacing; 40-metre grid cells) and covers most of the area (Figure 5).

A summary of survey acquisition parameters for the geophysical surveys used during the lineament study is provided in Table 3.

**Table 3: Summary of Geophysical Survey Acquisition Parameters for the Lineament interpretation**

Survey	Flight Line Spacing (m)	Grid Cell Size (m)	Sensor Height (m)	Flight Line Azimuth (0-359°)
Single Master Gravity and Aeromagnetic data for Ontario (SMGA; GDS1036)	805	200	305	0°
Schreiber Magnetic and Electromagnetic Supergrid (GDS1104)	200	40	30-45	0°
Schreiber Aeromagnetic Survey data (GSC2514)	1000	200	120	0°

### 3.1.2 Surficial Data

#### *Canadian Digital Elevation Data (CDED)*

CDED served as an important data source for analyzing and interpreting lineaments in the Schreiber area. The digital elevation model (DEM) used for this study was constructed by the Ontario Ministry of Natural Resources (MNR). The source data were acquired through the Ontario Base Mapping program, which was a major photometric program conducted across Ontario between 1978 and 1995. Four main data sets were used: contours, spot heights, stream networks, and lake elevations derived using spot heights and water features. CDED data sets are provided in geographic coordinates, referenced horizontally using North American Datum 1983 (NAD83) and vertically based on the Canadian Geodetic Vertical Datum 1928 (CGVD28). Ground elevations are recorded in metres relative to mean

sea level. It was determined that the resolution of the DEM data set was sufficient to undertake the lineament interpretation.

The CDED topography data for the Schreiber area is available in six USGS DEM format individual tiles, each tile covering approximately 600 km<sup>2</sup>, covering the entire area, including an area to the west of the Schreiber area. The tiles that cover the area have the following identifiers: 042e04\_0100\_deme; 042e03\_0100\_demw; 042e03\_0100\_deme; 042d13\_0100\_deme; 042d14\_0100\_demw; and 042d14\_0100\_deme. These files are accurate to within five metres and a resolution of 0.75 arc seconds (Table 4), which is equivalent to approximately 16 to 23 metres in the Schreiber area. The six individual tiles were merged, levelled, and a colour mosaic, shaded digital elevation model was created in ErMapper and saved as a compressed raster image. The DEM for the Schreiber area is shown in Figure 7.

**Table 4: Summary of 1:50,000 scale CDED tiles used for Lineament interpretation**

NTS Tiles	East/West Coverage	Ground Resolution (arc sec.)
042d/ 14	Both	0.75
042d/ 13	East	0.75
042e/ 04	Both	0.75
042e/ 03	East	0.75

*Systeme Pour l'Observation de la Terre (SPOT) and Landsat Imagery*

SPOT multispectral and panchromatic orthoimagery were used for identifying surficial lineaments and exposed bedrock within the Schreiber area. SPOT multispectral data consist of several bands, each band recording the reflected radiation within a particular spectral range, displayed with a radiometry of 8-bits (or a value ranging from 0 to 255). SPOT 5 images were acquired using the High Resolution Geometric (HRG) sensor. Each image covers an area of approximately 3,600 km<sup>2</sup>.

For quality control, Natural Resources Canada (NRCan) provides images that have a maximum of 5% snow and ice cover, 5% cloud cover and a maximum viewing angle of 15°. NRCan orthorectified the SPOT images using three data sources: 1:50,000 scale Canadian Digital Elevation Data (CDED), National Road Network (NRN), and Landsat 7 orthoimagery. The orthoimages are provided in GeoTIFF format, projected using Universal Transverse Mercator (UTM) projection referenced to the North American Datum 1983 (NAD83).

The SPOT 5 Geobase OrthoImage for the Schreiber area is available as one individual tile (Table 5), containing four Geotiff images representing spectral bands B1, B2, B3, and MIR. A false natural colour was created for this tile in ErMapper and saved as a compressed raster image.

**Table 5: Summary of SPOT imagery scenes used for the Lineament interpretation**

Scene ID	Image Center (Lat/Long)	Satellite	Date of Image
S5_08722_4857_20050706	48°57', -87°22'	SPOT 5	6-July-2005

The Landsat 7 Orthorectified Image for the Schreiber area is available as one individual tile from the Canadian Council of Geomatics (<http://www.geobase.ca>; Table 6), already with bands 7, 4, and 3 combined; with each tile approximately 33,400 km<sup>2</sup> in area. A false natural colour image (Landsat bands 4, 3 and 2) and short-wave infrared (SWIR; Landsat bands 7, 4 and 2) image were created for this tile in ErMapper and saved as a compressed raster images. Higher resolution Landsat 7 imagery was obtained as .Geotiff files from the Geogratis website (<http://geogratis.cgdi.gc.ca/>) and used as the main reference for lineament interpretation from satellite imagery (Figure 8). Figure 8 is an example of a colour

composite of the Landsat imagery that was created by assigning a primary colour (red, green and blue) to three of the spectral bands (bands 3, 2, 1). Different materials reflect and absorb solar radiation differently at different wavelengths and therefore have varying intensities within each of the Landsat bands. When combined into a single image, the colour assignment results in a pixel colour that tends to approach a “natural” representation. Image processing and different colour assignments can be used to enhance the presence of different material categories, such as vegetation type, water, soil or man-made features.

**Table 6: Summary of Landsat 7 imagery scenes used for the Lineament interpretation**

<b>Scene ID</b>	<b>Date of Image</b>
024026_0100_000729_17	29-Jul-2000

The SPOT satellite, Landsat satellite, and CDED topography data cover the entire Schreiber area with a good resolution (e.g., SPOT, 20-metre resolution). However, the bedrock structural information available from these three data sets is limited in the southeast portion of the area, near the town of Terrace Bay. In this area, Quaternary cover reduces the expression of bedrock structural information in the satellite imagery and topography data (Figure 4). This limits the use of satellite imagery and topography data to identify bedrock lineaments in this area. The area of Quaternary cover where the satellite (SPOT and Landsat) and CDED topography data were of limited use is approximately 65 km<sup>2</sup> (Figure 4). However, this area is covered by the higher resolution Schreiber Magnetic Supergrid, which allowed for the interpretation of reliable bedrock structural information from at least two data sets (magnetic and electromagnetic data). Ductile features (Figure 9) were only interpreted using the high resolution Schreiber Magnetic Supergrid (Figure 5).

## 3.2 Lineament Interpretation Workflow

Lineaments were interpreted using a workflow designed to address issues of subjectivity and reproducibility that are inherent to any lineament interpretation. The workflow follows a set of detailed guidelines using the publicly available surficial (DEM, SPOT) and geophysical (aeromagnetic and electromagnetic) data sets described above. The interpretation guidelines involved three steps:

- Step 1: Independent lineament interpretation by individual interpreters for each data set and assignment of certainty level (1, 2 or 3);
- Step 2: Integration of lineament interpretations for each individual data set and determination of reproducibility (Figures 10, 11, 12 and 13) and first determination of reproducibility (RA\_1); and
- Step 3: Integration of lineament interpretations for all data sets (Figure 14) and determination of coincidence (RA\_2).

Each identified lineament feature was classified in an attribute table in ArcGIS. The description of the attribute fields used is included in Table 7. Fields 1 to 9 are populated during Step 1. Fields 10 and 11 are populated during Step 2. Fields 12 to 19 are populated during Step 3, the final step. In addition, ductile geophysical lineaments (Figure 9) were interpreted using the aeromagnetic geophysical survey data by two specialist observers.

A detailed description of the three workflow steps is provided below; this includes the methodology for populating the associated attribute field for each interpreted lineament.

**Table 7: Summary of Attribute Table Fields Populated for the Lineament Interpretation**

ID	Attribute	Brief Description
1	Rev_ID	Reviewer initials
2	Feat_ID	Feature identifier
3	Data_typ	Data set used (MAG, EM, CDED, SPOT, LSAT)
<b>Type of feature used to identify each lineament</b>		
<b>Satellite Imagery:</b>		
		A. Lineaments drawn along straight or curved lake shorelines;
		B. Lineaments drawn along straight or curved changes in intensity or texture (i.e., vegetation);
		C. Lineaments drawn down centre of thin rivers or streams;
		D. Lineaments drawn along a linear chain of lakes; or
		E. Other (if other, define in comments).
4	Feat_typ	<b>Digital Elevation Model:</b>
		A. Lineaments drawn along straight or curved topographic valleys;
		B. Lineaments drawn along straight or curved slope walls; or
		C. Other (if other, define in comments).
		<b>Airborne Geophysics (magnetic and electromagnetic data):</b>
		A. Lineaments drawn along straight or curved magnetic high;
		B. Lineaments drawn along straight or curved magnetic low;
		C. Lineaments drawn along straight or curved steep gradient; or
		D. Other (if other, define in comments).
5	Name	Name of feature (if known)
6	Certain	Value describing the interpreters confidence in the feature being related to bedrock structure (1-low, 2-medium or 3-high)
7	Length*	Length of feature is the sum of individual lengths of mapped polylines (not end to end) and is expressed in kilometers
<b>Width of feature; This assessment is categorized into 5 bin classes:</b>		
8	Width**	A. < 100 m B. 100 – 250 m C. 250 – 500 m D. 500 – 1,000 m E. > 1,000 m
9	Azimuth	lineament orientation expressed as degree rotation between 0 and 180 degrees
10	Buffer_RA_1	Buffer zone width for first reproducibility assessment
11	RA_1	Feature value (1 or 2) based on first reproducibility assessment
12	Buffer_RA_2	Buffer zone width for second reproducibility assessment
13	RA_2	Feature value (1, 2, 3 or 4) based on second reproducibility assessment (i.e. coincidence)
14	MAG	Feature identified in geophysical data set (Yes or No)
15	EM	Feature identified in electromagnetic data set (Yes or No)
16	CDED	Feature identified in topography data set (Yes or No)
17	SAT	Feature identified in satellite data set (Yes or No)
18	F_Width	Final interpretation of the width of feature
19	Rel_age	Relative age of feature, in accord with regional structural history
20	Notes	Comment field for additional relevant information on a feature
21	Object	Geological element identified, e.g., dyke, fault, joint, contact

\*The length of each interpreted feature is calculated based on the sum of all segment lengths that make up that lineament.

\*\*The width of each interpreted feature is determined by expert judgement and utilization of a GIS-based measurement tool. Width determination takes into account the nature of the feature as assigned in the Feature type (Feat\_typ) attribute.



### 3.2.1 Step 1: Lineament Interpretation and Certainty Level

To accommodate the generation of the best possible, unbiased lineament interpretation, two individual interpreters followed an identical process for structural lineament analysis during Step 1. The first step of the lineament interpretation was to have each individual interpreter independently produce GIS lineament maps, and detailed attribute tables, for each of the four data sets. The following components were addressed in the order specified:

- **Magnetic Data**
  - Throughout the interpretation of magnetic data sets, priority was given to the highest resolution data set available (Figure 5). In general, for this study, this was the Schreiber Magnetic Supergrid data set. Other available magnetic data were only used where the Schreiber area was not covered by this data set. The interpretation of magnetic data included two steps:
- **Interpretation of Ductile Lineaments**
  - Drawing of stratigraphic and structural form lines using first vertical derivative magnetic data (Figure 9). The form lines trace the geometry of magnetic high lineaments and represent the geometry of stratigraphy within metavolcanic and metasedimentary rocks or the internal fabric (foliation) within granitoid batholiths and gneissic rocks. This process highlighted discontinuities between form lines, particularly in stratigraphic form lines (e.g., intersecting form lines) that represent structural lineaments (e.g., faults, folds, unconformities, or intrusive contacts).
  - For this study, form lines were drawn using the Schreiber Magnetic Supergrid first vertical derivative and the tilt derivative data. Where the Schreiber area was not covered by the Schreiber Magnetic Supergrid, no form lines were drawn, and lineaments representing magnetic minima and (or) maxima were interpreted directly from magnetic data with a coarser resolution (see below).
- **Interpretation of Structural Lineaments**
  - This part of the interpretation involved the drawing of lineaments, representing all interpreted faults regardless of interpreted age, style (e.g., brittle versus ductile) or kinematics. Evidence for interpreted brittle lineaments was derived from several sources in the magnetic data, including discontinuities between form lines (as outlined above), offset of magnetic units, or the presence of linear magnetic lows. Lineaments were drawn using the Schreiber Magnetic Supergrid first vertical derivative image, with the tilt derivative image for validation and enhancement. Where the Schreiber area was not covered by the Schreiber Magnetic Supergrid, the first vertical derivative SMGA and Schreiber Aeromagnetic data (GSC2514) were used.
- **Electromagnetic Data**
  - In the Schreiber area, electromagnetic data are only available from the Schreiber Magnetic Supergrid data. Lineaments were drawn on coloured images of electromagnetic data along discontinuities and linear zones of low resistivity that could be observed in the data.
- **Topography Data**
  - The lineament interpretation of topography data involved the drawing of lineaments along topographic valleys, slope walls or escarpments, drainage patterns and abrupt changes in topography that were visible in a colour mosaic constructed from the CDED topography data.

- Satellite Imagery
  - The lineament interpretation of satellite imagery involved the drawing of lineaments along linear features including changes in bedrock colour (changing lithology), vegetation cover, and drainage patterns, such as rivers and streams and linear chains of lakes that were visible in Landsat and SPOT satellite image data.

All lineaments were drawn up to a maximum of ten kilometers outside the Schreiber area boundary, to express their full extent, or in the case of longer lineaments, to better estimate their maximum length within a buffer around the Schreiber area. Lineaments displayed on maps are truncated at the boundary of the margins of the Schreiber area; however, the full length of the lineaments was included in the attribute table (Length; Table 7).

The higher resolution of the topography and satellite imagery data sets helped identify a greater density of smaller scale lineaments that were not evident in the lower resolution Schreiber Magnetic Supergrid (GDS1104), Schreiber Aeromagnetic Survey data (GSC2514) and SMGA Aeromagnetic data (GDS1036).

This Step 1 lineament analysis resulted in the generation of one interpretation for each data set (magnetic, electromagnetic, satellite imagery (SPOT and Landsat) and topography (CDED) for each interpreter, resulting in a total of eight individual GIS layer-based interpretations. Within these data sets, crosscutting relationships between individual lineaments were assessed. Following this assessment, based on the expert judgment of each interpreter, lineament segments were merged, resulting in lineament length corresponding to the sum of all parts.

During Step 1, identified lineaments were attributed with fields one to nine as listed in Table 7. For attribute field six, each interpreter assigned a certainty/uncertainty descriptor (attribute field 'Certain' = 1-low, 2-medium or 3-high) to each lineament feature in their interpretation based on their judgment concerning the clarity of the lineament within the data set. Where a surface lineament could be clearly seen on exposed bedrock, it was assigned a certainty value of 3. Where a lineament represented a bedrock feature that was inferred from linear features, such as orientation of lakes or streams or linear trends in texture, it was assigned a certainty value of either 1 or 2. For geophysical lineaments, a certainty value of 3 was assigned when a clear magnetic susceptibility contrast could be discerned and a certainty value of either 1 or 2 was assigned when the signal was discontinuous or more diffuse in nature. The certainty classification for all three data sets ultimately came down to expert judgment and experience of the interpreter.

In the determination of attribute field nine, SRK used ET<sup>TM</sup> EasyCalculate 10, an add-in extension to ArcGIS. This add-in provides a function (polyline\_GetAzimuth.cal) that calculates the azimuth of each polyline at a user-specified point and populates an assigned attribute field. SRK used the mid-point of each interpreted lineament to calculate the azimuth.

It is understood that some of the lineament attributes (e.g. width and relative age) will be further refined as more detailed information becomes available in subsequent stages of characterization, should the community be selected by the NWMO and remain interested in advancing in the site selection process.

### **3.2.2 Step 2: Reproducibility Assessment 1 (RA\_1)**

During Step 2, individual lineament interpretations produced by each interpreter were compared for each data set (Figures 10, 11, 12 and 13). This included a reproducibility assessment (RA\_1) based on the coincidence, or lack thereof, of interpreted lineaments within a data set-specific buffer zone. For example, if a lineament was identified by both interpreters within an overlapping buffer zone, then it

was deemed coincident. The two individual lineament interpretations for each data set were then integrated to provide a single interpretation for the aeromagnetic (Figure 10), electromagnetic (Figure 11), CDED (Figure 12) and Landsat (Figure 13) data that included the results of the first stage reproducibility assessment (RA\_1). A discussion of the parameters used during this step follows.

### **Buffer Size Selection**

Buffer sizes for lineaments in each data set were initially based on the (grid) resolution of each data set. It was determined using trial-and-error over a selected portion of the lineament interpretation that buffer sizes of five times the grid cell resolution of each data set provided a balanced result for assessing reproducibility.

A buffer of 200 metres (either side of the lineament) was generated for the magnetic and electromagnetic data. This value is equivalent to five times the data set grid cell resolution (40 metres) of the Schreiber Magnetic Supergrid data, which cover the majority of the Schreiber area.

A buffer of 150 metres (either side of the lineament) was generated for the satellite data. This value is equivalent to five times the resolution of the Landsat data (30 metres), which is the coarser of the two available satellite data sets.

A buffer of 125 metres (either side of the lineament) was generated for the topographic data. This value is approximately equivalent to five times the resolution of the CDED topography data (23 metres).

The buffers were used as an initial guide to determine coincidence between lineaments, with the expert judgement of the interpreter ultimately determining which lineaments were coincident. The buffer size widths were included in the attribute fields of each interpretation file (Table 7).

### **Reproducibility Assessment**

The generation of an integrated lineament interpretation for each data set, including the reproducibility assessment, utilized a three step process to combine the first interpreter's lineaments ("lead interpretation") and second interpreter's lineaments, as follows:

- Lineament buffers, described above, were overlain on top of the lead interpretation data set. The second interpreter's lineaments were overlain on top, and all lineaments that occurred within overlapping buffers were carried forward and copied into a new file for the next step. These lineaments were attributed with a reproducibility value (RA\_1; Table 7) of two in the Step 2 attribute table.
- The remaining lineaments of the lead interpreter's Step 1 interpretation were then manually analyzed by both interpreters on the basis of the available imagery for each data set. In some instances, this included adapting the shape and extent of individual lineaments to increase the accuracy of spatial location or length of the lineament, and carrying the adapted lineament forward into the Step 2 interpretation file. These lineaments were attributed a RA\_1 value of one in the Step 2 attribute table.
- Finally, the remaining lineaments of the second interpreter's Step 1 interpretation were then manually analyzed by both interpreters on the basis of the available imagery for each data set. In some instances, this included adapting the shape and extent of individual lineaments to increase the accuracy of spatial location or length of the lineament, and carrying the adapted lineament forward into the Step 2 interpretation file. These lineaments were attributed a RA\_1 value of one in the Step 2 attribute table.

As specified above, the decision on whether or not to adapt the shape and extent of an individual lineament and (or) whether the lineament was carried forward to the next step followed analysis of the specified lineament with the available imagery was based on expert judgement. The following guidelines were applied:

- If a lineament was drawn continuously by one interpreter but as individual, spaced or disconnected segments by the other interpreter, a single continuous lineament was carried forward to the Step 2 interpretation with a RA\_1 value of two, if expert judgement deemed the continuous lineament to be more correct.
- If more than two thirds of a lineament were identified by one interpreter compared to the other interpreter, the lineament was carried forward to the Step 2 interpretation with a RA\_1 value of two. If less than two thirds of a lineament were identified by one interpreter compared to the other interpreter, the longer lineament was segmented, and each portion was attributed with RA\_1 values accordingly.

The resulting Step 2 interpretations for each data set (magnetics, electromagnetics, topography, and satellite imagery) were then refined using expert judgement to avoid any structurally inconsistent relationships. This included adapting the lineaments within the limits of the assigned buffer zone to avoid any mutually crosscutting relationships, and updating the attribute fields.

### **3.2.3 Step 3: Coincidence Assessment 2 (RA\_2)**

During Step 3, the integrated lineament interpretations for each data set were amalgamated into one final interpretation, as shown in Figure 14, following a similar methodology as described above in Step 2. In this second assessment, reproducibility (RA\_2) is based on the coincidence, or lack thereof, of interpreted lineaments between different individual data sets within an assigned buffer zone (Buffer\_RA\_2). A discussion of the parameters used during this step follows below.

Geophysical data supply vital information about structures in the subsurface, whereas surficial data only provide information about the surface expression of structures and may include lineaments that may not be related to the bedrock structural framework. Since high resolution geophysical data are available over the majority of the Schreiber area it was determined that for this step of the interpretation, the lineaments derived from geophysical data would be given precedence over lineaments derived from surficial data.

On this premise, all lineaments derived from the magnetic data were included in the final interpretation. A buffer (200 metres either side) was generated around these lineaments, which was used for comparison with lineaments derived from electromagnetic data. This buffer size was included as an attribute field for all interpreted lineaments (Buffer RA\_2; Table 7). As part of this comparison, coincident lines were identified and attributed. Next, non-coincident lineaments were evaluated against the magnetic data by both interpreters, and if required, were adapted and carried forward to the final Step 3 data set. This resulted in a combined interpretation with lineaments derived from geophysical data (magnetic and electromagnetic).

The lineaments derived first from topographic and then satellite data were then evaluated against the combined geophysical interpretation in a similar fashion. During this process, each lineament was attributed with a text field highlighting in which data sets it was identified.

The following rules were applied for determining reproducibility between the data set-specific lineament maps:

- If any coincidence of lineaments occurred between two lineament data sets, the longest lineament was carried forward to the Step 3 interpretation and attributed as derived from two (or more) data sets, regardless of the length of overlap between the lineaments. This meant that if any part of a lineament derived from one data set was identified in another data set, it was considered that this lineament was reproduced.
- In the case that a lineament derived from topographic or satellite imagery data was longer than a coincident lineament derived from geophysical data, the former lineament was cut and the non-coincident portion was carried forward into the final Step 3 interpretation as a single entity. Both the lineament in the geophysical data and the non-coincident portion derived from another data set were then attributed accordingly in terms of reproducibility.
- A lineament derived from topographic and (or) satellite imagery data that would fall within the buffer of a lineament derived from geophysical data would be attributed as reproduced in the relevant data sets if the orientation of the lineaments did not deviate significantly.
- Short (less than 500 metres) discontinuous topographic and satellite imagery data lineaments that are at low angles to geophysical data lineaments but extending outside the geophysical lineament buffer were considered to be coincident.
- Short (less than 500 metres) topographic and satellite imagery data lineaments that are at high angles to geophysical data lineaments, largely overlapped with the buffer zone from the geophysical data lineament, and had no further continuity (i.e., singular elements), were not carried forward to the final interpretation. This was done on the basis that these short segments represent a subsidiary lineament that is related to a broader fault zone already included as a brittle lineament in the final interpretation based on identification in the geophysical data.

The final reproducibility value (RA\_2; Table 7) was then calculated as the sum of the number of data sets in which each lineament was identified (i.e. a value of 1-4).

The resulting lineament framework interpretation, representing the integration of all data sets, was then evaluated and modified (within the limits of relevant buffers) in order to develop a final lineament interpretation that is consistent with the known structural history of the Schreiber region. This included defining the age relationships of the interpreted lineaments on the basis of crosscutting relationships between different generations of brittle lineaments and populating attribute field for each lineament for the relative age (Rel\_Age; Table 7). This incorporated a working knowledge of the structural history of the Schreiber area, combined with an understanding of the fault characteristics in each brittle lineament population (e.g., brittle versus ductile). The structural history of the area is defined in Section 2.3.

The interpreted crosscutting and age relationships between different families of brittle lineaments and within individual families of brittle lineaments were refined using the available data. Crosscutting relationships were evaluated based on the through-going nature and termination of brittle lineaments and evaluated against the regional structural history as described below.

- D<sub>1</sub> deformation:
  - Development of S<sub>1</sub> compositional layering and localized isoclinal (overturned) F<sub>1</sub> folds and associated D<sub>1</sub> thrust faults in greenstone rocks; and
  - Not recognized in lineament analysis.
- D<sub>2</sub>-D<sub>4</sub> Deformation:
  - Only present in greenstone rocks;
  - Represents protracted north-south to northwest-southeast compression and transpression;
  - Brittle-ductile structures constrained between ca. 2.691 Ga and ca. 2.679 Ga; and
  - Interpreted to form foliations, D<sub>2</sub>-D<sub>3</sub> isoclinal folds, D<sub>2</sub>-D<sub>4</sub> thrust faults and D<sub>4</sub> kink folds.

- D<sub>5</sub> Deformation:
  - Present in greenstone and granitic supracrustal rocks;
  - Only described in literature as “post-D<sub>4</sub> brittle structures subparallel to S<sub>2</sub> foliation in the Hemlo greenstone belt” (Lin, 2001);
  - Occurred after emplacement of granites and Proterozoic dykes (post ca. 2.121 Ga), absolute age constraints are not available for this phase; and
  - Interpreted to form brittle faults.
- D<sub>6</sub> Deformation:
  - Present in greenstone and granitic supracrustal rocks;
  - Only described in literature as “post-D<sub>4</sub> southeasterly trending dextral strike-slip faults in the Hemlo greenstone belt” (Lin, 2001);
  - Other than post-dating Proterozoic dykes (post ca. 2.121 Ga), absolute age constraints are not available for this phase; and
  - Interpreted to form brittle faults.

This interpretation is preliminary and needs to be verified by field investigations.

Interpreted lineaments were amended by applying this structural framework where required. This resulted in a cohesive interpretation representing clearly-defined, consistent lineament network for the Schreiber area.

Finally, following the amendment of selected lineaments, the azimuth and length attribute fields were recalculated. The attribute field for the final interpretation of the width of each lineament (F\_Width; Table 7) remains unpopulated, since no information is available on the width of the known faults in the Schreiber area.

Additional analyses described further below in this report were carried out using the final interpretation. The final lineament interpretation shows a dense network of lineaments throughout the Schreiber area (Figures 14 and 15).

## 4 Findings

### 4.1 Description of Lineaments by Data Set

#### 4.1.1 Geophysical Data

Interpretation of geophysical data allows for the distinction between ductile, dyke and brittle lineaments. Features interpreted as ductile lineaments from the aeromagnetic geophysical data set are shown on Figure 9. Interpreted brittle and dyke lineaments from the aeromagnetic and electromagnetic geophysical data sets are shown on Figure 10 and Figure 11, respectively. The following paragraphs provide an overview of these interpretations.

A total of 419 lineaments comprise the data set (RA\_1) of merged lineaments identified by the two interpreters from the aeromagnetic data (Figure 10). Of the 419 lineaments, 243 are interpreted as brittle lineaments, while 176 are interpreted as dyke lineaments. The length of the aeromagnetic lineaments (including both brittle and dyke features) ranges from 160 metres up to 48.7 kilometres, with a

geometric mean length of 2.5 kilometres and a median length of 2.2 kilometres. Azimuth data, weighted by length, for the aeromagnetic lineaments interpreted as brittle lineaments exhibit a dominant orientation to the west-northwest (Figure 10 inset). Other prominent orientations include a northwest and minor east-northeast trend (Figure 10 inset). The 176 lineaments identified from the aeromagnetic data that are interpreted to represent dyke lineaments include dominant northwest, northeast and east-trending dyke sets that belong to several different suites.

Of the brittle lineaments interpreted from aeromagnetic data, 114 (47%) lineaments were assigned the highest level of certainty (certainty = 3), while 125 (51%) and 4 (2%) of the interpreted brittle lineaments were given certainty values of two and one, respectively. Of the dykes interpreted from aeromagnetic data, 150 (85%) dykes were assigned a certainty value of 3, while six (4%) and twenty (11%) dykes were given certainty values of two and one, respectively. The reproducibility assessment identified coincidence for 59 brittle lineaments (24%; RA\_1 = 2) and a lack of coincidence for 184 of the interpreted brittle lineaments (76%; RA\_1 = 1). The reproducibility assessment identified coincidence for 129 of the interpreted dykes (73%; RA\_1 = 2) and a lack of coincidence for 47 of the interpreted dykes (27%; RA\_1 = 1).

A total of 147 lineaments comprise the data set of merged lineaments identified by the two interpreters from the electromagnetic data (Figure 11). Of the 147 lineaments, 125 are interpreted as brittle lineaments, while 22 are interpreted as dyke lineaments. The length of the electromagnetic lineaments (including both brittle and dyke features) ranges from 260 metres up to 48.7 kilometres, with a geometric mean length of 5.0 kilometres and a median length of 5.8 kilometres. Azimuth data, weighted by length, for the electromagnetic lineaments interpreted as brittle lineaments exhibit a dominant orientation to the northwest (Figure 11 inset). Other prominent orientations include minor east-northeast and east-southeast trends (Figure 11 inset). The 147 lineaments identified from the electromagnetic data include dominant northwest, northeast and east-trending dyke sets that are interpreted to represent dyke lineaments that belong to several different suites.

Of the brittle lineaments interpreted from electromagnetic data, 74 (59%) lineaments were assigned the highest level of certainty (certainty = 3), while 51 (41%) were given certainty values of two. No brittle lineaments interpreted from the electromagnetic data were assigned a certainty value of one. Of the dyke lineaments interpreted from electromagnetic data, 17 (77%) dykes were assigned a certainty value of 3, while four (18%) and one (5%) dyke(s) were given certainty values of two and one, respectively. The reproducibility assessment identified coincidence for 50 brittle lineaments (40%; RA\_1 = 2) and a lack of coincidence for 75 of the interpreted brittle lineaments (60%; RA\_1 = 1). The reproducibility assessment identified coincidence for 15 of the interpreted dyke lineaments (68%; RA\_1 = 2) and a lack of coincidence for 7 of the interpreted dyke lineaments (32%; RA\_1 = 1).

Based on the combined interpretation of geophysical data (magnetic and electromagnetic), a total of 477 lineaments were identified in the Schreiber area, 177 of the which are interpreted as dyke lineaments. On the basis of their orientation, these 177 dyke lineaments were divided into several groups:

- Fifty-one dyke lineaments are interpreted to belong to the northwest-trending Matachewan Suite dykes (ca. 2.473 Ga; Buchan and Ernst, 2004);
- Twenty-one dyke lineaments are interpreted to belong to the north-northwest- to northeast-trending Marathon Suite dykes (ca. 2.121 Ga; Buchan et al., 1996); and
- Forty-three dyke lineaments are interpreted to belong to the east-west-trending, reversely polarized Keweenaw Suite dykes (ca. 1.100 Ga; Thurston, 1991). The justification for this interpretation is described in detail in Mira (2013).

Hamilton et al. (2002) described northeast-trending Biscotasing Suite dykes (ca. 2.167 Ga) in the Schreiber area. However, these could not be distinguished from northeast-trending Marathon Suite dykes, and therefore, sixty-one northeast-trending dyke lineaments are attributed as “Marathon/Biscotasing”. All other north-northwest- to north-trending interpreted dykes were only attributed as “Marathon”.

Also, given its distinct character in the magnetic data (a non-linear magnetic low), a single interpreted dyke lineament in the southeast of the Schreiber area was interpreted to be associated with the Coldwell alkalic complex.

#### **4.1.2 Surficial Data (CDED topography and satellite imagery)**

Interpreted lineaments from the CDED topography and satellite imagery data sets are shown on Figure 12 and 13, respectively. The following paragraphs provide an overview of these surface-based interpretations.

A total of 874 lineaments were identified by the two interpreters (Step 2) from the CDED topography data (Figure 12). These lineaments range in length from 110 metres to 38.1 kilometres, with a geometric mean length of 1.65 kilometres and a median length of 1.47 kilometres. CDED topography lineament orientations display a strong west-northwest trend and a prominent northwest trend (Figure 12 inset). A minor trend to the east-northeast is also present (Figure 12 inset). A total of 370 of the CDED topography lineaments (43%) were assigned a certainty value of 3. Certainty values of 2 and 1 were assigned to 503 (57%) and 1 of the CDED topography lineaments, respectively. The reproducibility assessment shows coincidence for 424 of the CDED topography lineaments (48%, RA\_1 = 2) and a lack of coincidence for 450 of the CDED topography lineaments (52%, RA\_1 = 1).

A total of 659 lineaments were identified by the two interpreters (Step 2) from the satellite imagery data (Figure 13). These lineaments range in length from 280 meters to 48.7 kilometers, with a geometric mean length of 1.96 kilometers and a median length of 1.83 kilometres. Satellite imagery lineament orientations display a strong northwest trend and a prominent north-northwest trend (Figure 13 inset). A minor trend to the east-southeast is also present (Figure 13 inset). A total of 174 of the satellite imagery lineaments (26%) were assigned a certainty value of 3. Certainty values of 2 and 1 were assigned to 457 (70%) and 29 (4%) of the satellite imagery lineaments, respectively. The reproducibility assessment shows coincidence for 309 of the satellite imagery lineaments (47%, RA\_1 = 2) and a lack of coincidence for 350 of the satellite imagery lineaments (53%, RA\_1 = 1).

## **4.2 Description and Classification of Integrated Lineament Coincidence (RA\_2)**

The integrated lineament data set produced by merging all lineaments interpreted from the geophysical (MAG and EM), CDED topography, and satellite imagery data is presented on Figure 14 and Figure 15. Figure 14 displays the lineament classification based on Reproducibility Analysis 2 (RA\_2). Figure 15 displays the lineament classification based on length of interpreted lineaments. The merged lineaments were classified by length using four length bins: >10 kilometres, 5-10 kilometres, 1-5 kilometres and <1 kilometre. These length bins were defined based on an analysis of the lineament length frequency distributions for the Schreiber area.

The merged lineament data set contains a total of 949 lineaments (brittle and dyke) that range in length from 140 metres to 46.5 kilometres. The geometric average length of these lineaments is 2.1 kilometres and the median length is 1.8 kilometres. Lineaments in the >10 kilometres and 5-10 kilometres length



bins represent 10% and 8% of the merged lineaments, respectively, while lineaments in the 1-5 kilometres and <1 kilometre length bins represent 60% and 22% of the merged lineaments, respectively. Orientation data for the merged lineament data set exhibit the same dominant trends as described in the previous section, namely dominant west-northwest and northwest-trending lineaments with a minor east-northeast trending lineament set (Figure 14 and 15 inset rose diagrams).

Results from the Reproducibility Assessment 2 (RA\_2), shown in Figure 14, for the merged lineament data set (brittle and dyke) show 77 lineaments (8%) were identified and coincident in all four data sets (RA\_2 = 4), and 234 lineaments (25%) were coincident with a lineament from two other data sets (RA\_2 = 3). A total of 484 lineaments (51%) were coincident with a lineaments from one other data set (RA\_2 = 2), while 154 lineaments lacked a coincident lineament from the other data sets (RA\_2 = 1).

Due to the absence of significant Quaternary cover in the Schreiber area, at least a portion of all lineaments identified in the CDED topography data were also identified in Landsat and SPOT satellite imagery. This is a result of the lineament integration process (as described in section 3), in which overlap and partial coincidence of lineaments observed in two data sets may result in a combined final lineament. This indicates that at least a portion of an interpreted lineament in the topography data was also observed in the satellite imagery data, or vice-versa. For this reason, all surficial lineaments (or parts thereof) were observed in both CDED topography and satellite imagery data. A total of 253 (27%) lineaments observed in aeromagnetic data were coincident with a mapped interpreted surficial lineament. A total of 135 (14%) lineaments observed in electromagnetic data were coincident with an interpreted surficial lineament.

Of all lineaments interpreted to represent brittle lineaments (Figure 14), 471 (61%) of the total 772 brittle lineaments have reproducibility values of two (RA\_2 = 2), as these were observed in both the CDED topography and satellite imagery data sets. A total of 234 (30%) brittle lineaments have a reproducibility value of three (RA\_2 = 3) as they were observed in the surficial data sets and at least one of the geophysical data sets. Sixty-seven (9%) brittle lineaments have been observed all data sets (RA\_2 = 4).

Given that dykes exhibit a limited surficial expression, 154 (87%) of the total 177 interpreted dyke lineaments (Figure 14) have reproducibility values of one (RA\_2 = 1), as they were only observed in the aeromagnetic data. However, a total of 23 dyke lineaments have been observed in multiple data sets, where 13 (7%) dyke lineaments have been observed in both the aeromagnetic and electromagnetic data (RA\_2 = 2), and 10 (6%) dyke lineaments have been observed in all data sets (RA\_2 = 4).

### 4.3 Description of Lineaments by Batholiths and Plutons in the Schreiber Area

As described in Section 2.2, the bedrock geology of the Schreiber area is dominated by large granitic bodies that intrude older metavolcanic and metasedimentary rocks associated with greenstone belts. These granitic bodies include the Whitesand Lake, Crossman Lake, and Terrace Bay batholiths and the Mount Gwynne pluton (Figure 3 and Figure 16). Rose diagrams for interpreted lineaments (brittle and dyke) on the batholiths and pluton are presented on Figure 16.

There were 133 interpreted lineaments (122 brittle, 11 dyke) identified that crosscut the Whitesand Lake batholith that covers most of the southwestern quadrant in the Schreiber area (approximately 123 km<sup>2</sup>). Of these, 46 brittle lineaments are interpreted as D<sub>5</sub> faults and 75 as D<sub>6</sub> faults. The remaining one brittle lineament is interpreted as a D<sub>2</sub>-D<sub>4</sub> fault. The interpreted lineaments that intersect the Whitesand Lake batholith range in strike length from 0.3 to 35 kilometres and largely trend west-northwest and northwest

within the Whitesand Lake batholith (Figure 16). Four dyke lineaments interpreted to be related to the Marathon Suite, four dyke lineaments related to the Matachewan Suite and three dyke lineaments interpreted to be related to the Keweenawan Suite also crosscut the Whitesand Lake batholith.

The Crossman Lake batholith covers a large part (~300 km<sup>2</sup>) of the northern half of the Schreiber area and is crosscut by 386 interpreted lineaments (315 brittle, 71 dyke). Fifty-six brittle lineaments are interpreted as D<sub>2</sub>-D<sub>4</sub> faults. This is consistent with overlap between the inferred age of the Crossman Lake batholith and the timing of D<sub>2</sub>-D<sub>4</sub> deformation. Alternatively, these faults may represent conjugate segments of D<sub>5</sub> faults. The D<sub>2</sub>-D<sub>4</sub> faults that intersect the Crossman Lake batholith range in strike length from 0.4 to 27.2 kilometres. 108 brittle lineaments are interpreted as D<sub>5</sub> faults, with the remaining 151 brittle lineaments interpreted as D<sub>6</sub> faults. The D<sub>5</sub> and D<sub>6</sub> faults that intersect the Crossman Lake batholith range in strike length from 0.4 to 37 kilometres and from 0.5 to 49 kilometres, respectively. D<sub>5</sub> faults are largely oriented west-northwest and D<sub>6</sub> faults are largely oriented northwest with subordinate south- and northeast-trending faults within the Crossman Lake batholith (Figure 16). A total of twenty Matachewan, one Keweenawan, ten Marathon, and forty Marathon/Biscotasing dyke segments are interpreted to crosscut the Crossman Lake batholith.

The segment of the Terrace Bay batholith that occurs in the southeastern portion of the Schreiber area covers an area of approximately sixty-seven km<sup>2</sup> and is crosscut by 65 interpreted lineaments (30 brittle, 35 dyke). Five of these are interpreted as D<sub>2</sub>-D<sub>4</sub> faults that overlap in age with the inferred age for emplacement of this batholith. Eleven brittle lineaments are interpreted to be D<sub>5</sub> faults, and the remaining fourteen as D<sub>6</sub> faults. D<sub>5</sub> and D<sub>6</sub> faults that intersect the Terrace Bay batholith range in strike length from 1 to 34 kilometres and from 3.5 to 49 kilometres, respectively. D<sub>5</sub> faults are largely oriented west-northwest and D<sub>6</sub> faults are largely oriented northwest within the Terrace Bay batholith (Figure 16). Twenty-seven Keweenawan, one Marathon, 6 Marathon/Biscotasing, and one suspected Coldwell dyke segments are interpreted to crosscut the Terrace Bay batholith.

The Mount Gwynne pluton, which covers approximately five km<sup>2</sup> along the southern margin of the Schreiber area, is crosscut by 19 lineaments (12 brittle, 7 dyke). One of these brittle lineaments is considered an extension of D<sub>2</sub>-D<sub>4</sub> faults, six are interpreted as D<sub>5</sub> faults and the remaining five are interpreted as D<sub>6</sub> faults. The D<sub>5</sub> and D<sub>6</sub> faults that intersect the Mount Gwynne pluton range in strike length from 1 to 24 kilometres and from 0.8 to 26 kilometres, respectively. D<sub>5</sub> faults are largely oriented west-northwest and D<sub>6</sub> faults are largely oriented northwest or northeast within the Mount Gwynne pluton (Figure 16). Six dykes of the Keweenawan Suite and one dyke of the Marathon/Biscotasing Suite are interpreted to crosscut the Mount Gwynne pluton.

## 5 Discussion

The following sections are provided to discuss the results of the lineament interpretation in terms of lineament density, reproducibility and coincidence, and lineament length, the relationship between mapped faults and interpreted lineaments, and the relative age relationships of the interpreted lineaments.

### 5.1 Lineament Density

The density of all interpreted brittle lineaments in the Schreiber area was determined by examining the statistical density of individual lineaments using ArcGIS Spatial Analyst. A grid cell size of 50 metres and a search radius of 1.5 kilometres (equivalent to half the size of the longest boundary of the minimum area size of a potential siting area) were used for this analysis. The spatial analysis used a circular search

radius examining the lengths of polylines intersected within the circular search radius around each grid cell, following this equation:

$$\text{Density} = (L1 + L2) / (\text{area of circle})$$

Where L1 represents the length of Line 1 within the circle and L2 represents the length of Line 2 in the circle, assuming that only two lineament polylines intersect the circle search radius.

Even though the density of brittle lineaments is relatively uniform and high in the Schreiber area, some variations can be described. The uniformity of the brittle lineament density can be attributed to the relatively high resolution of data sets used for the lineament interpretation combined with the absence of extensive areas of bedrock cover sequences (other than in the southeastern corner near the settlement of Terrace Bay).

The greatest density of lineaments occurs in areas underlain by Schreiber Assemblage metavolcanic rocks, as well as in a corridor approximately 10 kilometres wide crossing the Schreiber area from the northwest to the southeast. Among the granitic intrusions in the Schreiber area, the lowest lineament density is observed in the Terrace Bay batholith. However, this low brittle lineament density is likely an artefact related to the Quaternary cover that overlies most of the batholith in the area. Several relatively small areas of low lineament density occur throughout the Whitesand Lake and Crossman Lake batholiths in the Schreiber area.

## 5.2 Lineament Reproducibility and Coincidence

Reproducibility values assigned to the lineaments provide a measure of the significance of the bedrock structures expressed in the different data sets. The approach used to assign reproducibility values involved checking whether lineament interpretations from different interpreters (RA\_1), and from different data sets (RA\_2), were coincident within a specified buffer zone radius. Reproducibility values are discussed in detail in Sections 4.1 and 4.2.

The findings from the reproducibility assessment RA\_1 indicate that approximately 47 % of surficial lineaments were identified by both interpreters (see Figure 12 and Figure 13). Importantly, longer lineaments with higher certainty values were identified more often by both interpreters. The reproducibility assessment of the geophysical lineaments shows that over 24 % of the lineaments were identified by both interpreters (see Figure 10 and Figure 11). As with the surficial lineaments, longer geophysical lineaments with higher certainty values were also recognized more often by both interpreters.

There are some differences in the individual Step 1 lineament interpretations. These differences can be explained by two main factors: the person carrying out the interpretation and the lineament information that can be derived from specific data sets. The lineament interpretations carried out by two different interpreters is subjective and, in part, may be affected by the interpreter's experience. The lineament information that can be derived from each data set may have a strong impact on the quality and resolution of an interpretation. As discussed earlier in this report, topographic and satellite data only provide information about the potential surficial expressions of lineaments. However, these data sets may include lineaments that are related to erosional features, such as glacial features, that do not have a structural origin. It can be challenging to distinguish such features from structural features, and careful evaluation, combined with a working knowledge of the glacial history of the area is required. For the final lineament interpretation in the Schreiber area, lineaments that were interpreted during Step 1 and Step 2 that strike roughly south (i.e., parallel to the ice flow direction), with relatively short lengths and

discontinuous in nature, were considered as suspect and likely to represent glacial features that were incorrectly interpreted as structural features. Therefore these lineaments were not included in the final Step 3 interpretation.

The resolution of each available data set has a strong impact on the reproducibility and number of interpreted lineaments. The Schreiber Magnetic Supergrid data has a high resolution (40-metre grid cells) and covers most of the area. The SPOT satellite, Landsat satellite, and CDED topography data cover the entire Schreiber area with a 30-metre (and less) grid cell resolution. The better resolution of the surficial data sets may explain why a larger number of lineaments are identified from these data compared to the geophysical data sets. Importantly, all brittle lineaments observed from geophysical data sets were also observed in surficial data sets. Therefore, SRK infers that the resolution of the data sets used, in combination with the final interpretation originating from two individual interpreters, form a suitable basis to conduct a robust lineament interpretation in the Schreiber area.

The bedrock structural information available from surficial data sets (topography and satellite data) is limited only in the southeast portion of the area, due to the presence of relatively thick glaciolacustrine cover. In this area, high resolution Schreiber Supergrid magnetic and electromagnetic data are present, which provide the required information to complete a suitable structural lineament interpretation. The absence of thick or extensive bedrock cover sequences elsewhere in the Schreiber area facilitates the practical interpretation of lineaments from surficial data. This is particularly illustrated by the reproducibility values (RA\_2) of 100 % between surficial lineaments interpreted from CDED topography and satellite imagery data. This is explained by the fact that lineaments interpreted from the satellite imagery and the CDED topography data represent surficial expressions of the same bedrock features (that are not masked by any extensive bedrock cover sequences in the Schreiber area). For example, a lineament drawn along a stream channel shown on the satellite imagery is expected to be coincident with a lineament that captures the trend of the associated topographic valley expressed in the digital elevation data.

In contrast, only 311 (253 magnetic and an additional 58 electromagnetic) equivalent to approximately 33 % of the geophysical lineaments were coincident with interpreted surficial lineaments. Aside from the higher number of lineaments observed in surficial data, this relatively poor correlation between surficial and geophysical lineaments may be the result of various factors, such as: deeper structures identified in geophysics may not have a surface expression; surficial features may not extend to great depth; and, structural features may not possess a magnetic susceptibility contrast with the host rock. However, the recognition of more lineaments in the surficial data is likely associated with the difference in resolution between the geophysical and surficial data, where the latter data sets have a markedly higher resolution.

For these reasons, it is necessary to objectively analyze the results of the RA\_2 assessment with the understanding that  $RA_2 = 1$  does not necessarily imply a low degree of confidence that the specified lineament represents a true geological feature (i.e. a fracture). The true nature of the interpreted features will need to be investigated further during subsequent stages of the site evaluation process, if the community is selected by the NWMO, and remains interested in continuing with the site selection process.

### 5.3 Lineament Length

There is no information available on the depth extent into the bedrock of the lineaments interpreted for the Schreiber area. In the absence of available information, the interpreted length may be used as a proxy for the depth extent of the identified structures (Figure 15). A preliminary assumption may be that the

longer interpreted lineaments in the Schreiber area may extend to greater depths than the shorter interpreted lineaments.

As discussed in Section 5.2 above, longer interpreted lineaments generally have higher certainty and reproducibility values. Although the existence of interpreted lineaments would need to be confirmed through field observations, certainty and reproducibility values provide a preliminary indication that the longer features are related to bedrock structures.

## 5.4 Fault and Lineament Relationships

Regional geological maps (Figure 3) recognize three named southeast-trending faults (Sox Creek, Ross Lake and Cook Lake faults) and four northeast-trending faults (Syenite Lake, Schreiber Point, Worthington Bay and Ellis Lake faults) in the Schreiber area. These faults are interpreted as  $D_6$  structures in Section 3.2 (Carter, 1998). There are also several additional unnamed faults in the regional database (Figure 3). In comparison, as a result of lineament analysis, a total of 949 brittle and dyke lineaments were interpreted in the Schreiber area.

It should be noted that the majority of the mapped (and named) faults shown on Figure 3 were reproduced during the lineament analysis. Only the northeast-trending Ellis Lake fault was not identified during the lineament interpretation. All but one of the observed lineaments correlating with the mapped faults have a reproducibility rating (RA<sub>2</sub>) of four, even though the traces of the observed lineaments may diverge slightly from the mapped faults. A mapped fault in the southwest corner of the Schreiber area, parallel to the Sox Creek fault, correlates with an observed lineament with a reproducibility (RA<sub>2</sub>) rating of three. The north-trending segment of the Schreiber Point fault (Figure 3) was not reproduced as a brittle lineament, but a portion of an interpreted dyke lineament with reproducibility rating (RA<sub>2</sub>) of four corresponds with this mapped fault.

The principal neotectonic stress orientation in central North America is generally oriented approximately east-northeast (63 degrees  $\pm$  28 degrees; Zoback 1992) although anomalous stress orientations have also been reported in the mid-continent that include a 90-degree change in azimuth of the maximum compressive stress axis (Brown et al. 1995) and a north-south maximum horizontal compressive stress (Haimson 1990). Local variations, and other potential complicating factors involved in characterizing crustal stresses, including the effect of shear stress by mantle flow at the base of the lithosphere (Bokelmann 2002; Bokelmann and Silver 2002), the degree of coupling between the North American plate and the underlying mantle (Forte et al. 2010), the effects of crustal depression and Holocene rebound, and the influence of the thick lithospheric mantle root under the Canadian Shield, make it premature to correlate the regional neotectonic stress orientation with the orientation of mapped lineaments at the desktop stage.

However, it is possible to broadly speculate on the potential behavior of the identified lineaments if they were to be reactivated by the regional east-northeasterly neotectonic stress regime. The combined set of lineaments from all sources includes strong trends to the west-northwest (290 degrees), northwest (320 degrees) and a minor east-northeast orientation. These features were formed by Precambrian paleostress regimes and constitute zones of weakness that are more amenable to reactivation under certain stress conditions than the surrounding rock mass. On this basis, should the identified lineaments be reactivated under the current stress regime, the west-northwest and east-northeast oriented lineaments will likely reactivate as strike slip faults, and the northwest oriented lineaments likely as reverse faults.

## 5.5 Relative age relationships

The structural history of the Schreiber area, outlined in Section 2.3, provides a framework that may aid in constraining the relative age relationships of the interpreted bedrock lineaments. In brief summary, six regionally distinguishable deformation episodes ( $D_1 - D_6$ ) are inferred to have overprinted the bedrock geological units of the Schreiber area.

$D_1$  developed a compositional layering and isoclinal folds between ca. 2.719 and ca. 2.691 Ga.  $D_2$ - $D_4$  produced the dominant brittle-ductile structures observed within the greenstone belts, including steeply dipping foliations, isoclinal folds, and thrust faults prior to ca. 2.680 Ga.  $D_5$  was a brittle deformation event that involved the activation and possible re-activation of major regional faults sub-parallel to  $S_2$  between ca. 2.680 and ca. 1.100 Ga.  $D_6$  represents another regional brittle deformation event that occurred between ca. 2.680 and 1.100 Ga. The youngest major event of brittle fault displacement is constrained by the ca. 1.100 Ga Keweenawan dykes that transect the Schreiber area with no apparent fault offset. This suggests that only limited displacement could have occurred along the interpreted fault network since the intrusion of the Keweenawan dykes.

The 772 brittle lineaments identified in the Schreiber area are interpreted to represent successive stages of brittle-ductile and brittle deformation. These lineaments can therefore be classified into three main stages based on relative age and in accord with the structural history described above: 217  $D_2$ - $D_4$  lineaments, 240  $D_5$  lineaments, and 315  $D_6$  lineaments.  $D_2$ - $D_4$  brittle lineaments are interpreted as Archean brittle-ductile faults characterized as zones of pervasive foliation and phyllonite development, potentially with hydrothermal veining.  $D_5$  and  $D_6$  brittle lineaments are interpreted as brittle faults. Limited information exists on the character of each interpreted fault set. At the desktop stage of preliminary assessment, it is still uncertain whether or not each interpreted lineament is in fact an actual brittle-ductile or brittle geological feature with a significant expression at depth.

No information is available on the depth of fault penetration in the Schreiber area; however, brittle lineament strike length may be a proxy for the depth extent. In general,  $D_5$  and  $D_6$  faults have longer strike lengths than  $D_2$ - $D_4$  faults and may have a greater depth extent.

## 6 Summary

This report documents the source data, workflow and results from a lineament interpretation of publicly-available digital data sets, including geophysical (aeromagnetic, electromagnetic) and surficial (satellite imagery, topography) data sets for the Schreiber area (approximately 1,100 km<sup>2</sup>), in northwestern Ontario.

The lineament analysis provides an interpretation of the location and orientation of possible individual brittle features and dykes on the basis of remotely sensed data, and helps to evaluate their relative timing relationships within the context of the regional geological setting. The three step process involved a workflow that was designed to address the issues of subjectivity and reproducibility.

The distribution of lineaments in the Schreiber area reflects the bedrock structure, resolution of the data sets used, and surficial cover. Surface lineament density, as demonstrated in this study, is high and relatively uniform since only minor areas of significant overburden cover occur throughout the area that may mask the surficial expression of bedrock structures.

The greatest density of lineaments occurs within portions of the Schreiber area that are underlain by metavolcanic rocks of the Schreiber Assemblage. In addition, an approximately 10 kilometre wide corridor defines a zone of high lineament density through the center of the Schreiber area in a northwest-southeast direction.

Although the lineament density in the Schreiber area is generally high, several areas with a relatively low density of lineaments were identified. These were few in number, and restricted to granitoid batholiths, mostly within the Crossman Lake batholith. Within areas of exposed bedrock or thin drift, further investigations of bedrock formations and potential structures could be conducted through outcrop mapping and rock mass characterizations.

In terms of reproducibility, comparison between the various data sets (RA\_2) indicates that the best coincidence is between surficial lineaments interpreted from CDED topography and satellite imagery data. This is in part explained by the fact that lineaments interpreted from the satellite imagery and the CDED topography data represent surficial expressions of the same bedrock feature.

A poor correlation exists between surficial and geophysical lineaments, which, in addition to the difference in resolution between the data sets, may be the result of various factors, such as: deep structures identified in geophysics may not have a surface expression; surficial features may not extend to great depth; and, structures may not possess a magnetic susceptibility contrast with the host rock.

The combined set of lineaments from all sources includes strong trends to the west-northwest (290 degrees), northwest (320 degrees) and a minor east-northeast orientation. On the basis of the structural history of the Schreiber area, a framework was developed to constrain the relative age relationships of the interpreted lineaments.

772 brittle lineaments were noted in the Schreiber area, representing three main generations: 217 D<sub>2</sub>-D<sub>4</sub> lineaments, 240 D<sub>5</sub> lineaments, and 315 D<sub>6</sub> lineaments. In addition, a total of 177 dykes have been interpreted, including fifty-one Matachewan Suite dykes, twenty-one Marathon Suite dykes, sixty-one dykes related to the Marathon or Biscotasing Suite, forty-three Keweenawan Suite dykes and one dyke related to the Coldwell alkalic complex.

All interpreted brittle lineaments appear to be crosscut by east-west-trending Keweenawan diabase dykes (ca. 1.100 Ga) indicating only limited displacement may have occurred along the interpreted lineaments since the intrusion of the Keweenawan dykes.

Brittle lineaments interpreted as D<sub>2</sub>-D<sub>4</sub> features occur primarily within the metavolcanic and metasedimentary rocks of the Schreiber assemblage in the Schreiber-Hemlo greenstone belt. D<sub>2</sub>-D<sub>4</sub> faults are interpreted to have formed prior to ca. 2.680 Ga, and to be zones of pervasive foliation and phyllonite development, potentially with hydrothermal veining (quartz or calcite).

Brittle lineaments interpreted as D<sub>5</sub> and D<sub>6</sub> features are interpreted to have formed between ca. 2.680 Ga and ca. 1.100 Ga. The D<sub>5</sub> and D<sub>6</sub> faults are interpreted to represent a broad east-southeast- and southeast-trending fault network.

## 7 References

- AECOM Canada Ltd., 2013a. Phase 1 Geoscientific Desktop Preliminary Assessment of Potential Suitability for Siting a Deep Geological Repository for Canada's Used Nuclear Fuel, Township of Schreiber, Ontario. Prepared for Nuclear Waste Management Organization (NWMO). NWMO Report Number: APM-REP-06144-0035.
- AECOM Canada Ltd., 2013b. Phase 1 Geoscientific Desktop Preliminary Assessment, Terrain and Remote Sensing Study, Township of Schreiber, Ontario. Prepared for Nuclear Waste Management Organization (NWMO). NWMO Report Number: APM-REP-06144-0036.
- Barnett, P.J., Henry, A.P. and Babuin, D. 1991. Quaternary geology of Ontario, west central sheet; Ontario Geological Survey, Map 2554, scale 1:1,000,000.
- Barnett, P.J. 1992. Quaternary Geology of Ontario. *In* Geology of Ontario, Ontario Geological Survey, Special Volume 4, Part 2, p.1010–1088.
- Berman, R.G., Easton, R.M. and Nadeau, L. 2000. A New Tectonometamorphic Map of the Canadian Shield: Introduction; *The Canadian Mineralogist*, v. 38, p.277-285.
- Berman, R.G., Sanborn-Barrie, M., Stern, R.A. and Carson, C.J. 2005. Tectonometamorphism at *ca.* 2.35 and 1.85 Ga *in* the Rae Domain, western Churchill Province, Nunavut, Canada: Insights from structural, metamorphic and *in situ* geochronological analysis of the southwestern Committee Bay Belt; *The Canadian Mineralogist*, v. 43, p.409-442.
- Bleeker, W. and Hall, B. 2007. The Slave Craton: Geology and metallogenic evolution; *In* Goodfellow, W.D., ed., Mineral Deposits of Canada: A Synthesis of Major Deposit-Types, District Metallogeny, the Evolution of Geological Provinces, and Exploration Methods: Geological Association of Canada, Mineral Deposits Division, Special Publication No. 5, p.849-879.
- Bokelmann, G.H.R. 2002. Which forces drive North America?, *Geology*, v.30, p.1027-1030
- Bokelmann, G.H.R. and Silver, P.G. 2002. Shear Stress at the Base of Shield Lithosphere. *Geophysical Research Letters*, v. 29, p.61-64
- Bostock, H.S. 1970. Physiographic subdivisions of Canada. *In* Geology and Economic Minerals of Canada, Geological Survey of Canada, Economic Geology Report no. 1, p.11-30.
- Breaks, F.W. and Bond, W.D. 1993. The English River Subprovince – An Archean Gneiss Belt: Geology, geochemistry and associated mineralization; Ontario Geological Survey, Open File Report 5846, v. 1, 483p.
- Brown, A., Everitt, R.A., Martin C.D. and Davison, C.C. 1995. Past and future fracturing *In* AECL research areas in the Superior Province of the Canadian Precambrian Shield, with emphasis on the Lac Du Bonnet Batholith; Whiteshell Laboratories, Pinawa, Manitoba.
- Buchan, K.L., Halls, H.C. and Mortensen, J.K. 1996. Paleomagnetism, U-Pb geochronology, and geochemistry of Marathon dykes, Superior Province, and comparison with the Fort Frances swarm. *Canadian Journal of Earth Sciences*, v. 33, pp. 1583-1595.



- Buchan, K.L. and Ernst, R.E. 2004. Diabase dyke swarms and related units in Canada and adjacent regions. Geological Survey of Canada, Map 2022A, scale 1:5,000,000.
- Campbell, D.A., Scott, J.F., Cooke, A., Brunelle, M.R., Lockwood, H.C. and Wilson, A.C. 2012. Report of Activities 2011, Resident Geologist Program, Thunder Bay South Regional Resident Geologist Report: Thunder Bay South District; Ontario Geological Survey, Open File Report 6273, 59p.
- Carter, M.W. 1988. Geology of Schreiber-Terrace Bay area, District of Thunder Bay. Ontario Geological Survey, Open File Report 5692, 287p.
- Corfu, F. and Muir, T.L. 1989. The Hemlo-Heron Bay greenstone belt and Hemlo Au-Mo deposit, Superior Province, Ontario, Canada: 1. Sequence of Igneous activity determined by zircon U-Pb geochronology. *Chemical Geology*, v. 79, pp. 183-200.
- Corfu, F., Stott, G.M. and Breaks, F.W. 1995. U-Pb geochronology and evolution of the English River Subprovince, an Archean low P – high T metasedimentary belt in the Superior Province; *Tectonics*, v.14, p.1220-1233.
- Corrigan, D., Galley, A.G. and Pehrsson, S. 2007. Tectonic evolution and metallogeny of the southwestern Trans-Hudson Orogen, in Goodfellow, W.D., ed., *Mineral Deposits of Canada: A Synthesis of Major Deposit-Types, District Metallogeny, the Evolution of Geological Provinces, and Exploration Methods*: Geological Association of Canada, Mineral Deposits Division, Special Publication No. 5, p.881-902.
- Davis, D.W., and Lin, S. 2003. Unraveling the geologic history of the Hemlo Archean gold deposit, Superior Province, Canada; a U-Pb geochronological study. *Economic Geology and the Bulletin of the Society of Economic Geologists* 98, pp. 51–67.
- Easton, R.M. 2000a. Metamorphism of the Canadian Shield, Ontario, Canada. I. The Superior Province; *The Canadian Mineralogist*, v. 38, p.287-317.
- Easton, R.M. 2000b. Metamorphism of the Canadian Shield, Ontario, Canada. II. Proterozoic metamorphic history; *The Canadian Mineralogist*, v. 38, p.319-344.
- Farrand, W.R. and Drexler, C.W. 1985. Late Wisconsinan and Holocene history of the Lake Superior basin; *In Quaternary Evolution of the Great Lakes*, Geological Association of Canada, Special Paper 30, p.17-32.
- Forte, A., Moucha, R., Simmons, N., Grand, S., and Mitrovica, J., 2010. Deep-mantle contributions to the surface dynamics of the North American continent. *Tectonophysics*, v. 481, p. 3–15.
- Fralick P., Davis, D.W. and Kissin, S.A. 2002. The age of the Gunflint Formation, Ontario, Canada: single zircon U-Pb age determinations from reworked volcanic ash. *Canadian Journal of Earth Sciences*, v.39, p.1085-1091.
- Fraser, J.A. and Heywood, W.W. (editors) 1978. *Metamorphism in the Canadian Shield*; Geological Survey of Canada, Paper 78-10, 367p.
- Gartner, J.F. 1979a. Schreiber area (NTS 42D/NW), District of Thunder Bay; Ontario Geological Survey, Northern Ontario Engineering Geology Terrain Study 59, 15p.

- Gartner, J.F. 1979b. Roslyn Lake area (NTS 42E/SW), District of Thunder Bay; Ontario Geological Survey, Northern Ontario Engineering Geology Terrain Study 43, 12p.
- Haimson, B.C. 1990. Scale effects in rock stress measurements. In Proceedings international workshop on scale effects in rock masses, Loen, AA Balkema, Rotterdam, p.89-101.
- Hamilton, M.A., David, D.W., Buchan, K.L. and Halls H.C. 2002. Precise U-Pb dating of reversely magnetized Marathon diabase dykes and implications for emplacement of giant dyke swarms along the southern margin of the Superior Province, Ontario. Geological Survey of Canada, Current Research 2002-F6, 10p.
- Hayek, S., J.A. Drysdale, V. Peci, S. Halchuk, J. Adams and P. Street. 2009. Seismic Activity in the Northern Ontario Portion of the Canadian Shield. Progress Report for the Period of January 01 to December 31, 2008; NWMO TR-2009-05, 30p.
- Jackson, S.L. 1998. Stratigraphy, structure and metamorphism; Part 1, p.1--58, *in* S.L. Jackson, G.P. Beakhouse and D.W. Davis, Geological Setting of the Hemlo Gold Deposit; an Interim Progress Report, Ontario Geological Survey, Open File Report 5977, 121p.
- Johnson, M. D., Armstrong, D.K., Sanford, B.V., Telford, P.G. and Rutka, M.A. 1992. Paleozoic and Mesozoic geology of Ontario. *In* Geology of Ontario, Ontario Geological Survey, Special Volume 4, Part 2, p.907-1008
- Jolly, W.T. 1978. Metamorphic history of the Archean Abitibi Belt; *In* Metamorphism in the Canadian Shield; Geological Survey of Canada, Paper 78-10, p.63-78.
- Kamineni, D.C. Stone, D. and Peterman Z.E. 1990. Early Proterozoic deformation in the western Superior Province, Canadian Shield. Geological Society of America Bulletin, v. 102, p. 1623-1634.
- Kraus, J. and Menard, T. 1997. A thermal gradient at constant pressure: Implications for low- to medium-pressure metamorphism in a compressional tectonic setting, Flin Flon and Kiseynew domains, Trans-Hudson Orogen, Central Canada; The Canadian Mineralogist, v. 35, p.1117-1136.
- Lin, S. 2001. Stratigraphic and Structural Setting of the Hemlo Gold Deposit, Ontario, Canada. Economic Geology, v. 96, pp. 477–507.
- Manson, M.L. and Halls, H.C. 1994. Post-Keweenaw compressional faults in the eastern Lake Superior region and their tectonic significance; Can. J. Earth Sciences, v.31, p.640-651.
- Marmont, S. 1984. The Terrace Bay Batholith and Associated Mineralization. Ontario Geological Survey Open File Report 5514, 95p.
- Menard, T. and Gordon, T.M. 1997. Metamorphic P-T paths from the Eastern Flin Flon Belt and Kiseynew Domain, Snow Lake, Manitoba; The Canadian Mineralogist, v. 35, p. 1093-1115.
- Ministry of Natural Resources (MNR), 2012a.  
[http://www.mnr.gov.on.ca/en/Business/Forests/2ColumnSubPage/STEL02\\_163522.html](http://www.mnr.gov.on.ca/en/Business/Forests/2ColumnSubPage/STEL02_163522.html)

- Ministry of Natural Resources (MNR), 2012b. Licence and permit list.  
[http://www.mnr.gov.on.ca/en/Business/Aggregates/2ColumnSubPage/STDPROD\\_091593.html](http://www.mnr.gov.on.ca/en/Business/Aggregates/2ColumnSubPage/STDPROD_091593.html)
- Ministry of Northern Development and Mines (MNR), 2012. Geology Ontario. Internet Application.  
<http://www.geologyontario.mndm.gov.on.ca/>
- Mira Geoscience Ltd., 2013. Phase 1 Geoscientific Desktop Preliminary Assessment, Processing and Interpretation of Geophysical Data, Township of Schreiber, Ontario. Prepared for Nuclear Waste Management Organization (NWMO). NWMO Report Number: APM-REP-06144-0037.
- Morris, T.F. 2000. Quaternary geology mapping and overburden sampling, Schreiber area, northwestern Ontario; *In* Summary of Field Work and Other Activities 2000, Ontario Geological Survey, Open File Report 6032, p.33-1 to 33-7.
- Morris, T.F. 2001. Geochemical and till pebble lithology data related to the Schreiber-Killala Lake overburden mapping and sampling program, Northwestern Ontario; Ontario Geological Survey, Miscellaneous Release – Data 74.
- Muir, T.L. 2003. Structural evolution of the Hemlo greenstone belt in the vicinity of the world-class Hemlo gold deposit. *Canadian Journal of Earth Sciences*, vol. 40, pp. 395-430.
- NWMO, 2010. Moving Forward Together: Process for Selecting a Site for Canada's Deep Geological Repository for Used Nuclear Fuel. Nuclear Waste Management Organization, May 2010.
- NWMO, 2013. Preliminary Assessment for Siting a Deep Geological Repository for Canada's Used Nuclear Fuel - Township of Schreiber, Ontario - Findings from Phase One Studies. NWMO Report Number APM-REP-06144-0033.
- Ontario Geological Survey (OGS), 1997. Quaternary Geology. Seamless coverage of the Province of Ontario: Ontario Geological Survey, Data Set 14.
- Ontario Geological Survey (OGS), 1999. Single Master Gravity and Aeromagnetic Data for Ontario; ERLIS Data Set # 1035 (ASCII Format) and # 1036 (Geosoft Format).
- Ontario Geological Survey (OGS), 2003. Ontario airborne geophysical surveys, magnetic and electromagnetic data, Schreiber area; Ontario Geological Survey, Geophysical Data Set 1104 - Revised.
- Ontario Geological Survey (OGS), Ministry of Northern Development and Mines, and Northeast Science and Information Section, Ministry of Natural Resources 2005. Digital Northern Ontario Engineering Geology Terrain Study (NOEGTS); Ontario Geological Survey, Miscellaneous Release Data 160.
- Ontario Geological Survey (OGS), 2011. 1:250 000 scale bedrock geology of Ontario; Ontario Geological Survey, Miscellaneous Release–Data 126 - Revision 1. <http://www.mndm.gov.on.ca>
- Osmani, I.A. 1991. Proterozoic mafic dyke swarms in the Superior Province of Ontario. *in* *Geology of Ontario*, Ontario Geological Survey, Special Volume 4, Part 1, pp. 661-681.
- Pease, V., Percival, J., Smithies, H., Stevens, G. and Van Kranendonk, M. 2008. When did plate tectonics begin? Evidence from the orogenic record; in *Condie, K.C. and Pease, V., eds., When*

- Did Plate Tectonics Begin on Earth?; Geological Society of America Special Paper 440, p.199-228.
- Percival, J.A., Sanborn-Barrie, M., Skulski, T., Stott, G.M., Helmstaedt, H. and White, D.J. 2006. Tectonic evolution of the western Superior Province from NATMAP and Lithoprobe studies; *Can. J. Earth Sciences* v.43, p.1085-1117.
- Percival, J.A. and R.M. Easton. 2007. *Geology of the Canadian Shield in Ontario: an update*. Ontario Power Generation, Report No. 06819-REP-01200-10158-R00.
- Peterman, Z.E. and Day, W. 1989. Early Proterozoic activity on Archean faults in the Western Superior Province – evidence from pseudotachylite. *Geology*, vol. 17, pp. 1089-1092
- Polat, A. 1998. Geodynamics of the Late Archean Wawa Subprovince greenstone belts, Superior Province, Canada. PhD Thesis, Department of Geological Sciences, University of Saskatchewan, Saskatoon, 249p.
- Polat, A. and Kerrich, R. 1999. Formation of an Archean tectonic mélangé in the Schreiber-Hemlo greenstone belt, Superior Province, Canada: Implications for Archean subduction-accretion process. *Tectonics*, v. 18, pp. 733–755.
- Polat, A., Kerrich, R. and Wyman, D.A. 1998. The late Archean Schreiber–Hemlo and White River–Dayohessarah greenstone belts, Superior Province: collages of oceanic plateaus, oceanic arcs, and subduction–accretion complexes. *Tectonophysics*, v. 289, pp. 295–326.
- Powell, W.G., Carmichael, D.M. and Hodgson, C.J. 1993. Thermobarometry in a subgreenschist to greenschist transition in metabasites of the Abitibi greenstone belt, Superior Province, Canada; *J. Metamorphic Geology*, v.11, p.165-178.
- Sado, E.V. and Carswell, B.F. 1987. *Surficial geology of northern Ontario*; Ontario Geological Survey, Map 2518, scale 1:1,200,000.
- Santaguida, F. 2002. *Precambrian geology compilation series – Schreiber sheet*; Ontario Geological Survey, Map 2665-revised, scale 1:250,000.
- Shirota, J. and Barnett, P.J. 2004. *Lineament extraction from digital elevation model (DEM) for the province of Ontario*; Ontario Geological Survey, Miscellaneous Release—Data 142.
- Skulski, T., Sandeman, H., Sanborn-Barrie, M., MacHattie, T., Hyde, D., Johnstone, S., Panagapko, D. and Byrne, D. 2002. *Contrasting crustal domains in the Committee Bay belt, Walker Lake – Arrowsmith River area, central Nunavut*; Geological Survey of Canada, Current Research 2002-C11, 11p.
- Smyk, M.C. and Schnieders, B.R. 1995. *Geology of the Schreiber Greenstone Assemblage and its Gold and Base Metal Mineralization*. Institute on Lake Superior Geology 41st Annual Meeting, Proceedings Volume 41, Field Trip Guidebook, 86p.
- Sutcliffe, R.H. 1991. *Proterozoic Geology of the Lake Superior Area*; *In Geology of Ontario*, Ontario Geological Survey, Special Volume 4, Part 1, p.627-658.

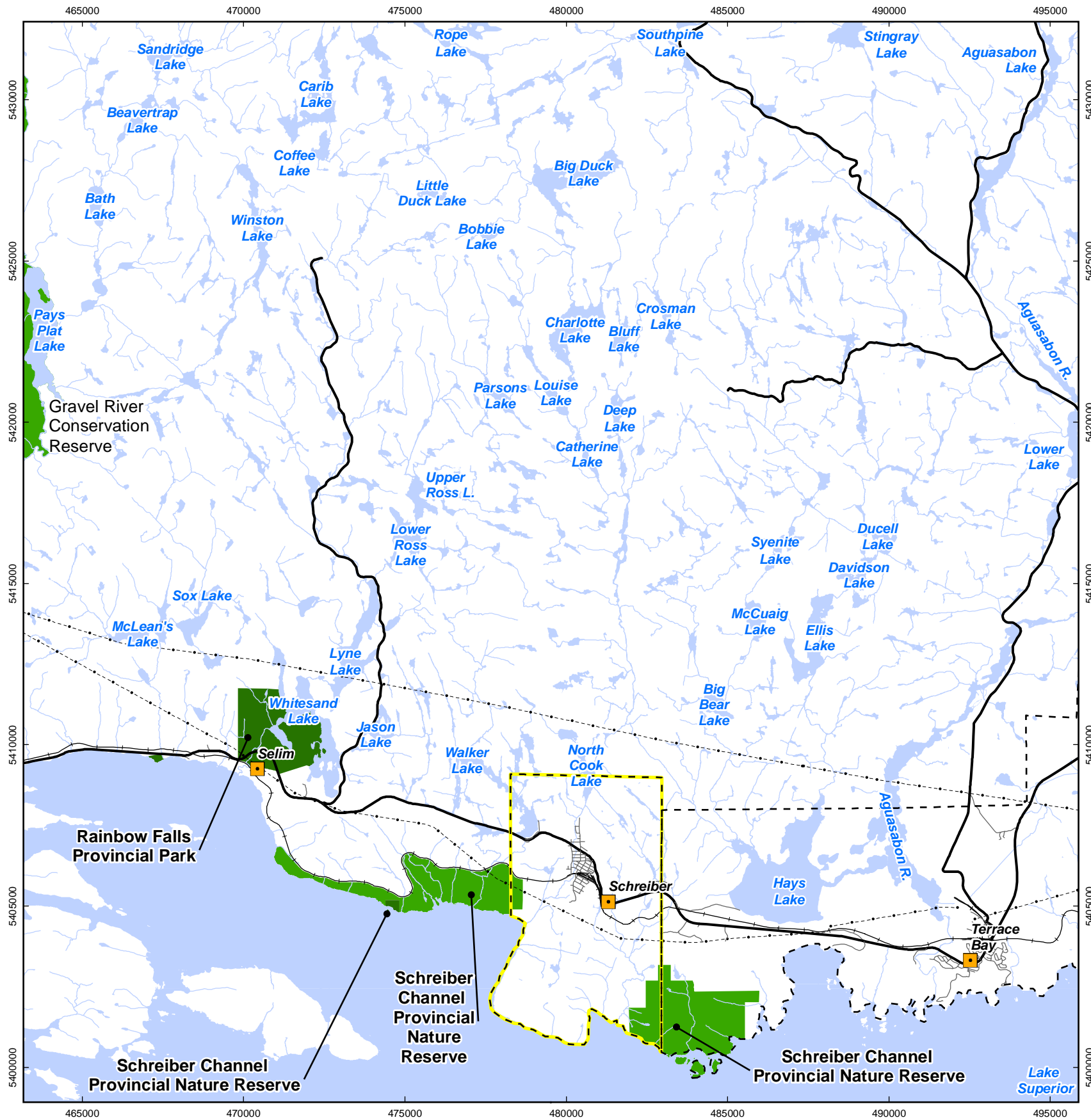
- Thurston, P.C. 1991. Archean Geology of Ontario: Introduction. *in* Geology of Ontario, Ontario Geological Survey, Special Volume 4, Part 1, pp. 3-25.
- Tollo, R.P., Corriveau, L., McLelland, J. and Bartholomew, M.J. (eds.) 2004. Proterozoic tectonic evolution of the Grenville orogen in North America; Geological Society of America Memoir 197, 820p.
- Williams, H. R., G.M. Stott, K.B. Heather, T.L. Muir and R.P. Sage. 1991. Wawa Subprovince. *in* Geology of Ontario, Ontario Geological Survey, Special Volume 4, Part 1, pp. 485-525.
- Young, G.M., Long, D.G.F., Fedo, C.M., Nesbitt, H.W., 2001. Paleoproterozoic Huronian basin: Product of a Wilson cycle punctuated by glaciations and a meteorite impact. *Sediment. Geol.* 141–142, p.233–254.
- Zoback, M.L., 1992. First- and second-order patterns of stress in the lithosphere: the world stress map project; *Journal of Geophysical. Research.*, 97, p.11,703-11,728.
- Zoltai, S. C. 1965. Surficial geology of the Thunder Bay map area; Ontario Department of Lands and Forests. Map S265.



## **FIGURES**





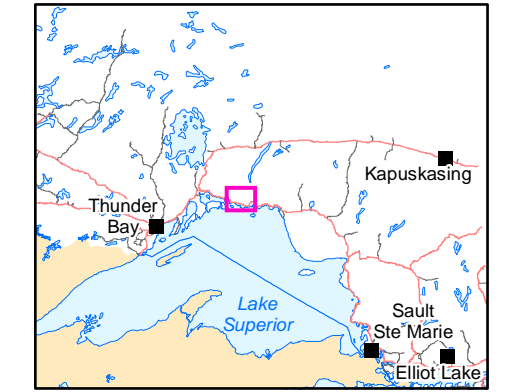


**Legend**

- City / Towns
- Township of Schreiber
- Township of Terrace Bay
- Main Road
- Local Road
- Railway
- Transmission Line
- Watercourse
- Waterbody

**Protected Areas**

- Provincial Park
- Conservation Reserve



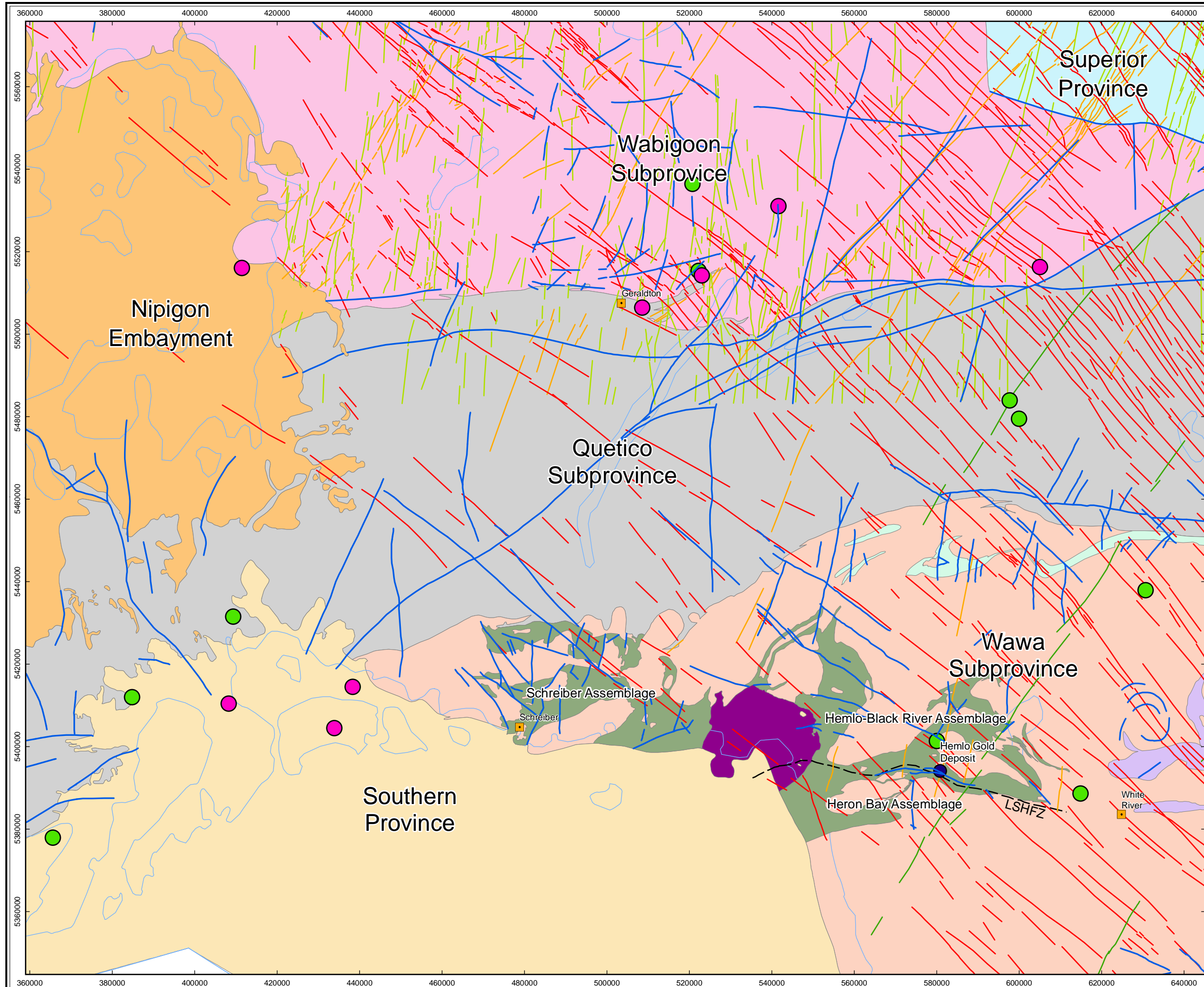
Data Sources:  
 Parks: LIO CLUPA designation  
 Rail: LIO Railway  
 Road: LIO Road Segment  
 Township: LIO Township  
 Utility: LIO Utility Line  
 Waterbody: LIO Waterbody  
 Watercourse: LIO Watercourse  
 Figure reproduced from AECOM (2013)

NORTH  
 5 km

PROJECT  
 Phase 1 Geoscientific Desktop Preliminary Assessment,  
 Lineament Analysis, Schreiber Area, Ontario

TITLE  
**Township of Schreiber and Surrounding Area**

DESIGN	GHF	14 Aug 2012	<b>Figure 1</b>	REVISION 7
GIS	JA	02 Aug 2013		UTM ZONE 16
CHECK	IV	02 Aug 2013		NAD 1983
REVIEW	IV	02 Aug 2013		1:150,000



**Legend**

- Community
- Waterbody
- Hemlo Gold Deposit
- Lake Superior-Hemlo Fault Zone (LSHFZ)
- Geological Subprovince Boundary
- Fault

**Seismic Events (Magnitude)**

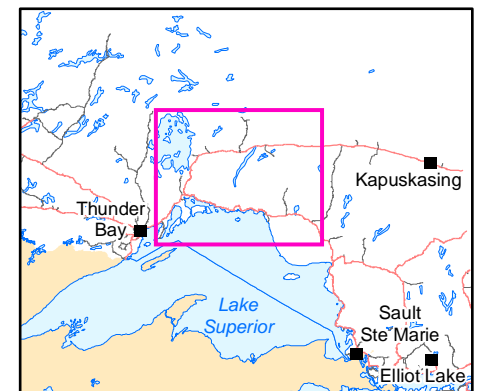
- 1.0 - 2.0
- 2.1 - 3.0

**Dykes**

- Biscotasing mafic dyke
- Marathon mafic dyke
- Marathon, Kapuskasing or Biscotasing mafic dyke
- Matachewan mafic dyke

**Regional Tectonic Geology**

- Nipigon Embayment
- Quetico Subprovince
- Southern Province
- Superior Province
- Wabigoon Subprovince
- Wawa Subprovince
- Schreiber-Hemlo Greenstone Belt
- Coldwell Alkalic Complex
- Manitouwadge-Hornepayne Greenstone Belt
- White River-Dayohessarah Greenstone Belt



Data Sources:  
 Bedrock: OGS MRD 126-REV-1 (1:250,000)  
 Earthquake: NRCAN Earthquake Database  
 Figure reproduced from AECOM (2013)

NORTH  
30 km

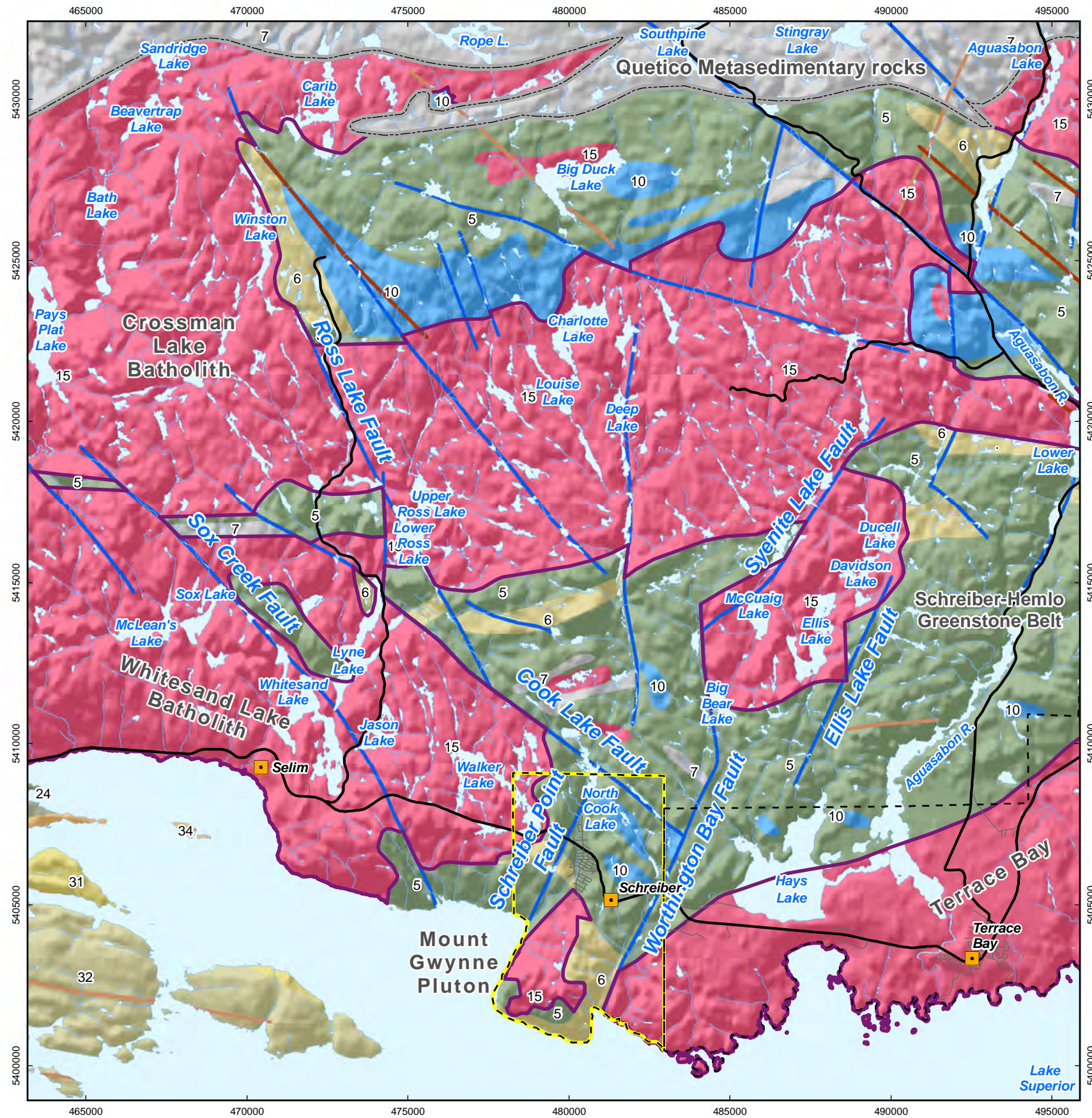
**AECOM**

PROJECT  
Phase 1 Geoscientific Desktop Preliminary Assessment,  
Lineament Analysis, Schreiber Area, Ontario

TITLE  
**Regional Tectonic Setting of  
Schreiber and Surrounding Area**

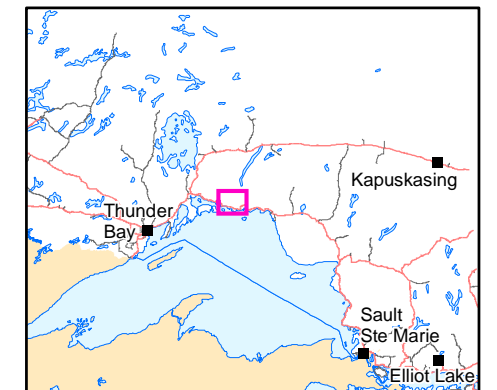
DESIGN	GHF	14 Aug 2012	<b>Figure 2</b>	REVISION 3
GIS	GHF	30 Nov 2012		UTM ZONE 16
CHECK	IV	08 Aug 2013		NAD 1983
REVIEW	IV	08 Aug 2013		1:892,000





**LEGEND**

- City / Towns
  - Township of Schreiber
  - Township of Terrace Bay
  - Main Road
  - Local Road
  - Watercourse
  - Waterbody
- Dykes**
- Marathon, Kapuskasing or Biscotasing Mafic Dyke
  - Matachewan Mafic Dyke
  - Dyke (other)
  - Mapped Fault
  - Quetico/Wawa Subprovince boundary
- Bedrock Geology (Youngest to Oldest)**
- 34. Mafic dykes and related intrusive rocks (Keweenawan age) (circa 1.1 to 1.2 Ga)
  - 32. Osler Gp., Maminse Point Fm., Michipicoten Island Fm.
  - 31. Sibley Gp.
  - 24. Sedimentary rocks
  - 15. Massive granodiorite to granite
  - 11. Gneissic tonalite suite
  - 10. Mafic and ultramafic rocks
  - 7. Metasedimentary rocks
  - 6. Felsic to intermediate metavolcanic rocks
  - 5. Mafic to intermediate metavolcanic rocks
  - 2. Felsic to intermediate metavolcanic rock
  - Batholith / Pluton



Data Sources:  
 Bedrock: OGS MRD 126-REV1 (1:250,000)  
 Faults: OGS MRD 126-REV1 (1:250,000)  
 Dike: OGS MRD 126-REV1 (1:250,000)  
 Batholith: Generalized from OGS 2006  
 Cities/Towns: LIO Cities and Towns  
 Road: LIO Road Segment  
 Township: LIO Township  
 Waterbody: LIO Waterbody  
 Watercourse: LIO Watercourse  
 Figure reproduced from AECOM (2013)

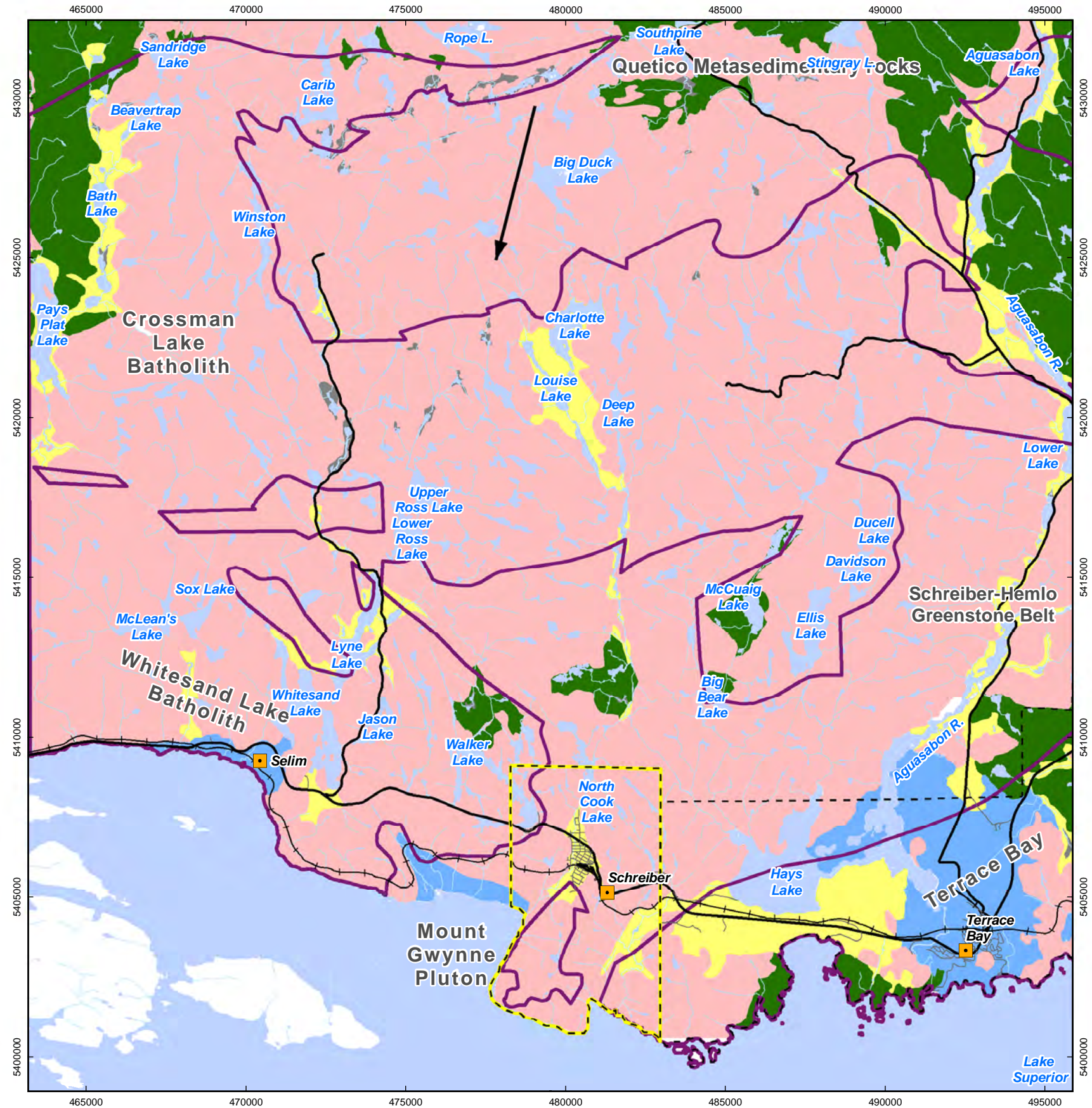


PROJECT  
 Phase 1 Geoscientific Desktop Preliminary Assessment,  
 Lineament Analysis, Schreiber Area, Ontario

TITLE  
**Local Bedrock Geology of the Schreiber Area**

DESIGN	GHF	14 Aug 2012	<b>Figure 3</b>	REVISION 7
GIS	GHF/JA	02 Aug 2013		UTM ZONE 16
CHECK	IV	02 Aug 2013		NAD 1983
REVIEW	IV	02 Aug 2013		1:150,000





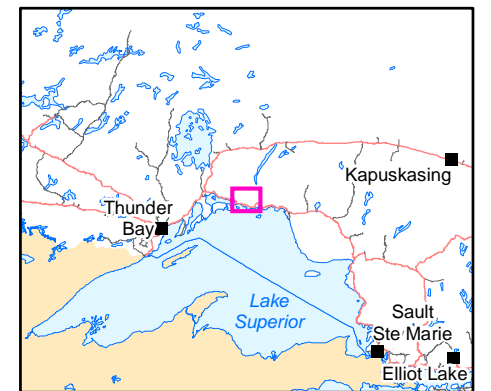
**LEGEND**

- Cities/Towns
- ▭ Township of Schreiber
- ▭ Township of Terrace Bay
- Main Road
- Local Road
- Railways
- Watercourse
- Waterbody
- ▭ Outline of Batholith / Pluton

**Surficial Geology**

- Morainal Terrain
- Glaciofluvial Terrain
- Glaciolacustrine Terrain
- Organic Terrain
- Bedrock Terrain

➔ Average Ice-Flow Direction for Area



Data Sources:  
 Overburden: OGS MRD-160 (1:100,000)  
 Batholith: Generalized from OGS 2006  
 Cities/Towns: LIO Cities and Towns  
 Road: LIO Road Segment  
 Township: LIO Township  
 Waterbody: LIO Waterbody  
 Watercourse: LIO Watercourse  
 Figure reproduced from AECOM (2013)

NORTH  
 4.5 km

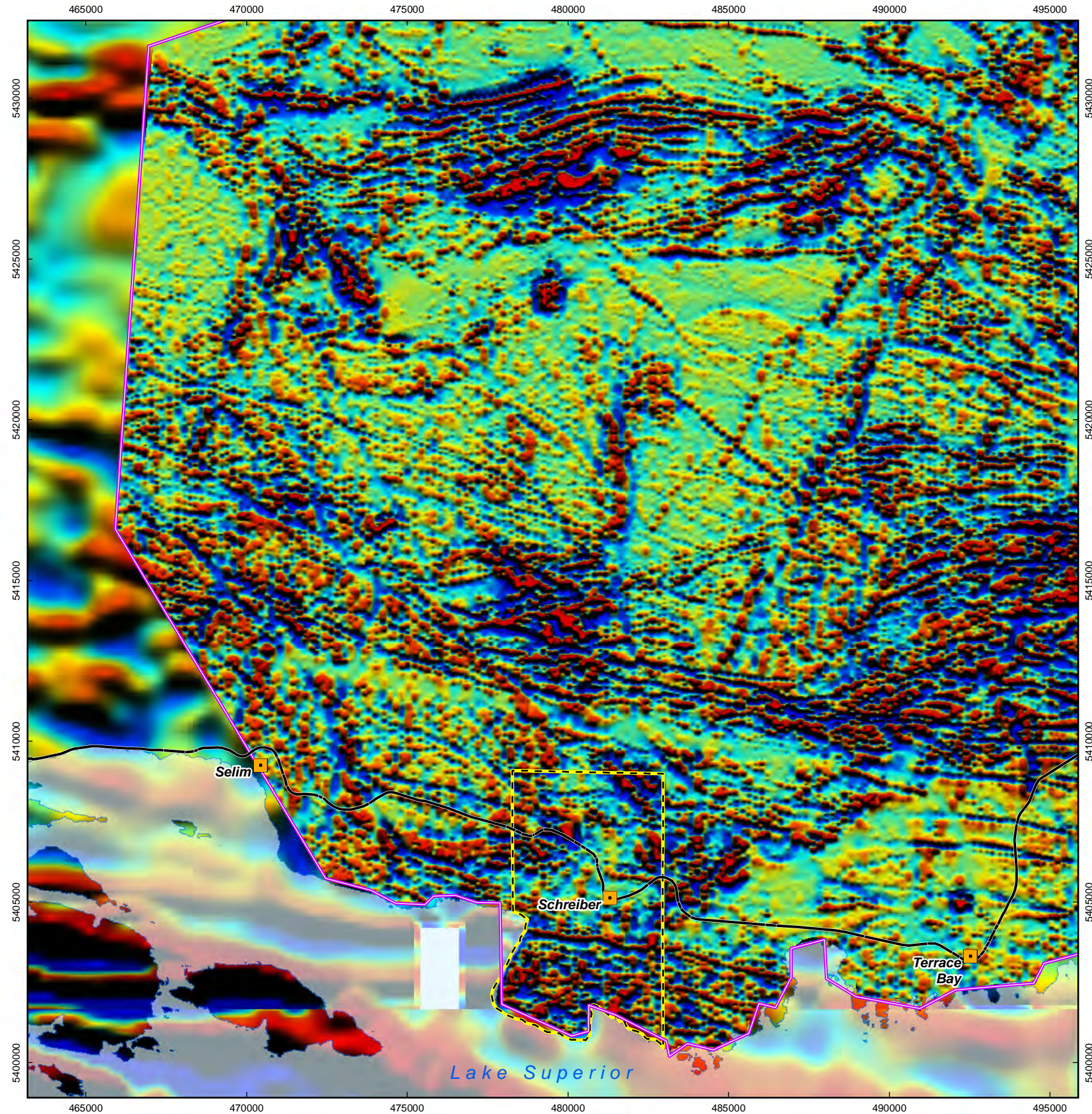
**AECOM**

PROJECT  
 Phase 1 Geoscientific Desktop Preliminary Assessment,  
 Terrain and Remote Sensing Study, Schreiber Area, Ontario

TITLE  
**Terrain Features of the Schreiber Area**

DESIGN	GHF	14 Aug 2012	<b>Figure 4</b>	REVISION 7
GIS	GHF/JA	02 Aug 2013		UTM ZONE 16
CHECK	IV	02 Aug 2013		NAD 1983
REVIEW	IV	02 Aug 2013		1:150,000

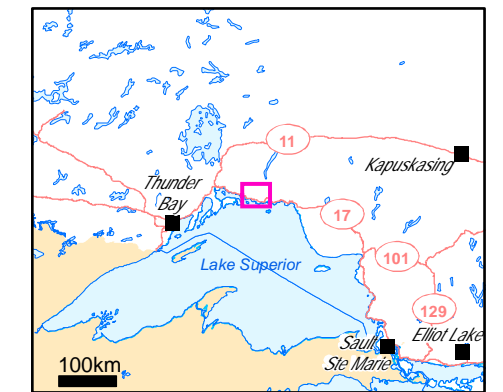
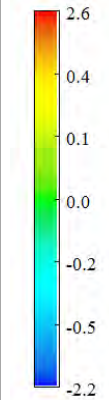




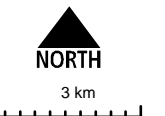
**Legend**

- City / Towns
- Township of Schreiber
- Major Roads
- Lake Superior
- High resolution "Supergrid" data

*Residual Total  
Magnetic Field (nT)*



Data Sources:  
 Road: LIO Road Segment  
 Township: LIO Township  
 Waterbody: LIO Waterbody  
 OGS Schreiber Magnetic Supergrid (GDS1104);  
 OGS SMGA (GDS1036); GSC Schreiber  
 Aeromagnetic Survey Data (GSC2514)

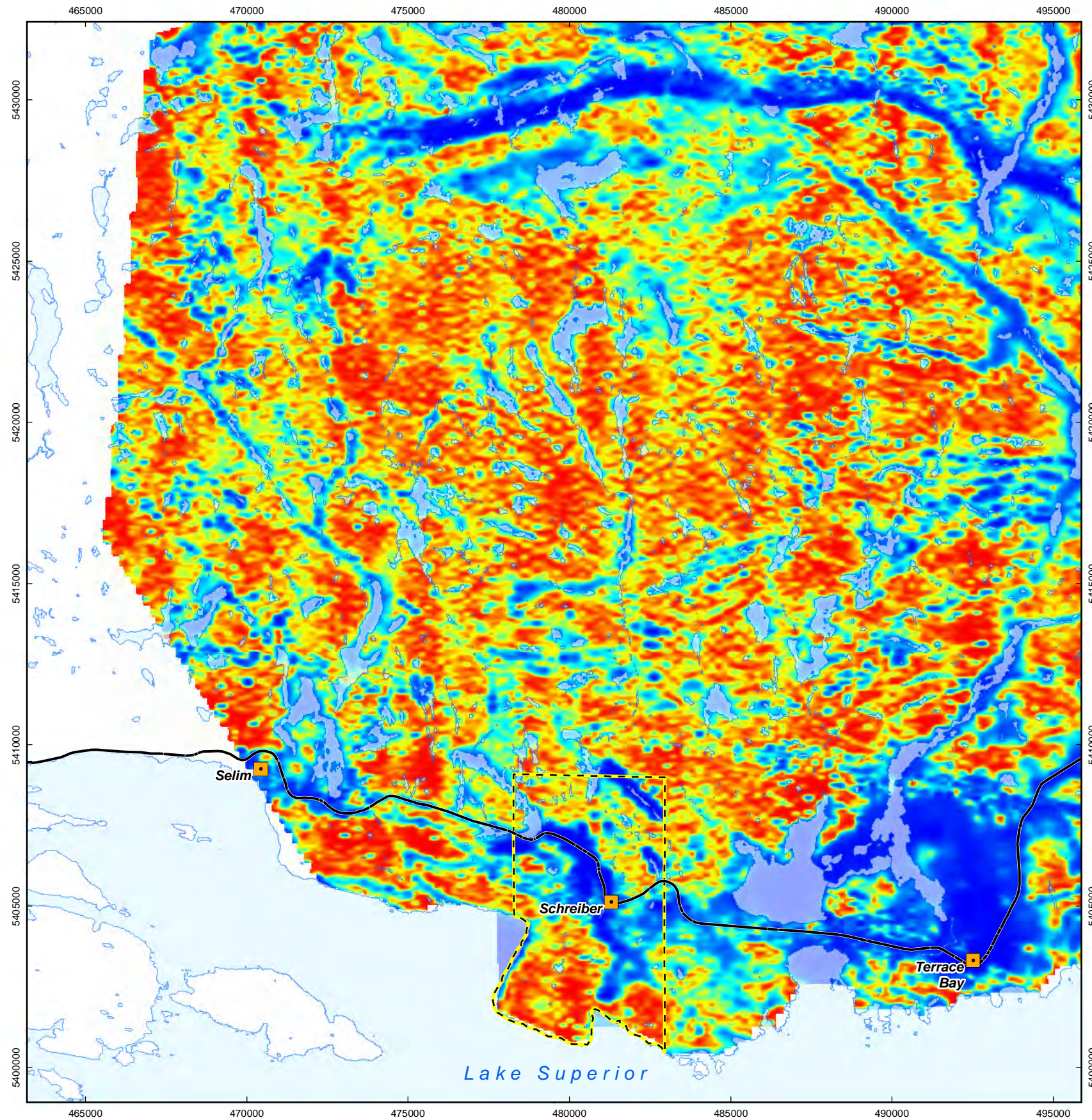


PROJECT  
 Phase 1 Geoscientific Desktop Preliminary Assessment,  
 Lineament Analysis, Schreiber Area, Ontario

TITLE  
**Pole Reduced Magnetic Data  
 (first vertical derivative)  
 for the Schreiber Area**

DESIGN	GHF	14 Aug 2012	<b>Figure 5</b>	REVISION 7
GIS	JA	02 Aug 2013		UTM ZONE 16
CHECK	IV	02 Aug 2013		NAD 1983
REVIEW	IV	02 Aug 2013		1:150,000

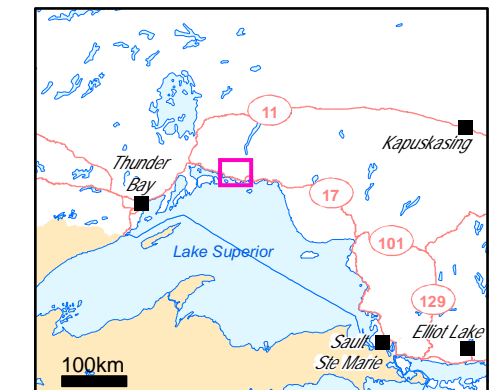
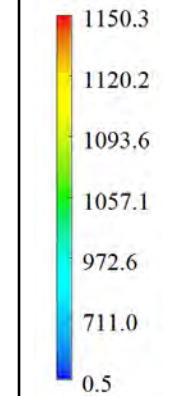




**Legend**

- City / Towns
- Township of Schreiber
- Major Roads
- Waterbody

Resistivity  
(ohm-metre)



Data Sources:  
 Road: LIO Road Segment  
 Township: LIO Township  
 Waterbody: LIO Waterbody  
 OGS Schreiber Magnetic Supergrid (GDS1104)



3 km

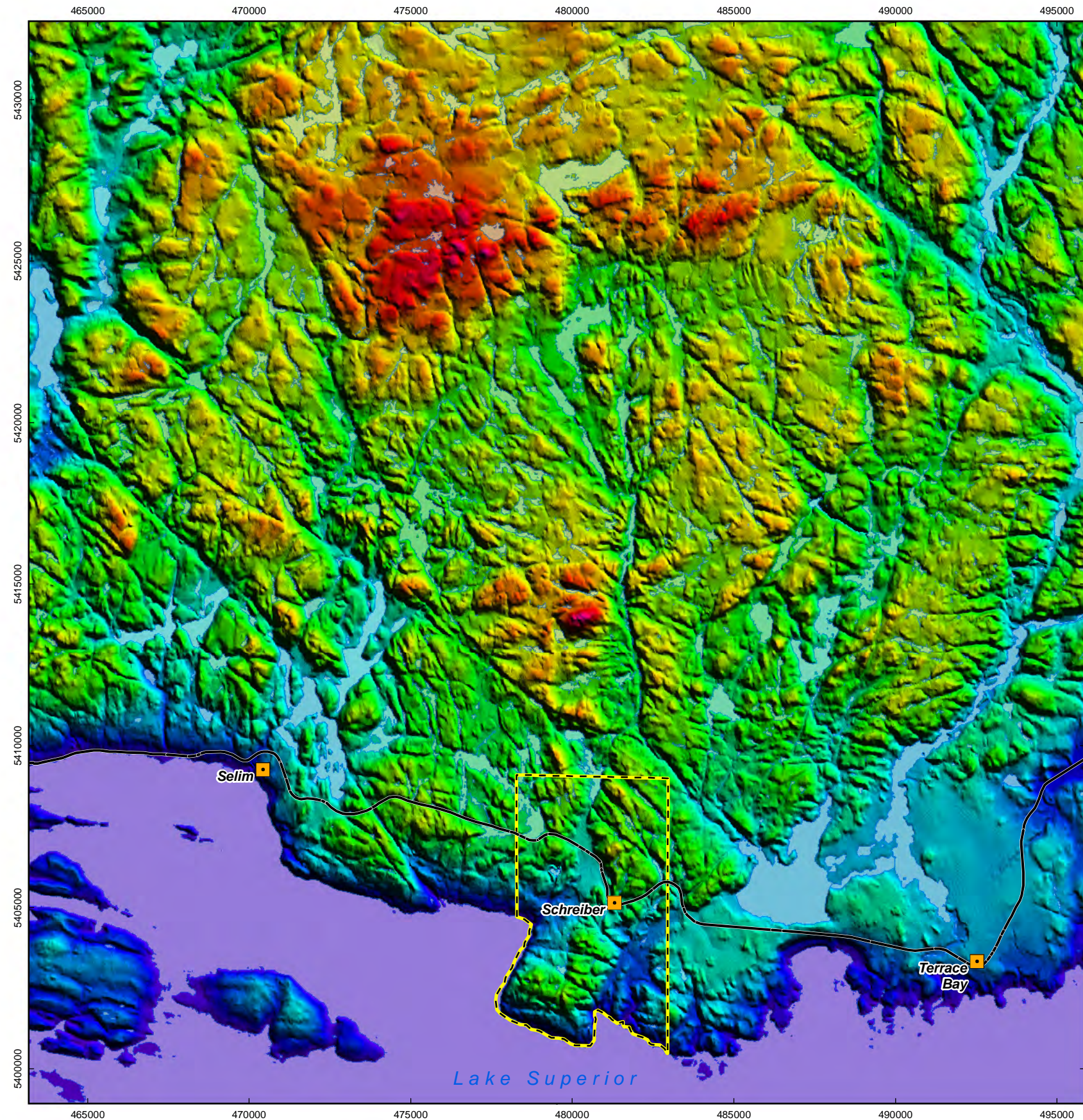


PROJECT  
 Phase 1 Geoscientific Desktop Preliminary Assessment,  
 Lineament Analysis, Schreiber Area, Ontario

TITLE  
**Apparent resistivity from low-frequency (877 Hz)  
 electromagnetic data for the Schreiber area**

DESIGN	GHF	14 Aug 2012	<b>Figure 6</b>	REVISION 7
GIS	JA	02 Aug 2013		UTM ZONE 16
CHECK	IV	02 Aug 2013		NAD 1983
REVIEW	IV	02 Aug 2013		1:150,000

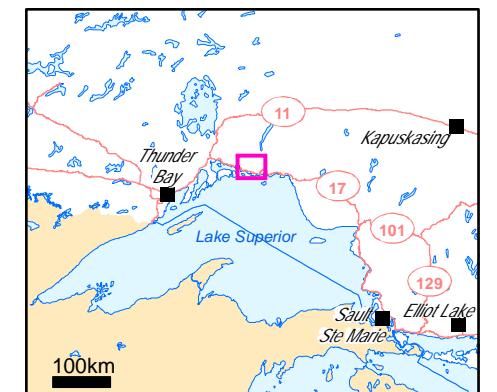
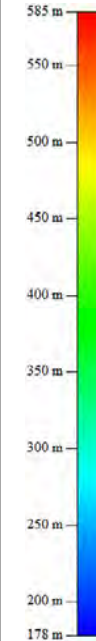




**Legend**

- City / Towns
- Township of Schreiber
- Major Roads
- Waterbody

*Elevation (metres)*



Data Sources:  
 Road: LIO Road Segment  
 Township: LIO Township  
 Waterbody: LIO Waterbody  
 NRC CDED Topography Data



**NORTH**



PROJECT  
 Phase 1 Geoscientific Desktop Preliminary Assessment,  
 Lineament Analysis, Schreiber Area, Ontario

TITLE  
**CDED digital elevation model  
 for the Schreiber area**

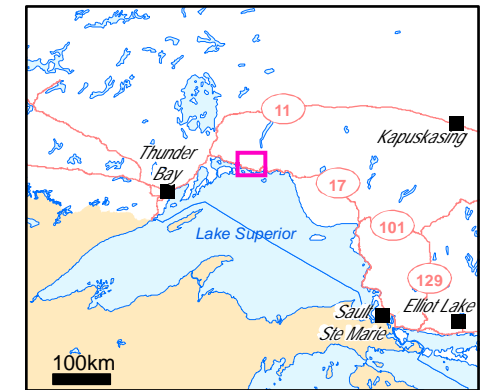
DESIGN	GHF	14 Aug 2012	<b>Figure 7</b>	REVISION 7
GIS	JA	02 Aug 2013		UTM ZONE 16
CHECK	IV	02 Aug 2013		NAD 1983
REVIEW	IV	02 Aug 2013		1:150,000





**Legend**

- City / Towns
- Township of Schreiber
- Major Roads
- Waterbody



Data Sources:  
 Road: LIO Road Segment  
 Township: LIO Township  
 Waterbody: LIO Waterbody  
 NRC LandSAT 7 OrthoImage (CanImage)  
 ESRI/Bing Maps Aerial

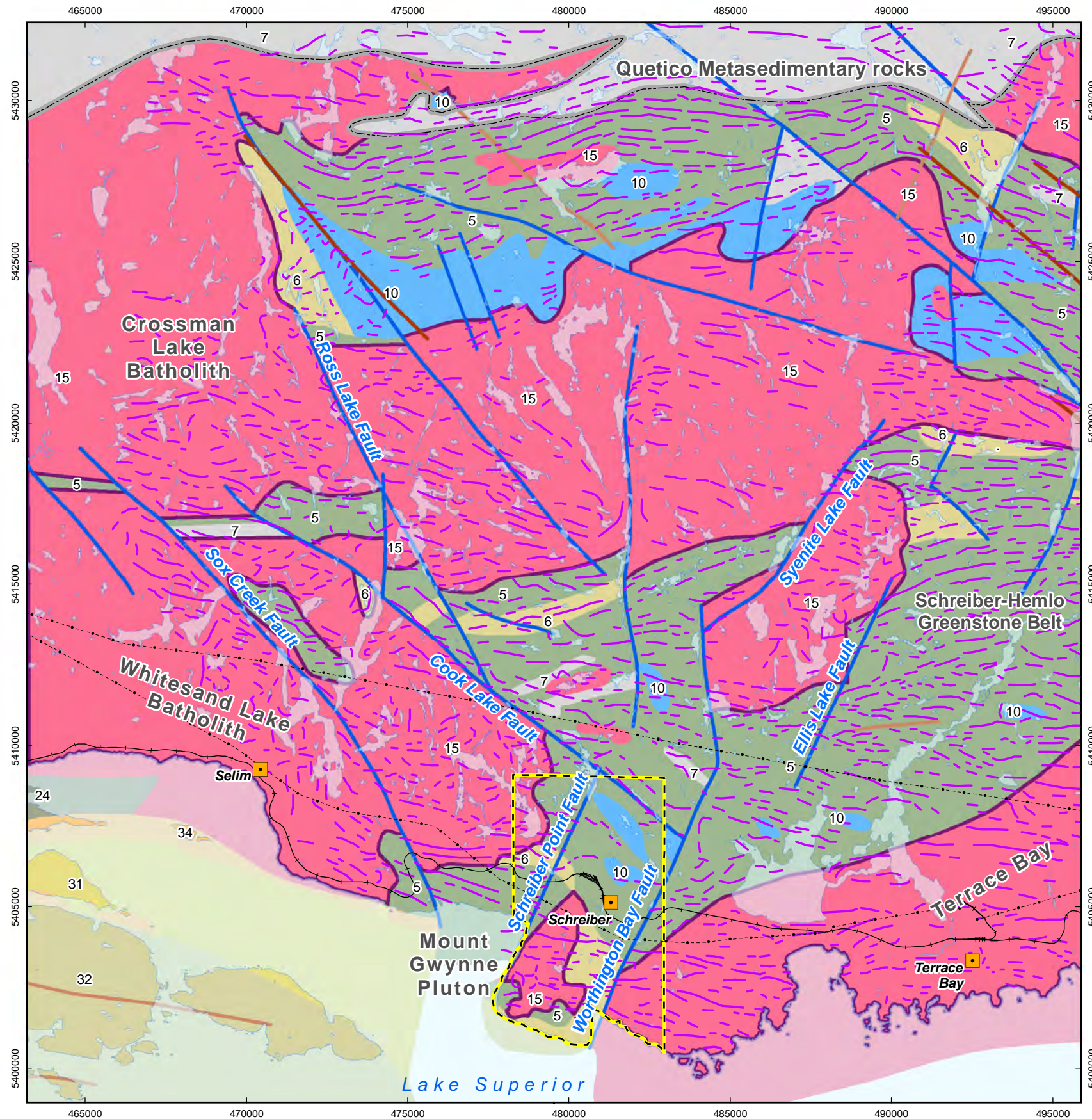


PROJECT  
 Phase 1 Geoscientific Desktop Preliminary Assessment,  
 Lineament Analysis, Schreiber Area, Ontario

TITLE  
**Satellite Data (LandSAT)  
 for the Schreiber Area**

DESIGN	GHF	14 Aug 2012	<b>Figure 8</b>	REVISION 7
GIS	JA	02 Aug 2013		UTM ZONE 16
CHECK	IV	02 Aug 2013		NAD 1983
REVIEW	IV	02 Aug 2013		1:150,000





**Legend**

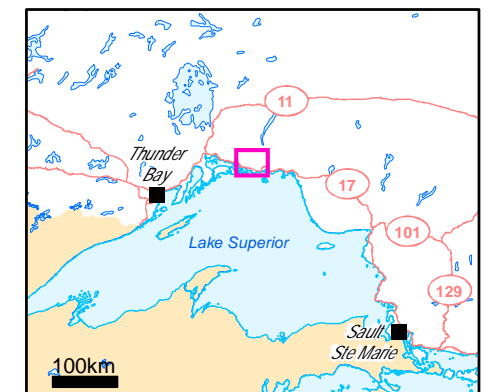
- City / Towns
- Township of Schreiber
- Main Road
- Local Road
- Waterbody
- Mapped Fault
- Ductile lineament
- Quetico-Wawa Subprovince boundary

**Dykes**

- Marathon, Kapuskasing or Biscotasing Mafic Dyke
- Matachewan Mafic Dyke
- Dyke (other)

**Bedrock Geology (Youngest to Oldest)**

- 34. Mafic dykes and related intrusive rocks (Keweenaw age) (circa 1.1 to 1.2 Ga)
- 32. Osler Gp., Maminse Point Fm., Michipicoten Island Fm.
- 31. Sibley Gp.
- 24. Animikie Group (Sedimentary)
- 15. Massive granodiorite to granite
- 11. Gneissic tonalite suite
- 10. Mafic and ultramafic rocks
- 7. Metasedimentary rocks
- 6. Felsic to intermediate metavolcanic rocks
- 6a. Felsic to intermediate metavolcanic rocks
- 5. Mafic to intermediate metavolcanic rocks
- 2. Felsic to intermediate metavolcanic rock
- Outline of Batholith / Pluton



Data Sources:  
 Road: LIO Road Segment  
 Township: LIO Township  
 Waterbody: LIO Waterbody  
 OGS Ontario Bedrock Geology  
 Compilation, Revision 1  
 SRK Lithotectonic, Linear Interpretation

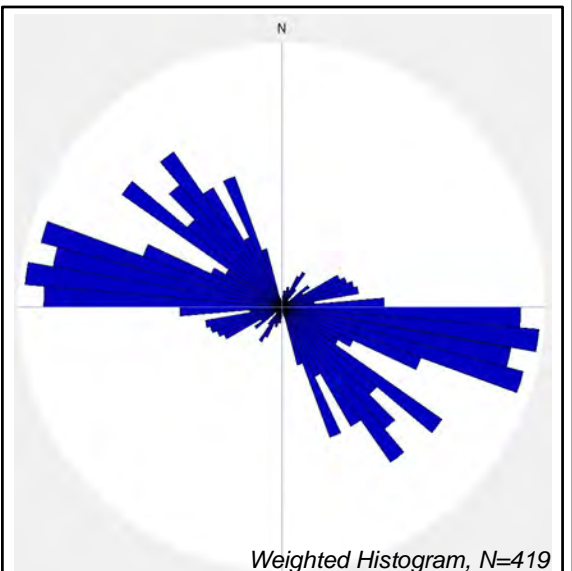
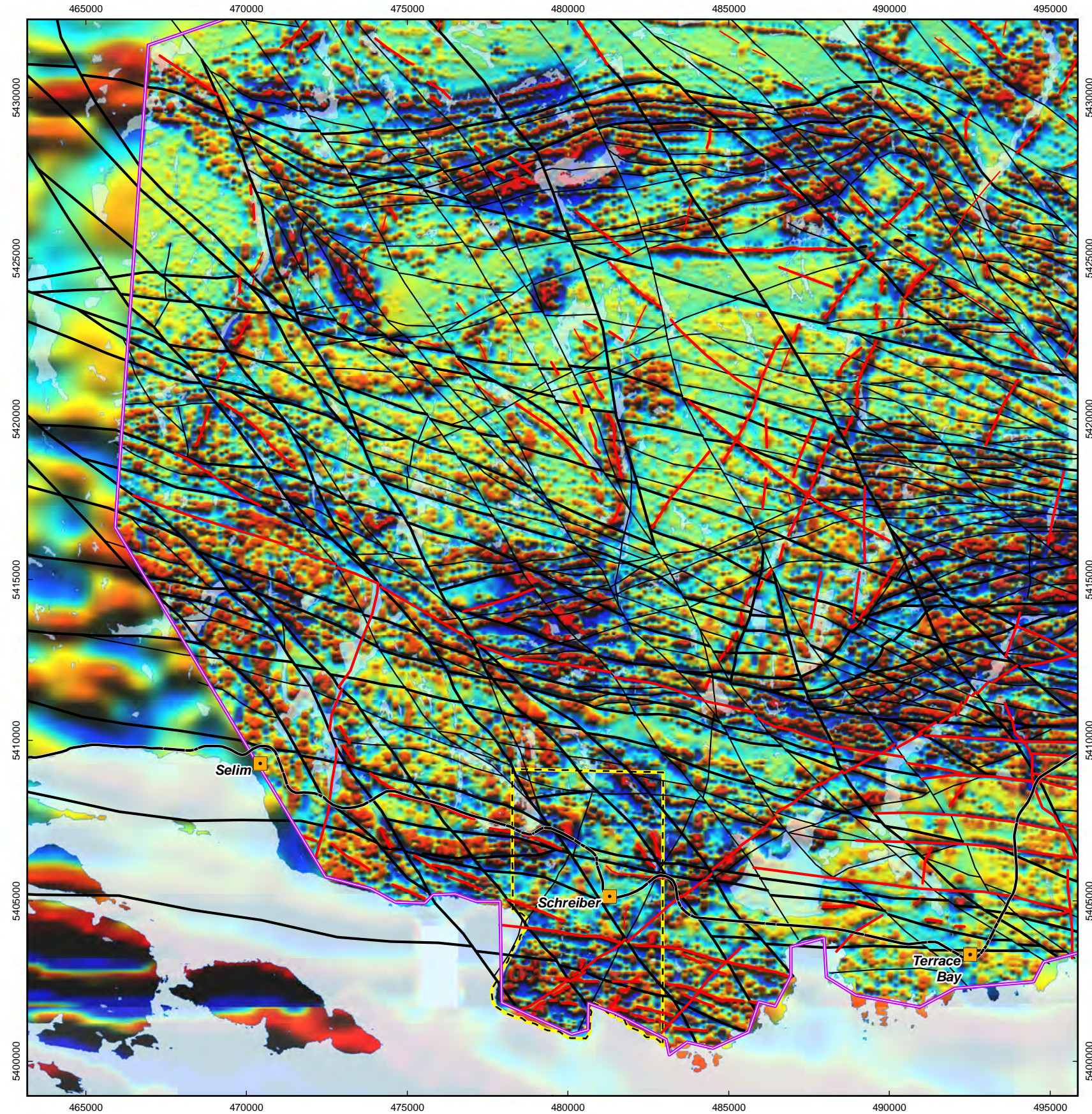


PROJECT  
 Phase 1 Geoscientific Desktop Preliminary Assessment,  
 Lineament Analysis, Schreiber Area, Ontario

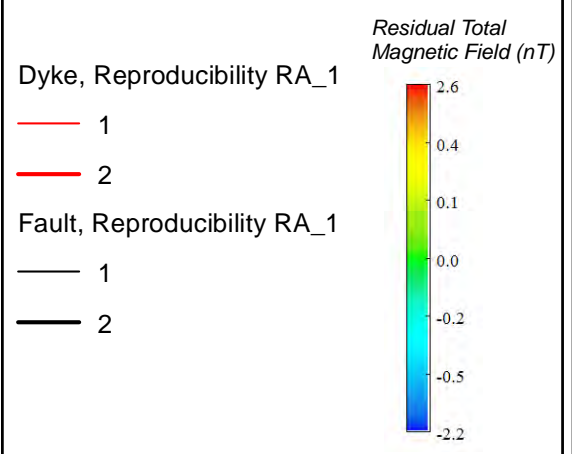
TITLE  
**Ductile Features  
 for the Schreiber Area**

DESIGN	GHF	14 Aug 2012	<b>Figure 9</b>	REVISION 7
GIS	JA	02 Aug 2013		UTM ZONE 16
CHECK	IV	02 Aug 2013		NAD 1983
REVIEW	IV	02 Aug 2013		1:150,000





- Legend**
- City / Towns
  - Township of Schreiber
  - Major Roads
  - Waterbody
  - High resolution "Supergrid" data



Data Sources:  
 Road: LIO Road Segment  
 Township: LIO Township  
 Waterbody: LIO Waterbody  
 OGS Schreiber Magnetic Supergrid (GDS1104);  
 OGS SMGA (GDS1036); GSC Schreiber  
 Aeromagnetic Survey Data (GSC2514)

**NORTH**  
3 km

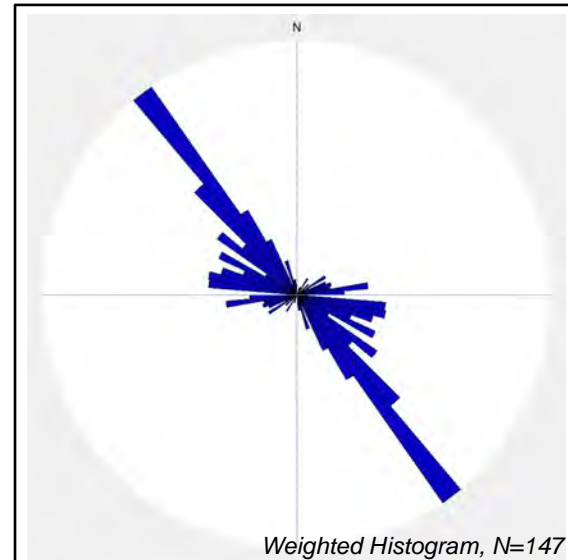
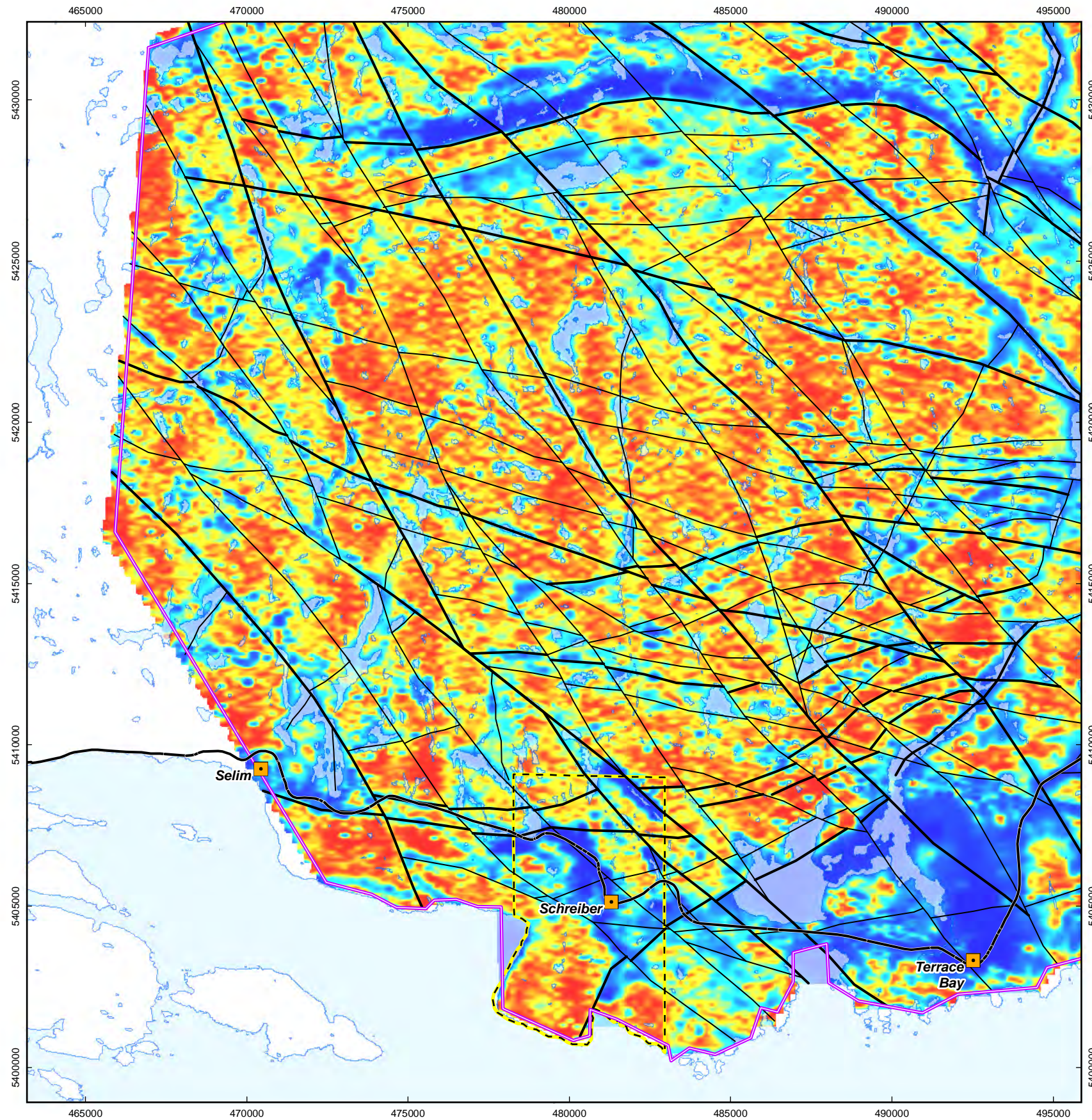
**srk consulting**

PROJECT  
Phase 1 Geoscientific Desktop Preliminary Assessment,  
Lineament Analysis, Schreiber Area, Ontario

TITLE  
**Lineaments by Reproducibility (RA\_1)  
interpreted from Pole Reduced Magnetic Data (1VD)  
for the Schreiber Area**

DESIGN	GHF	14 Aug 2012	<b>Figure 10</b>	REVISION 10
GIS	JA	06 Aug 2013		UTM ZONE 16
CHECK	IV	06 Aug 2013		NAD 1983
REVIEW	IV	06 Aug 2013		1:150,000



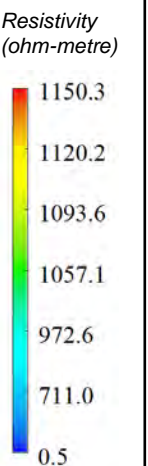


**Legend**

- City / Towns
- Township of Schreiber
- Major Roads
- Waterbody
- High resolution "Supergrid" data

**Fault, Reproducibility RA\_1**

- 1
- 2



Data Sources:  
 Road: LIO Road Segment  
 Township: LIO Township  
 Waterbody: LIO Waterbody  
 OGS Schreiber Magnetic Supergrid (GDS1104)

NORTH  
3 km

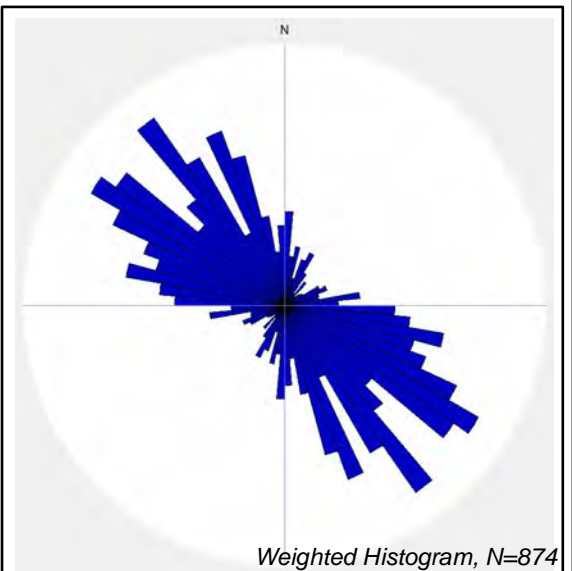
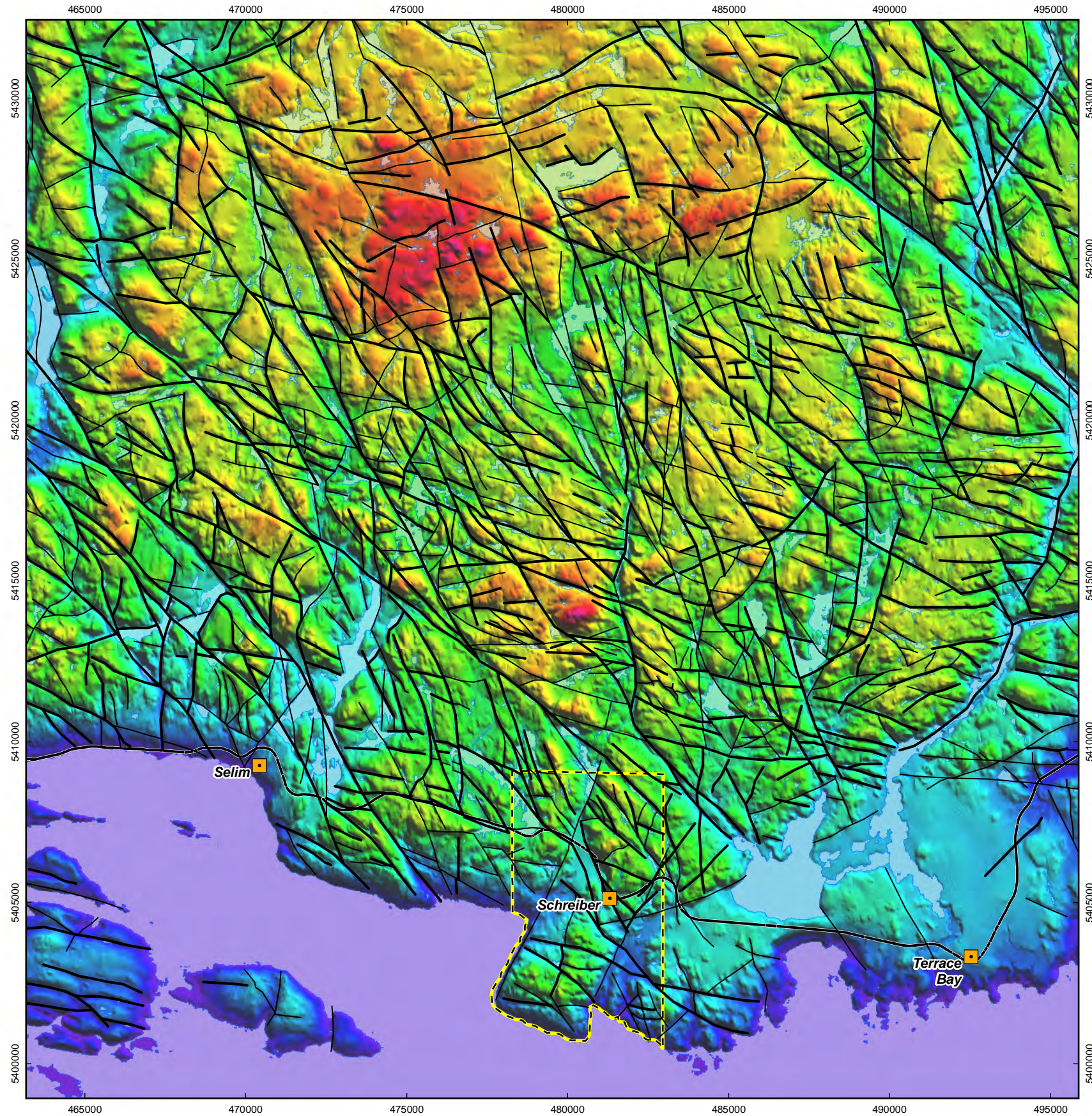


PROJECT  
 Phase 1 Geoscientific Desktop Preliminary Assessment,  
 Lineament Analysis, Schreiber Area, Ontario

TITLE  
**Lineaments by reproducibility (RA\_1)  
 interpreted from low-frequency (877 Hz) EM data  
 for the Schreiber Area**

DESIGN	GHF	14 Aug 2012	<b>Figure 11</b>	REVISION 10
GIS	JA	06 Aug 2013		UTM ZONE 16
CHECK	IV	06 Aug 2013		NAD 1983
REVIEW	IV	06 Aug 2013		1:150,000





**Legend**

- City / Towns
- Township of Schreiber
- Major Roads
- Waterbody

**Fault, Reproducibility RA\_1**

- 1
- 2

**Elevation (metres)**

585 m  
550 m  
500 m  
450 m  
400 m  
350 m  
300 m  
250 m  
200 m  
178 m

Data Sources:  
 Road: LIO Road Segment  
 Township: LIO Township  
 Waterbody: LIO Waterbody  
 NRC CDED Topography Data

**NORTH**  
3 km

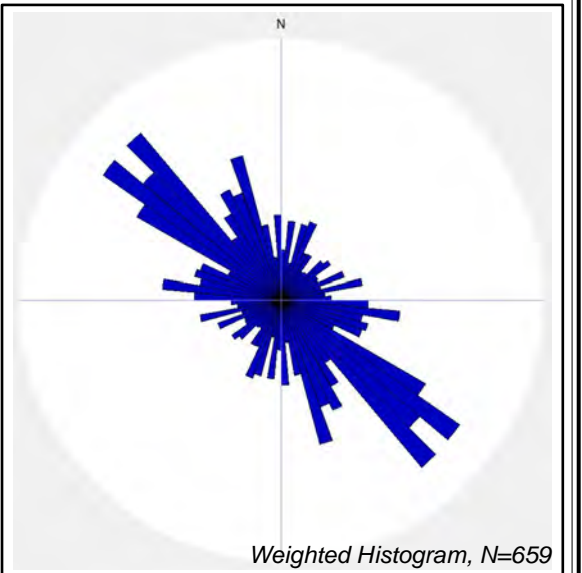
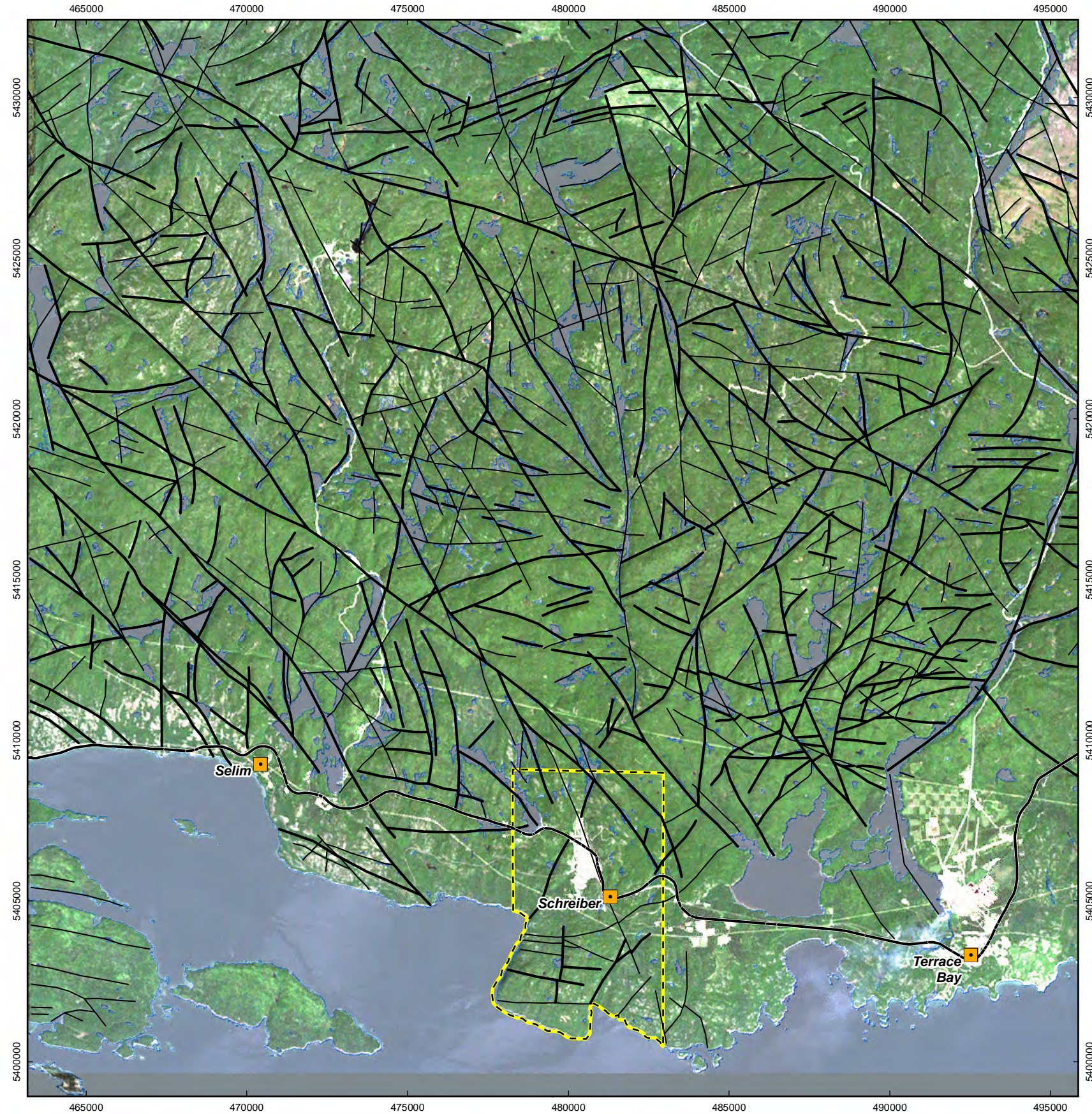
**srk consulting**

PROJECT  
Phase 1 Geoscientific Desktop Preliminary Assessment,  
Lineament Analysis, Schreiber Area, Ontario

TITLE  
**Lineaments by reproducibility (RA\_1)  
Interpreted from CDED digital elevation data  
for the Schreiber area**

DESIGN	GHF	14 Aug 2012	<b>Figure 12</b>	REVISION 10
GIS	JA	06 Aug 2013		UTM ZONE 16
CHECK	IV	06 Aug 2013		NAD 1983
REVIEW	IV	06 Aug 2013		1:150,000





**Legend**

- City / Towns
- Township of Schreiber
- Major Roads
- Waterbody

**Fault, Reproducibility RA\_1**

- 1
- 2

Data Sources:  
 Road: LIO Road Segment  
 Township: LIO Township  
 Waterbody: LIO Waterbody  
 NRC LandSAT 7 Ortholmage (CanImage)  
 ESRI/Bing Maps Aerial

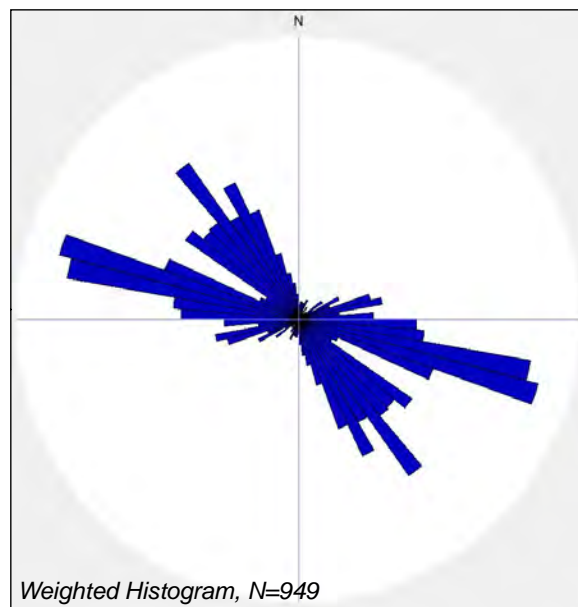


PROJECT  
 Phase 1 Geoscientific Desktop Preliminary Assessment,  
 Lineament Analysis, Schreiber Area, Ontario

TITLE  
**Lineaments by reproducibility (RA\_1)  
 Interpreted from Satellite Data (LandSAT)  
 for the Schreiber Area**

DESIGN	GHF	14 Aug 2012	<b>Figure 13</b>	REVISION 10
GIS	JA	06 Aug 2013		UTM ZONE 16
CHECK	IV	06 Aug 2013		NAD 1983
REVIEW	IV	06 Aug 2013		1:150,000





Weighted Histogram, N=949



**Legend**

- City / Towns
  - Township of Schreiber
  - Major Roads
  - Waterbody
  - Mapped Dyke
  - Mapped Fault
- Bedrock Geology (Youngest to Oldest)**
- 34. Mafic dykes and related intrusive rocks (Keweenawan age) (circa 1.1 to 1.2 Ga)
  - 32. Osler Gp., Maminse Point Fm., Michipocoten Island Fm.
  - 31. Sibley Gp.
  - 24. Animikie Group (Sedimentary)
  - 15. Massive granodiorite to granite
  - 11. Gneissic tonalite suite
  - 10. Mafic and ultramafic rocks
  - 7. Metasedimentary rocks
  - 6. Felsic to intermediate metavolcanic rocks
  - 6a. Felsic to intermediate metavolcanic rocks
  - 5. Mafic to intermediate metavolcanic rocks
  - 2. Felsic to intermediate metavolcanic rock

**Dyke, Reproducibility RA\_2**

- 1
- 2
- 4

**Fault, Reproducibility RA\_2**

- 2
- 3
- 4

Data Sources:  
 Road: LIO Road Segment  
 Township: LIO Township  
 Waterbody: LIO Waterbody  
 OGS Ontario Bedrock Geology  
 Compilation, Revision 1  
 SRK, Linear Interpretation

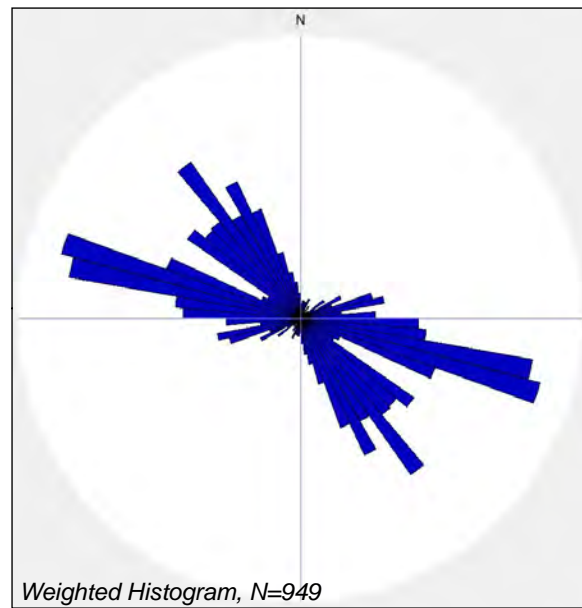


PROJECT  
 Phase 1 Geoscientific Desktop Preliminary Assessment,  
 Lineament Analysis, Schreiber Area, Ontario

TITLE  
**Interpreted Lineaments by Reproducibility (RA\_2)  
 overlying bedrock geology for the Schreiber Area**

DESIGN	GHF	14 Aug 2012	<b>Figure 14</b>	REVISION 10
GIS	JA	06 Aug 2013		UTM_ZONE 16
CHECK	IV	06 Aug 2013		NAD 1983
REVIEW	IV	06 Aug 2013		1:150,000





**Legend**

- City / Towns
  - Township of Schreiber
  - Major Roads
  - Waterbody
  - Mapped Dyke
  - Mapped Fault
- Bedrock Geology (Youngest to Oldest)**
- 34. Mafic dykes and related intrusive rocks (Keweenaw age) (circa 1.1 to 1.2 Ga)
  - 32. Osler Gp., Maminse Point Fm., Michipicoten Island Fm.
  - 31. Sibley Gp.
  - 24. Animikie Group (Sedimentary)
  - 15. Massive granodiorite to granite
  - 11. Gneissic tonalite suite
  - 10. Mafic and ultramafic rocks
  - 7. Metasedimentary rocks
  - 6. Felsic to intermediate metavolcanic rocks
  - 6a. Felsic to intermediate metavolcanic rocks
  - 5. Mafic to intermediate metavolcanic rocks
  - 2. Felsic to intermediate metavolcanic rock

- |  |  |
|--|--|
| Dyke, Length   | Fault, Length  |
| <span style="display: inline-block; width: 20px; border-bottom: 1px dashed red; margin-right: 5px;"></span> <1 km  | <span style="display: inline-block; width: 20px; border-bottom: 1px dashed black; margin-right: 5px;"></span> <1 km  |
| <span style="display: inline-block; width: 20px; border-bottom: 1px solid red; margin-right: 5px;"></span> 1-5 km  | <span style="display: inline-block; width: 20px; border-bottom: 1px solid black; margin-right: 5px;"></span> 1-5 km  |
| <span style="display: inline-block; width: 20px; border-bottom: 2px solid red; margin-right: 5px;"></span> 5-10 km | <span style="display: inline-block; width: 20px; border-bottom: 2px solid black; margin-right: 5px;"></span> 5-10 km |
| <span style="display: inline-block; width: 20px; border-bottom: 3px solid red; margin-right: 5px;"></span> >10 km  | <span style="display: inline-block; width: 20px; border-bottom: 3px solid black; margin-right: 5px;"></span> >10 km  |

Data Sources:  
 Road: LIO Road Segment  
 Township: LIO Township  
 Waterbody: LIO Waterbody  
 OGS Ontario Bedrock Geology  
 Compilation, Revision 1

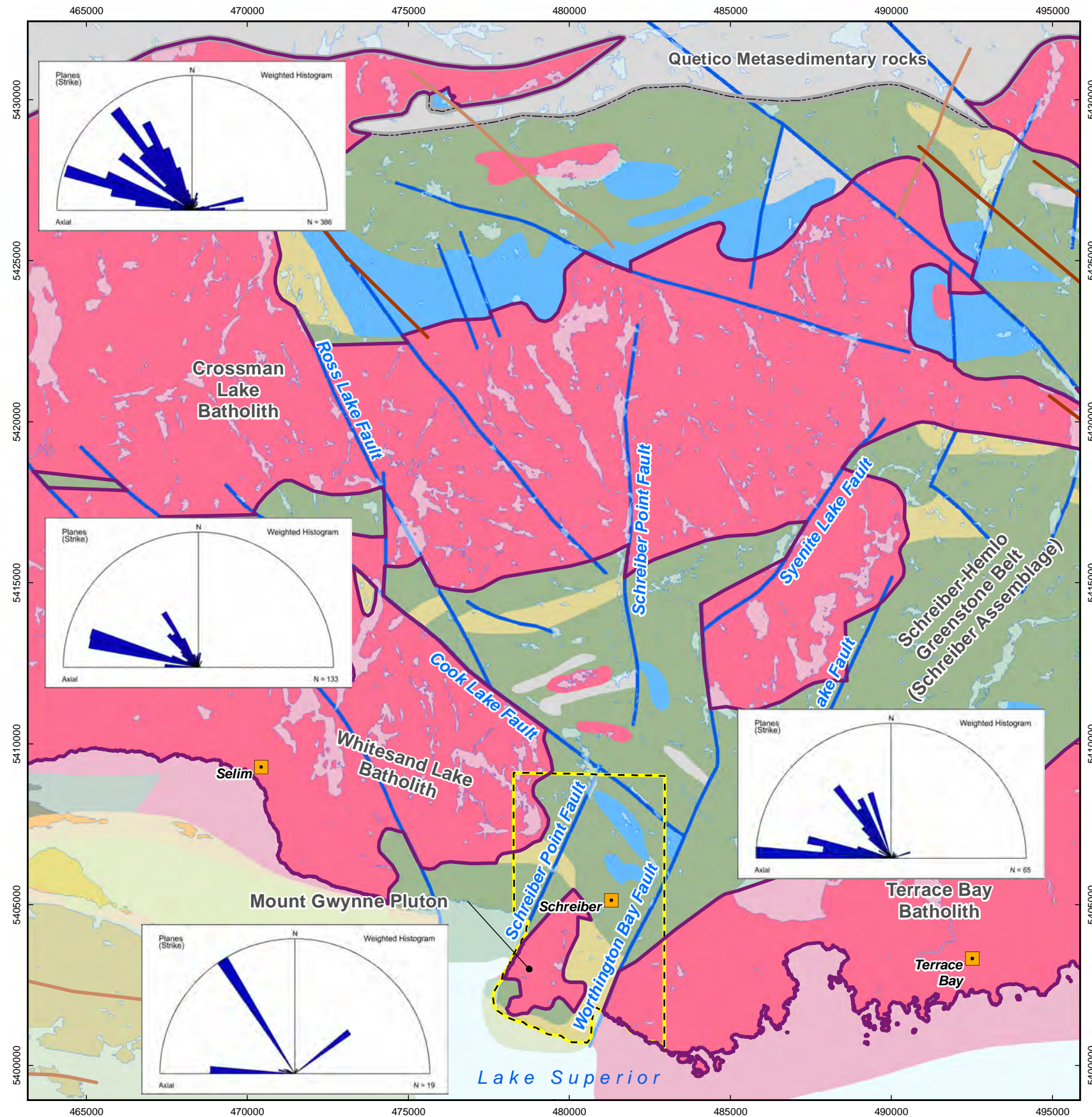


PROJECT  
 Phase 1 Geoscientific Desktop Preliminary Assessment,  
 Lineament Analysis, Schreiber Area, Ontario

TITLE  
**Interpreted Lineaments by Length  
 overlying bedrock geology for the Schreiber Area**

DESIGN	GHF	14 Aug 2012	<b>Figure 15</b>	REVISION 10
GIS	JA	06 Aug 2013		UTM ZONE 16
CHECK	IV	06 Aug 2013		NAD 1983
REVIEW	IV	06 Aug 2013		1:150,000

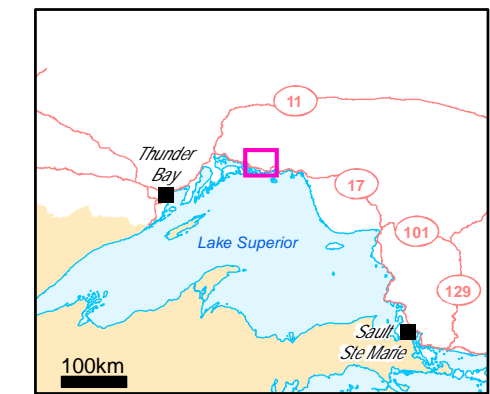




**Legend**

- City / Towns
  - Township of Schreiber
  - Main Road
  - Local Road
  - Waterbody
- Dykes**
- Marathon, Kapuskasing or Biscotasing Mafic Dyke
  - Matachewan Mafic Dyke
  - Dyke (other)
  - Mapped Fault
  - Quetico/Wawa Subprovince boundary

- Bedrock Geology (Youngest to Oldest)**
- 34. Mafic dykes and related intrusive rocks (Keweenawan age) (circa 1.1 to 1.2 Ga)
  - 32. Osler Gp., Maminse Point Fm., Michipicoten Island Fm.
  - 31. Sibley Gp.
  - 24. Animikie Group (Sedimentary)
  - 15. Massive granodiorite to granite
  - 11. Gneissic tonalite suite
  - 10. Mafic and ultramafic rocks
  - 7. Metasedimentary rocks
  - 6. Felsic to intermediate metavolcanic rocks
  - 6a. Felsic to intermediate metavolcanic rocks
  - 5. Mafic to intermediate metavolcanic rocks
  - 2. Felsic to intermediate metavolcanic rock
  - Batholiths/Pluton



Data Sources:  
 Road: LIO Road Segment  
 Township: LIO Township  
 Waterbody: LIO Waterbody  
 OGS Ontario Bedrock Geology  
 Compilation, Revision 1



PROJECT  
 Phase 1 Geoscientific Desktop Preliminary Assessment,  
 Lineament Analysis, Schreiber Area, Ontario

TITLE  
**Interpreted Lineaments by Length  
 overlying bedrock geology for the Schreiber Area**

DESIGN	GHF	14 Aug 2012	<b>Figure 16</b>	REVISION 10
GIS	JA	06 Aug 2013		UTM ZONE 16
CHECK	IV	06 Aug 2013		NAD 1983
REVIEW	IV	06 Aug 2013		1:150,000